Uncertainties in Modelling Atmospheric Dispersion of Radioactive Contaminants

PhD Thesis

Csilla Rudas

Supervisor: Dr. Tamás Pázmándi

Consultant: Dr. Szabolcs Czifrus

Budapest

2024

TABLE OF CONTENTS

LIST OF ABBREVIATIONS

BfS	Bundesamt für Strahlenschutz, German Federal Office for Radiation Protection
CARC	Calculating Atmospheric Release Criteria, computational tool developed by the Centre for Energy Research for deterministic safety assessment to evaluate compliance with release criteria
CER	Centre for Energy Research
CLI	Criteria for Limited Impact
CONFIDENCE	COping with uNcertainties For Improved modelling and DEcision making in Nuclear emergenCiEs
COSYMA	COde SYstem for MAria, a computational tool for assessing consequences of nuclear accidents
DBC	Design Basic Conditions
DCF	Dose Conversion Factor
DEC	Design Extension Condition
DSS	Decision Support System
DTU	Technical University of Denmark
ECMWF	European Center for Medium-range Weather Forecasts
EEAE	Ελληνική Επιτροπή Ατομικής Ενέργειας: Greek Atomic Energy Commission
EPS	Ensemble Prediction System
EUR	European Utility Requirements
FSAR	Final Safety Analysis Report
IRSN	Institut de Radioprotection et de Sûreté Nucléaire
JRODOS	Real-time On-line DecisiOn Support system in java programing language
NPP	Nuclear Power Plant
NWP	Numerical Weather Prediction
OBEIT	Országos Balesetelhárítási Intézkedsi Terv: National Nuclear Emergency Response Plan
OIL	Operational Intervention Level

PHE	Public Health England
REM	"Radiological Ensemble Modelling", the title of a series of case studies performed as part of the CONFIDENCE project
RIVM	National Institute for Public Health and the Environment in The Netherlands
WMO	World Meteorological Organization
WP	Work Package

1. INTRODUCTION

Since the emergence of nuclear power in the energy industry, the safety of nuclear facilities has been a critical issue, as the release of radioactive material from such installations to the environment may have a significant health impact on the population [1]. Among the various types of nuclear facilities, such as power plants, research reactors, and waste disposal sites, nuclear power plants (NPPs) are the most important in terms of the magnitude of the potential radioactive releases. In addition to the normal and anticipated operational states of NPPs, during which the amount of radioactive material that is released to the environment is minimal, it is crucial to consider accidents that could result in significant radioactive releases.

The release of radioactive contaminants from a nuclear facility can occur either as airborne material into the air or as liquid effluents into surface waters. The released radioactive material migrates through the atmosphere, surface water and groundwater and the food chain, reaching populated areas. To assess the impact of a radioactive release on the population, this environmental transport can be modelled and the radioactive concentration in the air, on the ground, in waters and in foodstuff can be determined in order to estimate the doses received by the members of public. Evaluating these individual doses is essential to correctly demonstrate the safety of a nuclear facility. In my research, I focus on atmospheric releases as in most cases the dose consequences associated with airborne releases are significantly more severe, often differing by several orders of magnitude, compared to those resulting from liquid releases.

Modelling of the atmospheric dispersion of airborne radionuclides has been utilized in the nuclear industry for decades. This approach supplements environmental radiation measurements by enabling analysis of processes and quantities that are either impossible or difficult to measure directly. In addition, it provides estimation of the special and temporal distribution of the results rather than being limited to specific points and times. Contrary to measurements, estimations made through modelling can provide information for hypothetical scenarios which are necessary to assess the safety of nuclear installations without the occurrence of an actual release.

There are various atmospheric dispersion models that can be used to simulate the spread of radioactive contaminants in the atmosphere for different types of nuclear assessments depending on their goals and calculational approaches. The most widely applied models are the box models, particle model, Gaussian plume and puff models. These models describe the dispersion of the radioactive contaminants with different approaches, which I present in more detail in section 2.1.

The input data required for the calculation of atmospheric dispersion of radioactive material are the meteorological data and the release characteristics (the source term containing detailed nuclide composition and activity, release elevation and release timing). The meteorogical parameters, such as the wind vector, atmospheric turbulence and precipitation vary in space and time, affecting the amount and extent of the radioactive material dispersion into the environment [2]. The release characteristics similarly influence the spatial distribution of the contaminants but also significantly affects the magnitude of the consequences [3].

A model is a generalized description of a phenomenon focusing on the most important processes while omitting other mechanisms that are less relevant to the phenomenon under investigation. In addition to these omissions in consideration of mechanisms, there are different types of uncertainties, which can occur in modelling and may affect the accuracy of the modelled quantities:

- aleatory uncertainty, resulting from the unpredictability and the natural variability of the modelled phenomena (also called stochastic uncertainty);
- epistemic uncertainty resulting from the lack of knowledge about the modelled system
  - model uncertainty, arising from simplifications, numerical approximations or incomplete treatment of the modelled phenomena, which can be assessed by comparing different models that compute the same quantity,
  - parameter uncertainty, resulting from the uncertainties of the model parameters and input data, that can be evaluated through sensitivity analysis by perturbing single parameters, or uncertainty analysis, when multiple parameters are varied simultaneously.

My thesis focuses on the model uncertainties and parameter uncertainties. I have made code-to-code comparisons to evaluate model uncertainties and applied sensitivity analysis to estimate input parameter uncertainties of atmospheric dispersion and dose calculations.

These types of uncertainties are also present in atmospheric dispersion model calculations and can significantly influence the modelled dispersion, the calculated radioactivity concentrations and the resulting doses [4]. It is therefore crucial to quantify the model uncertainties and parameter uncertainties and assess their effect on calculated population doses. This is also particularly important considering the fact that modelling the atmospheric dispersion of radioactive material is performed to assess off-site consequences of releases with various goals in the field of nuclear safety and radiation protection. These goals include a) safety analysis calculations such as deterministic and probabilistic safety analyses, and b) emergency preparedness and response calculations.

a) Safety analysis calculations are conducted to verify that for all reasonably possible occurrences which result in the spread of radioactivity in the environment, the resulting exposure consequences remains below a pre-defined regulatory limit (e.g. dose or risk criterion) to ensure that the facility is safe in case of a wide range of events [5][6]. The different scenarios are categorized based on their probability of occurrence such as normal operation, design basis conditions (DBCs) and design extension conditions (DECs) [7][8]. It is imperative that these assessments are transparent and well documented to enable comparison of the safety of different installations.
b) In nuclear emergency preparedness and response, atmospheric dispersion calculations have a crucial role in decision support systems (DSSs). These computations aim to provide estimations in the event of a real releases based on which recommendations can

be made regarding countermeasures to ensure the protection of the public [2][9]. Given that the decisions are based on these estimations, the estimated results (i.e. environmental contamination and resulting effect on the population) need to be reliable and robust. Estimations are made to support decision making both in the preparedness phase when response plans are being elaborated and during the early phase of a major accident when the extension of urgent countermeasures based on plant conditions is examined. It is important to point out that during the early phase of an emergency situation, there is a limited amount of information available about the release and the meteorological conditions. In these assessments, the atmospheric dispersion calculations rely only on the predictions about the environmental conditions such as meteorological data from weather prediction models.

1.1. Key challenges in atmospheric dispersion calculations

1.1.1. Challenges related to the approaches to be used in atmospheric dispersion calculations

Deterministic safety assessments are conducted with the goal of verifying compliance with safety requirements, and the analysis must show that in case of a wide range of operating conditions of the nuclear power plant the consequences do not exceed a given criterion (which be different for various operating states). Based on the 2009 IAEA Specific Safety Guide [10], it is necessary to define the acceptance criteria so that it can be shown that the operation of a given unit is in compliance with the safety requirements. If the criteria are related to dose of members of public, appropriate methods of environmental transport calculation and dose estimation are required. Different acceptance criteria can be assigned to events with various probabilities of occurrence, with higher incidence rates being subject to lower dose criteria [11]. There are different approaches and models utilized in deterministic safety assessments of releases from a nuclear facility around the world, as there are no harmonized requirements for the specific details of application of the concept. Even though there are international guidance and various national regulations aimed at avoiding accidents that could lead to large or early radioactive environmental release, e.g. the Council Directive 2014/87/Euratom [12], these do not oblige the countries to adopt identical methodologies. It would be beneficial to have harmonized methodologies for such calculations, allowing the safety of nuclear facilities to be evaluated on the same basis worldwide. To support this harmonization effort, a simplified and easy-to-use computational methodology has been developed in the last decade in the Centre for Energy Research so that compliance with atmospheric release criteria for nuclear facilities can be confirmed. The main novelty of the method is that with appropriate boundary conditions the released source term, the environmental transport and the exposure can be separated and computed independently. As the transport and the exposure is only dependent on external conditions and features of the site and generally do not change considerably for longer time periods, these can be computed only periodically and regarded to be constant otherwise. For a specific site, these can be updated during periodical safety analysis review of a facility e.g. once every 10 years, or when there is a significant change in the meteorological conditions or the characteristics of the population. (The developed method is described in more detail in Annex I.) This methodology has eventually been incorporated into the CARC (Calculating Atmospheric Release Criteria) software, which, however, needed to be validated and its practical applicability to be verified. I joined this work and participated in the implementation of these methods into the software. In Section 3, I describe my work that I carried out relating to deterministic safety assessment and present my results. .In Section 3.1 I show the validation of the newly developed methodology through the comparison of the internal results of the models integrated in the CARC code with the corresponding values computed with widely used and accepted commercially available programs, namely with PC-COSYMA [13] and MicroShield [14]. . I describe in Section 3.2 the verification of the practical applicability of the new methods through a hypothetical case study. In addition to the investigation of the uncertainties of atmospheric dispersion modelling, in Section 3.3, I present the sensitivity assessment of the exposure calculation module of the CARC code to habit characteristics such as exposure parameters and food consumption data.

Regarding the decision support systems, various methods can be used to calculate the dispersion of the contaminants in the atmosphere, and the difference between these also need to be evaluated as they can have a great influence on the final results of the calculation. With these type of assessments, the goal is to estimate consequences as precisely as possible which requires detailed calculations. However, there is a need to communicate the results promptly, which limits the computation time and restricts the complexity of the model. Hence, an optimum is needed to be found between the complexity allowing precise results and simplicity supporting fast data provisions. During my work, I joined the development of the SINAC (Simulator Software for Interactive Modelling of Environmental Consequences of Nuclear Accidents) [15][16] decision support system which has been developed by my research group at the Centre for Energy Research (CER) and has been used in the Hungarian Atomic Energy Authority's Centre for Emergency Response, Training and Analysis (OAH/HAEA CERTA). To optimize the atmospheric dispersion calculation, new methods have been implemented in SINAC to compute the propagation of the contaminants that are released from a nuclear power plant. In order to evaluate these new methods, a comparison of their influence on the environmental activity concentrations is required. The goal of the assessment was to identify which method produces the most precise result but with the additional consideration of the computation time which is limited in case of such simulations. I present the details of these evaluations in Section 5.

1.1.2. Challenges related to the input parameters to consider in atmospheric dispersion calculations

The evaluation of uncertainty (both parameter and model uncertainty) in atmospheric dispersion and dose calculation has been an important topic in the last couple of years (e.g. [17][18][19]).

In atmospheric dispersion modeling, the attributes of the release point and site specific meteorological conditions and environmental characteristics should be taken into account. In the atmospheric dispersion modeling for deterministic safety assessments, it should be assumed that during and after the emission, unfavorable meteorological condition exists [11]. The assessments are carried out for single scenarios which are characterized by conservative input parameters (e.g. release characteristics, meteorological conditions, exposure duration and habits of the population), and the atmospheric release is usually considered to be continuous from a point source. For this type of calculation, the stationary Gaussian plume model is the most suitable atmospheric dispersion model that applies meteorological input parameters that are constant over time (i.e. for the time interval of the release) and spatially uniform.

To ensure conservativity in the calculations using input parameters that describe the worst case scenario is straightforward in case of an initiating event of the accident (e.g. fuel damage can be considered for the highest possible number of fuel rods). However, when it comes to meteorological data, choosing a conservative scenario is more complicated. The worst meteorological characteristics differ depending on the distances and endpoints being considered. For instance, heavy rain around the release point is considered conservative if the receptor points are close to the release. However, as the distance increases, the doses decrease due to the washout resulting in less radioactive material to reach the receptor points located at larger distances.

Instead of relying on worst case meteorological scenario, an alternative approach is to use meteorological data from an extended time period (e.g. years) covering a wide range of conditions [6]. For example, the Regulatory Guide 1.145 of the American Nuclear Regulatory Commission [20] describes that concerning the meteorological data the directional dependence of the wind vector should be considered and a given percentile (99.5th) of the computed relative air concentrations for different meteorological conditions should be used as the final result. Similarly, a selected dose percentile (95^{th}) of the computations with different meteorological conditions was used for the definition of the acceptance criteria for the accidental releases from nuclear power in the European Utility Requirements [21]. Nevertheless, it is evident that there is no uniform procedure for selecting the percentile value, while it can significantly influence the variability of the results.

Regarding these types of assessments, two questions arise that I investigated in my thesis. Firstly, how does the variation in the meteorological data affect the results of deterministic safety analysis, and secondly how do different percentiles of the results respond to the variations. To demonstrate how these questions can be answered in case of a given nuclear facility, I conducted a study with the newly developed CARC software where I performed calculations using different subsets of a meteorological database compiled from real measurements and compared the values of various percentiles which I describe in Section 4. In Section 4.1 I compare the differences in the resulting doses when a real meteorological database or a hypothetical worst case meteorology is used. In Section 4.2, I evaluate different dose percentiles computed with a real, 5-years-long meteorological database with the goal of confirming that that using the 95^{th} percentile determined from a meteorological database as the final endpoint of the deterministic safety assessment provides robust results. Furthermore, I investigate how the imperfections of a one-year long meteorological database could affect the dose results of the calculations, to verify which percentile shows the lowest variation compared to the usage of the full, 5-year database in Section 4.3.

In decision support calculations, meteorological data covering a wide spatial domain with appropriate temporal resolution for the duration of the release and the atmospheric dispersion of the contaminants is required. Usually the source of such meteorological data is a numerical weather prediction (NWP) model, due to the limited availability of real meteorological measurements and observation [22][23]. The uncertainties of meteorological data obtained from NWP models are in the same order of magnitude as those of the meteorological measurements [24][25]. My research regarding the evaluation of meteorological uncertainties is described in Section 6. To assess the influence of meteorological uncertainties in the SINAC DSS, I conducted a sensitivity analysis by perturbing the meteorological parameters separately one by one. I describe the details of these assessments and my results in Section 6.1.

Another approach to assess the effect of the meteorological uncertainties on the results of decision support systems is to use ensemble meteorological data for atmospheric dispersion simulations. Meteorological ensembles consist of multiple sets of meteorological data produced by running the NWP model several times with slightly different initial conditions or parameter sets [26]. Using the ensemble meteorological data is advantageous because it inherently incorporates the meteorological uncertainties with their influence directly appearing in the results of the atmospheric dispersion calculations. Due to the large amount of data that is provided by the NWP models, the number of ensemble members that are generated is usually around 10. It is important to acknowledge that there is a disadvantage associated with using such meteorological data as well, namely the increased computational burden of running the simulations multiple times which is not optimal in an emergency situation. Despite this limitation, the method of using ensemble meteorological data to characterize the uncertainties has gained popularity in the last decade. For example, from 2017 to 2020 there has been an international project with the goal of identifying and reducing uncertainties in nuclear emergencies titled CONFIDENCE (COping with uNcertainties For Improved modelling and DEcision making in Nuclear emergenCiEs). The first workpackage of this project, investigated the influence of the input uncertainties of atmospheric dispersion and dose calculation models. The aim was to evaluate the uncertainties and assess how they propagate through the models by simulating the atmospheric dispersion of radioactive release scenarios in a series of case studies. The case studies were titled "Radiological Ensemble Modelling" (henceforth referred to as REM) due to the usage of ensemble input data.

I participated the first workpackage of this project. To be able to use the SINAC DSS in the uncertainty assessments, I integrated a new module into the software to consider not just one meteorological data but ensembles as well. I developed this new module in a way that made it possible to handle not just the meteorological ensembles used in the project but also the ensemble data that is produced by the Hungarian Meteorological Service (OMSZ). With the new module, I first conducted a simple case study considering a radioactive release from the Paks NPP with two meteorological scenarios provided for the site. I present these results in the first part of Section 6.2. In the second part of Section 6.2, I describe the main results of the "Radiological Ensemble Modelling" (REM) case study in which I participated with the developed SINAC DSS. As part of the CONFIDENCE project we also investigated how the atmospheric dispersion and dose calculations could be optimized in order to be sufficient for operational usage. I made assessments as part of this investigation and show my results in Section 6.3.

In Section 7, I summarize my thesis and describe my thoughts about the future of these topics.

2. METHODS

In this section I give a general overview of the atmospheric dispersion, deposition and dose calculation models available in the literature and describe in more detail those which I used in my thesis.

2.1. Atmospheric dispersion models

There are various atmospheric dispersion models that can be used to simulate the spread of radioactive contaminants in the atmosphere for different types of nuclear assessments depending on their goals, calculational approaches and applicability ranges. In my thesis, the distance of application ranged from a couple of kilometers to several 10 kilometers from the point of emission (without the consideration of building effects). The most widely applied atmospheric dispersion models are the box model, the particle model and the Gaussian plume and puff models [27]. In the following subsections, I provide brief summary of the box model and particle model, and give more detailed information about the Gaussian plume and puff models which I used in my work presenting the basic equations of these.

2.1.1. Box model

In the box or compartment model, the space in which the particles move is divided into compartments and it is assumed that the contaminants are uniformly mixed within them. The equations of the atmospheric dispersion are solved for each compartment for a given time step, and the activity concentration is determined by the number of particles within and the volume of the box. The concentration is the same at all points within a compartment (grid element) at the same time. The compartments can be distributed or re-distributed based on the geographic coordinate system or the coordinate system can be fixed to the release point. With a coarse spatial resolution, the compartment model is suitable for characterizing large-scale atmospheric dispersion and with a fine spatial resolution the model can also be used for providing more precise calculation, however a higher resolution requires more computing capacity. Compartment models are used to characterize both short-term and long-term releases with a grid network of 1–5 km at the urban scale and 10–50 km at the regional scale [28].

2.1.2. Particle model

In the particle or trajectory model (also widely mentioned as Lagrangian models), the dispersion in the atmosphere is characterized by following the movement of a large number of particles representing air parcels which move along flow trajectories determined by the meteorological parameters. The activity concentration can only be determined from the distribution of a large number of particles examined at given times, therefore a large number of trajectories must be computed. An advantage of this model is that as the particles are not linked to a spatial element, the result can be projected to any resolution. Particle models are primarily used for modeling long-range and mesoscale propagation, however, since greater computing capacity became available, they are increasingly used to describe atmospheric dispersion on a local scale. The most well-known particle models used in the nuclear field are the open-source FLEXPART [29] and HYSPLIT [30], and NAME [31].

2.1.3. Gaussian plume model

The Gaussian plume model [32] is suitable for characterizing the effect of emissions from a point source that can be considered either instantaneous or constant in time. The spatial distribution of the activity concentration of the released material can be described by a two-dimensional Gaussian function considering advection and diffusion as the main processes governing dispersion. In this range the modifying effects of chemical transformations, the topography (such as the different characteristics of land and water surface) can usually be omitted. The plume model assumes a constant wind vector in a fixed direction during propagation (along the x-axis) and takes into account the advection in this direction, while the diffusion is described by vertical and horizontal dispersion parameters (σy, σz) perpendicular to the wind direction. Such a model is used for the atmospheric dispersion calculation in the CARC software [33] and the PC-COSYMA program package [13].

The time-integrated activity concentration of a given nuclide at a specific point can be determined with the Gaussian plume model as follows:

$$C_{air,i}(x,y,z) = \frac{Q_i}{u} \cdot \frac{1}{2\pi\sigma_y\sigma_z} \exp\left(-\frac{(y-y_p)^2}{2\sigma_y^2}\right) \cdot \sum_{n=-N}^{N} \left\{ \exp\left[-\frac{(z-H+2nL)^2}{2\sigma_z^2}\right] + \exp\left[-\frac{(z+H+2nL)^2}{2\sigma_z^2}\right] \right\} \cdot \exp^{-\lambda_i \cdot t} \tag{1}$$

where

$C_{air,i}$ time-integrated activity concentration of isotope i [Bq s/m^3],
x, y, z are the coordinates [m],
Q_i released activity of isotope i [Bq],
$t = x/u$ the time from the start of the release [s],
u wind velocity in direction x [m/s],
$\sigma_y(x)$ horizontal dispersion parameter [m],
$\sigma_z(x)$vertical dispersion parameter [m],
y_p distance of plume centreline from axis z [m],
H distance of plume centreline from ground level [m],
L inversion layer height [m],
N number of reflections considered from the ground and the inversion layer,
λ_i decay factor of isotope i [1/s].

A scematic vizualization of the Gaussian plume model can be seen in Figure 1.

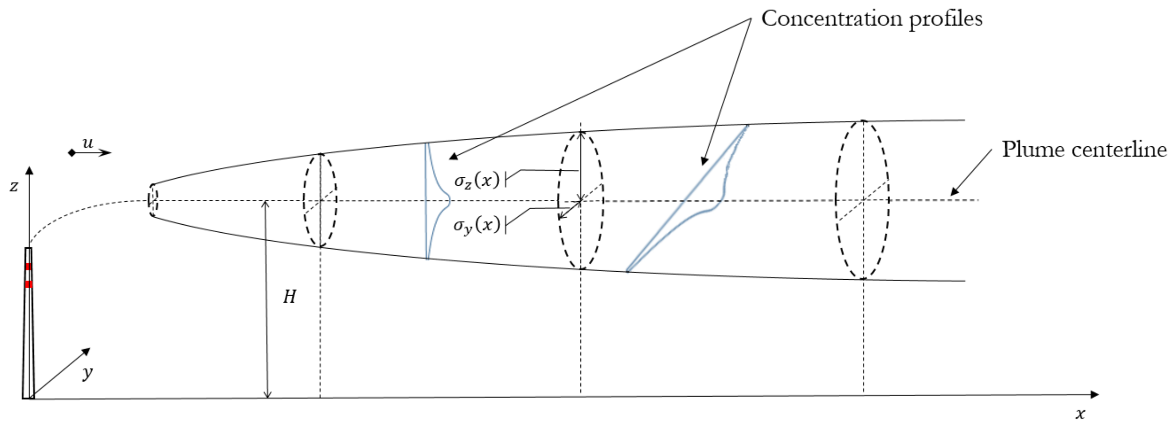

Figure 1. A schematic visualization of the Gaussian plume model

To simplify the computation, the y axis of the grid can be fixed to the release point thus $y_p = 0$. Due to the heat flux of the released material, the initial release height can differ from the distance of the centerline of the plume from ground level. This difference is the plume rise which can be computed with various models (for further details about the plume rise models see [34]). As a simplification, the plume rise can be neglected and an effective release height can be assumed to be equal to H, regarded as an input parameter for the computation (e.g. in the CARC software).

The dispersion of pollutants is mainly determined by the stability of the atmosphere. Under unstable atmospheric conditions, the dilution and mixing of plume is faster, whereas under stable stratification this process is slower. Atmospheric stability can be characterised by several methods, one of which is the Pasquill stability classification system [35]. This method distinguishes between six different stability categories: extremely unstable class A, moderately unstable class B, slightly unstable class C, neutral class D, slightly stable class E and stable class F. An advantage of this method is that it very simple and that the stability categories can be determined based on routinely measures meteorological quantities such as the near-surface wind speed (measured at 10 m), incoming solar radiation and ratio of cloud coverage. According to this method, the dispersion parameter values are dependent on the distance from the release point along the wind direction and can be calculated from the stability categories using the fllowing empirical formulae:

$$\sigma_y(x) = ax^b \tag{2}$$

$$\sigma_z(x) = cx^d \tag{3}$$

where a, b, c and d diffusion constants based on Pasquill parametrization with values taken from selected literature (e.g. [36][37] in case of PC-COSYMA and CARC).

The time dependence of the release is considered by splitting the total duration into time periods. At the kth time period, an instantaneous release is considered with the activity integrated over the given time period as follows:

$$Q_i^k = \int_{t_{k-1}}^{t_k} q_i(t)\mathrm{d}t \tag{4}$$

where

$t_k - t_{k-1} = \Delta t$ is the length of the time step [s],
$q_i(t)$ is the time dependent release rate for nuclide i [Bq/s].

The time-integrated activity concentration is computed for each time step and considering the release to be instantaneous at time k with released activity of Q_i^k. In practice the release is considered to change hourly, so Q is considered as cumulative value for every hour and is released instantaneously.

The consideration of very low wind values – where linear (Darcy) velocity of the diffusion is assumed to be lower than the advection – is problematic in the Gaussian plume model, as the wind speed is in a reciprocal position in the formula, causing near-zero values to result in unrealistic concentration. A method to address this is to expand the horizontal dispersion parameter with the ratio of minimum threshold of the measurement system and the measured wind speed as follows [38]:

$$\sigma_y(x) = a(x \cdot \frac{u_c}{u})^b \tag{5}$$

where a and b are the coefficients of the horizontal dispersion parameter, x is the distance from release point u_c is a constant [m/s] representing the minimum wind speed threshold of the measurement system, u is the measured wind speed [m/s]. The parameter of the wind speed threshold can be changed based on the meteorological measurement system but a default value of 0.5 m/s can be considered (like in the CARC software) taken as the starting threshold of a Vaisala WA15 wind vane [39].

The meteorological input data requirement of the method are the following parameters for the release location: wind vector, precipitation intensity, Pasquill category, inversion layer height. The meteorological data is assumed to be temporally and spatially constant for one simulation of release but it is also possible to consider the time dependence of the meteorological data by dividing the emission into stages, assuming that each stage is instantaneous within the given time period. However, the spatial dependence of the input data cannot be taken into account in the model. The plume model cannot be used in the immediate vicinity of the emission point or at a great distance from the emission point due to the high degree of uncertainty of the result, thus the reliable application distance of the plume model is between a few kilometers and a few tens of kilometers [40].

2.1.4. Gaussian puff model

The Gaussian puff model [41] assumes that the contaminants are released instantaneously, in packages called puffs at given times. The dispersion of the contaminant is characterized by several puffs with a spatial distribution of a three-dimensional Gaussian function determined by the vertical and horizontal dispersion parameters (σx, σy, σz). The instantaneous position of each puff is characterized by the trajectory, which is determined by the wind vector field around the release point. The time-dependent activity concentration at a location is determined by the superposition of all of the puffs in the vicinity. The influence of the reflection from the inversion layer and the ground can be taken into account which modifies the symmetry of the Gaussian function. A well-known example of the Gaussian puff model is the RIMPUFF model [42] developed by the Technical University of Denmark (DTU) and used in the JRODOS system (Real-time On-line Decision Support System) [43]. The SINAC decision support system [16] also applies a Gaussian puff model to compute the spread of radioactive material released to the atmosphere from a nuclear power plant.

The activity concentration of a given nuclide at a specific time and point can be calculated with the Gaussian puff model as follows:

$$C_{air,i}(x,y,z) = \frac{Q_i}{(2\pi)^{3/2}\sigma_r^2\sigma_z} \exp\left(-\frac{(x-ut)^2+(y-vt)^2}{2\sigma_r^2}\right) \cdot \sum_{n=-N}^{N}\left\{\exp\left[-\frac{(z-H+2nL)^2}{2\sigma_z^2}\right] + \exp\left[-\frac{(z+H+2nL)^2}{2\sigma_z^2}\right]\right\} \cdot \exp^{-\lambda_i t} \tag{6}$$

where

$C_{air,i}$ time-integrated activity concentration of isotope i [Bq/m^3],
x, y the horizontal distances from the release point [m],
z the height above the ground level [m],
Q_i the activity of isotope i in the given puff [Bq],
σ_r horizontal dispersion parameter [m],
σ_z vertical dispersion parameter [m],
u, v components of the wind vector in x and y direction [m/s],
t time from the start of the release [s],
H distance (height) of plume centerline from ground level [m],
L inversion layer height [m],
N number of reflections considered from the ground and the inversion layer,
λ_i decay factor of isotope i [1/s].

A scematic visualization of the Gaussian puff model can be found in Figure 2.

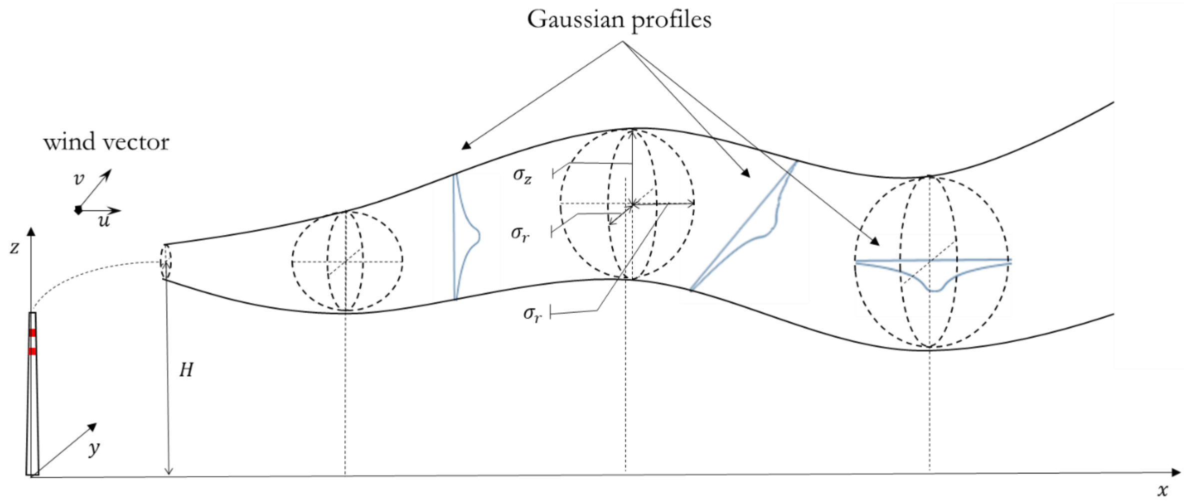

Figure 2. A schematic visualization of the Gaussian puff model

Similarly to the Gaussian plume model, the dispersion parameters are dependent on the distance from the release point.

Modifications can be included in the model to consider the effect of the buildings or the topography. For example, the modifying effect of the surface roughness on the vertical dispersion of the puffs can be taken into account with a correction factor for the vertical dispersion parameter:

$$\sigma_z = \zeta \cdot c\, r^d \tag{7}$$

where $r = \sqrt{x^2 + y^2 + (z - H)^2}$ is the distance from the release point [m], $\zeta = (z/z_0)^{0.2}$ is the correction factor, z characterizes the roughness of the surface and can take various values depending on the type of surface and z_0 is a constant (in SINAC, the default of these are z = 30 cm, and z_0 = 3 cm) [16][44].

A limitation of the model is that – similarly to the Gaussian plume model – its application distance ranges between a few kilometers and a few tens of kilometers, however with appropriate modifications and corrections it can be used at closer or at greater distances. An advantage of the model is that it can consider spatial and temporal variation of meteorological parameters while enabling relatively fast calculation. This aspect of the model makes it suitable to be used for emergency preparedness and response calculations in decision support systems [28].

2.2. Deposition model

The ground activity concentration is the sum of the material deposited by dry deposition (fallout) and wet deposition (wash-out). The dry deposition can be simply computed as a proportion of the air activity concentration on ground level with the following equation:

$$D_{dry,i}(x, y) = v_{dep,i} C_{air,i}(x, y, 0) \tag{8}$$

where

$C_{air,i}(x, y, 0)$ time-integrated activity concentration on ground level [Bq s/m^3],
$D_{dry,i}(x, y)$ deposited activity by dry deposition [Bq/m^2],
$v_{dep,i}$ deposition velocity [m/s].

With this formula, it is assumed that the deposition velocity contains the effects of gravity impaction and diffusion (for more detail see [45]). This deposition scheme is applied in the CARC, PC-COSYMA and SINAC programs. The deposition velocity depends on – among other parameters – the chemical form of the radionuclides and the size of the particles with radioactive content, usually these can be specified as input parameters. In consequence assessment codes, due to the need for limiting the computational burden, it is common practice to consider only the chemical form of the nuclides via four categories, namely noble gasses, aerosols, and the elemental and organic form of iodine (e.g. in PC-COSYMA, CARC, SINAC and JRODOS). Even though the dry deposition occurs near ground level, according to the source depletion model, the distribution of the air activity concentration can be assumed not to be affected by the deposition in order for the Gaussian distribution to be valid, and the deposited amount can be uniformly subtracted from the vertical profile of the radioactive cloud (plume or puff) [46]. This simplification is considered in CARC and SINAC software.

Wet deposition can be modelled with the well-known and commonly used exponential washout function [47], which expresses how much activity is washed from the plume due to precipitation:

$$\varepsilon_w = 1 - exp^{-\lambda_w \Delta t} \tag{9}$$

where

ε_w washout fraction [-],
$\lambda_w = \alpha \cdot p^{\beta}$ scavenging coefficient [1/s], α, β linear and exponential factors,
p precipitation intensity [mm/h],
Δt time it takes the radioactive material to reach the receptor point [s].

The linear and exponential factors can take different values depending on the type of precipitation (e.g. rain or snow) or if the scavenging occurs in or below the cloud. The values of these two factors are determined based on measurements and can usually be specified as input parameters in computer programs as in CARC, PC-COSYMA and SINAC.

2.3. Dose calculation models

2.3.1. Dose quantities

The dose quantities that are used in radiation protection and dose assessments are the absorbed dose, equivalent dose, effective dose and committed dose. The absorbed dose D [Gy] is the mean energy ($\mathrm{d}\bar{E}$ [joule]) of the ionizing radiation that is imparted in unit mass ($\mathrm{d}m$ [kg]):

$$D = \frac{\mathrm{d}\bar{E}}{\mathrm{d}m} \tag{10}$$

In radiation protection the energy of the radiation is averaged over specific organs or tissues. The equivalent dose (H_T [Sv]) is the absorbed dose of a specific tissue (T) or organ summed up for various types of ionizing radiation (R) (i.e. alpha, beta, gamma and neutron) taking into account their biological effect (their ability to damage human cell DNA causing stochastic radiation effects) with the radiation weighting factor (w_R):

$$H_T = \sum_R w_R \cdot D_{T,R} \tag{11}$$

The radiation weighting factor refers to the stochastic effects of radiation and its value is determined based on the relative biological effectiveness. The effective dose (E [Sv]) is the averaged equivalent dose summed up for the human body considering the different radiation vulnerability of the various tissues and organs with the tissue weighting factor (w_T):

$$E = \sum_T w_T \cdot H_T \tag{12}$$

The tissue weighting factors represent the relative contribution of the specific tissues and organs to the total radiation detriment assumed to be uniformly irradiated ($\sum w_T = 1$) and the values are averaged for both sexes and all ages. The committed dose is the dose that is received from the incorporated radionuclides within a specific time period (τ) starting from the intake (t_0). The committed equivalent dose ($H_T\ (\tau)$) is the time integral of the equivalent dose rate for a given tissue or organ, and the committed effective dose is:

$$E(\tau) = \sum_T w_T \cdot H_T\ (\tau) = \sum_T w_T \int_{t_0}^{t_0+\tau} \dot{H}_T\ (t)\mathrm{dt} \tag{13}$$

The commitment time is 50 years for workers and adult members of the public, and 70 years for children and infants [48].

The dose conversion factors (DCFs) or internal dose coefficients describe the effective dose per unit intake. The DCF values are determined based on biokinetic models and computational phantoms that have been continuously developed. The expression of "dose factors" is usually used for external coefficients that connect a dose quantity (dose rate) with unit activity or activity concentration of a given nuclide at a specific location, frequently marked as k_γ. The DCF and k_γ values are computed for the various radionuclides, types of exposure, age groups and for workers and members of the public.

For external exposure, the latest dose coefficient values are published in the ICRP Publication 116 [49] which were determined based on the recommendations and models of the ICRP Publication 103 [50]. The values differ only slightly from those in the previous ICRP Publication 74 publication [51] (the difference does not exceed 20-30%) due to the use of new computational phantoms and the higher gamma energy range from 0.01 MeV to 10 GeV. The coefficients are provided in the document for various idealized irradiation geometries with the radiation incident on the front of the body (antero-posterior), on the back of the body (postero-anterior), on the either side of the body (left lateral and right lateral), rotating at a uniform rate around the body (rotational) and assuming a radiation field with an angle that is independent of direction and location in space (isotropic). At the time of my work, the ICRP Publication 116 was the latest available document containing the dose coefficients, but since then, the ICRP Publication 144 [52] was published containing effective dose, ambient dose equivalent, and air kerma rate coefficients for external exposure from soil contamination, air submersion and water immersion.

Regarding the DCFs for internal exposure, the most current values are published in the IAEA General Safety Requirements Part 3 [53], which considered the recommendations and models of the ICRP Publication 103 [50] and contains the DCFs for ingestion and inhalation for workers, and for the members of public for six age groups.

2.3.2. International and national requirements related to dose quantities

The EUR Association, an organization formed by the major European electricity producers developed the European Utility Requirements (EUR) [21], a common specification for new fission reactor designs proposed by vendors in Europe. I note that here, I describe the details of the EUR version D published in 2012, but the newest, version F is currently being developed. The purpose of this document is to introduce a clear, complete statement of the utilities' expectations for 3rd generation nuclear power plants for the promotion of harmonization in requirements across Europe and worldwide. The EUR propose acceptance criteria for the release in relation to its dose consequences and thus eliminate the uncertainties arising from the calculation of the dose. Acceptance criteria for Design Basic Conditions 3 and 4 (DBC-3 and DBC-4) and Design Extension Condition (DEC) cases are defined. Release coefficients representing the environmental consequence of unit emission are defined for a maximum of 9 reference isotopes (Xe-133, I-131, Cs-137, Te-131m, Sr-90, Ru-103, La-140, Ce-141, Ba-140). The reference isotopes are key nuclides, nuclide groups containing all the isotopes that have similar physical and radiochemical properties. Different release coefficients apply for emissions through the building at ground level and stack releases. To verify the fulfillment of the acceptance criteria, the product of the release quantities of the reference nuclides and these release coefficients need to be evaluated and compared with the criteria depending on the DBC or DEC category. The verification of the fulfillment of the acceptance criteria for DBC-3, DBC-4 and DEC can be determined as follows:

$$A_{crit} > \sum_{i=1}^{n} R_{ig} \cdot C_{ig} + \sum_{i=1}^{n} R_{ie} \cdot C_{ie} \tag{14}$$

where A_{crit} is the acceptance criteria, R_{ig} and R_{ie} is the cumulative released activity of nuclide i at ground level (g) and stack level (e), respectively. The release coefficients C_{ig} and C_{ie} are given for each considered nuclide (i), for ground level (g) and stack level (e) emissions, which are available in the EUR document [21]. n is the number of nuclides needed for the calculation of the criteria which differs for the DBC and DEC cases. The different characteristics of the accident (e.g. the relative quantities of isotopes and the duration of releases) require the definition of a new set of coefficients. The acceptance criteria, the number of key nuclides and the time interval for the cumulated released activity for DBC and DEC cases are summarized in Table 1.

Table 1. Summary of the DBC and DEC acceptance criteria [21]

	Number of key nuclides (n)	Acceptance criteria (A_crit) [mSv]	Time interval for the cumulated released activity
DBC-3	3 (Xe-133, I-131, Cs-137)	1	the entire release time
DBC-4		5	the entire release time
DBC economic consequences	2 (I-131, Cs-137)	*	the entire release time
DEC criteria no. 1)	9 (Xe-133, I-131, Cs-137, Te-131m, Sr-90, Ru-103, La-140, Ce-141, Ba-140)	50	first 24 hours
DEC criteria no. 2)		30	first 4 days
DEC criteria no. 3)		100	the entire release time
DEC criteria no. 4)	3 (I-131, Cs-137, Sr-90)	*	the entire release time

* The acceptance criteria for economic effects is expressed with release quantities of the key nuclides given in Bq.

For events exceeding the design basis (turning to DEC from DBC), the emissions are limited by the fulfillment of the Criteria for Limited Impact (CLI) containing four independent targets (projected dose of the representative members of the public) for which the goal is not to exceed the value

1) which would justify the introduction of urgent countermeasures beyond 800 m;
2) which would justify early phase countermeasures (evacuation) beyond 3 km;
3) which would require late phase countermeasures (relocation) beyond 800 m;
4) which would require significant economic consequences (food and feed bans limited in space and in time).

The value of the first DEC acceptance criterion is the intervention dose criterion for evacuation (50 mSv). As the goal is to avoid the introduction of early countermeasures beyond 800 meters, the limit refers to the cumulative released activity over the first 24 hours of the release. It is important to note that these criteria are applied in the planning and siting process of a future NPP. Value of the second acceptance criterion is the intervention dose criterion for temporary relocation (30 mSv). The limit (to avoid intermediate phase countermeasures beyond 3 km) refers to the cumulative released activity over the first 4 days of the release. Value of the third DEC acceptance criterion is 100 mSv calculated for the total cumulated activity for the entire release. The fourth DEC acceptance criterion is based on the economic consequences, which is given for 3 key nuclides and for the cumulated activity over the entire release time. For the definition of the release limits and coefficients, several assumptions were taken into account such as the meteorological conditions were chosen to be characteristic for most of the European sites, the 95th percentile dose values of the probabilistic calculation were used and constant emissions were assumed in time from the end of the 1st hour to the times indicated in Table 1.

Similarly to the EUR criteria, in the IAEA Safety Standard No. GSR Part 7 "Preparedness and Response for a Nuclear or Radiological Emergency" [54], the safety requirements are also linked to protective measures. However, on the contrary to previous publications, the projected dose is introduced instead of the avoidable dose. The recommends setting an appropriate reference level for major emergencies and document provides generic criteria not only for doses for which protective actions and other response actions are expected to be undertaken under any circumstances in case of emergency to avoid or to minimize severe deterministic effects, but also for doses for which protective actions and other response actions are expected to be taken, if they can be taken safely to reasonably reduce the risk of stochastic effects. Such generic criteria are – among other values – 100 mSv projected effective dose in the first 7 days for urgent protective action and 100 mSv projected effective dose in the first year for early protective actions, deduced from a reference level of 100 mSv per event that shall not be exceeded considering all exposure routes together.

The IAEA also describe general principles of radiation protection and within, methods for determining release criteria and dosimetric quantities for the verification of compliance. According to the 2009 IAEA Specific Safety Guide [10], it is necessary to define the acceptance criteria to enable the verification that the operation of a given unit is in compliance with the safety requirements. The criteria may apply to emissions, in which case the most important volatile radionuclides (e.g. noble gases, iodine and cesium isotopes) must be taken into account. In atmospheric dispersion modeling, the attributes of the release point and site specific meteorological conditions and environmental characteristics should be taken into account. In general, it should be assumed that during and after the emission, unfavorable meteorological condition exist [11]. Criteria should normally be defined without restriction on the food chain, at least for events with higher frequencies. Accordingly, the contribution of the consumption of foodstuff from the contaminated area must also be taken into account. Conservative approaches in the determination of public doses should be used for the exposure duration, weather conditions and habits (e.g. outdoors activities, breathing rate, food consumption, etc.). An IAEA document [55] describing the methods for determining population doses contains detailed recommendations for the data required for analysis.

There are documents published by the U.S. Nuclear Regulatory Commission (NRC) that also define requirements for calculating the consequences of radioactive releases. According to the RG 1.145 guide [17], the atmospheric dispersion calculation should be performed for 16 spatial sectors and the maximum relative air concentrations (χ/Q) for each sector should be determined. For this, the χ/Q values for each hour must be computed, then the 99.5th percentile for every sector must be calculated. The largest of these 16 values should be selected as the final result. Population doses can be determined on the basis of the time integrated activity concentration at the receptor point, taking into account the different exposure pathways. Based on RG 1.183 [56], the total effective dose equivalent should be taken into account for population doses, which is the sum of the committed effective dose equivalent from inhalation and the deep dose equivalent for external exposure. In the calculations, all the isotope and progenies should be considered. The guide also specifies the time period for which the calculations should be made. Differing from the European Utility Requirements, where the 95th percentile of the dose values is used as the criteria, here the 99.5th percentile is applied Due to considerable conservativism in the atmospheric dispersion model and the omission of several mechanisms such as the deposition of the radioactive material this difference is acceptable as the doses computed by this method will be higher compared to the criteria defined by the EUR which presents a calculation method with more realistic assumptions. Thus, this is in line with the higher acceptance criteria set out in Regulations 10 CFR paragraph 50.67. [57] as 25 rem (250 mSv) which is also higher than the dose criteria of the EUR. This difference highlights that the limit value for a specific criteria and the calculation process of verifying its fulfillment should be treated together, they are closely linked and are not interchangeable with other criteria and method for demonstrating complience.

In the Hungarian regulatory system, the Act CXVI of 1996 on Atomic Energy (Atomic Act) [58] stipulates to protect the health and safety of the public and the environment from the use of atomic energy. Section 4 point 3. c) and d) state that:“ It shall be ensured in the use of atomic energy that (…) c) the annual radiation exposure of the employees and the public from all sources shall not exceed the dose limit determined by the respective safety requirements, which incorporate the latest and justified scientific results and recommendations of the international and domestic professional organizations; radiation exposure shall be reduced to as low as reasonably achievable, and the maximum quantity determined in terms of physical or chemical or other properties, concentration and method of release of radioactive materials allowed to be released to the environment shall be regulated accordingly; d) the risk of occurrence of an extraordinary event shall be decreased, its occurrence shall be preventable, its consequences shall be eliminated in a planned manner, harmful effects of the potentially released radioactive material and ionizing radiation shall be decreased to the lowest reasonably achievable level.” [58]

The national dose criteria for accidental conditions are defined in the Nuclear Safety Codes, which are the Annexes of the Govt. Decree 118/2011. (VII. 11.) on the nuclear safety requirements of nuclear facilities and on related regulatory activities [59] (current versions: 1/2022. and 9/2022. HAEA decrees). The acceptance criteria for operating NPPs (according to point 3.2.4.0100.), requires the demonstration that the dose for a person of the reference group of the population does not exceed:

- the public dose constraint for processes originating from initiating events resulting in DBC2, and
- the 5 mSv/event value for processes originating from initiating events resulting in DBC4.

It is also stated that outside the controlled area of the NPP:

- DBC2 conditions shall not cause doses exceeding 1 mSv/event/person and
- DBC4 conditions shall not cause a dose exceeding 10 mSv effective dose or 100 mGy absorbed dose for the thyroid.

For new NPPs, the requirements are (according to point 3a.2.4.0100.) the demonstration that the dose determined for a person of the reference group of the population does not exceed:

- the value of the public dose constraint for processes originating from initiating events resulting in DBC2;
- 1 mSv/event for processes originating from initiating events resulting in DBC3, and
- 5 mSv/event for processes originating from initiating events resulting in DBC4 and DEC1.

Some aspects of these requirements are not completely clear in terms of the dose calculation. It is stated that the effective dose for a person of the reference group should be computed, but the characteristics of this group (e.g. age, habit) is not defined, and the duration of the exposure that needs to be considered is not specified either in this document. The group of the population for which the dose needs to be determined is called reference group but in the 2/2022. (IV. 29.) HAEA Decree [60] it is stated the dose of the critical population group shall be evaluated, which corresponds with the term "critical group", defined in the international terminology [61]. In addition, the wording "for a person of the reference group" is imprecise and does not indicate that the doses should be determined for a representative person. According to the above HAEA decree, the representative person is a person that receives a dose that is representative of the doses to the more highly exposed individuals in the population, except for individuals with extreme or rare habits. The representative person is usually not a real individual but a hypothetical construct defined for the purpose of verifying compliance with regulatory criteria [61]. According to these requirements, the consequences of DBC need to be computed for a reference person residing at a specific location, which means that in the atmospheric dispersion calculation, the consideration of the wind direction is essential and it can significantly influence the dose results. The characteristics of the representative person (i.e. the critical group) is defined for atmospheric releases and the Paks NPP operating in Hungary, as the 1-2 year-old children residing at the Csámpa puszta bus station, at a 1300 m distance.

In the Nuclear Safety Codes, the dose requirements for DEC are only defined for the new NPPs and not for the operating ones. However, these requirements are similar to the IAEA generic criteria [54] and the EUR CLIs [21] as follows:

"3a.2.4.0700. For the fulfilment of the criterion of limited environmental impacts, for events resulting in DEC1 and for events resulting in DEC2 (…), it shall be demonstrated that

a) no urgent protective measures are required beyond a distance of 800 m from the nuclear reactor;
b) there is no need for any kind of temporary action, i.e. the temporary evacuation of the population, beyond a distance of 3 km from the nuclear reactor;
c) there is no need for any kind of late protective action, i.e. the permanent relocation of the population, beyond a distance of 800 m from the nuclear reactor;
d) there is no need for any long-term restriction on food consumption." [59]

There is no indication in the Nuclear Safety Codes about what dose quantities are connected to the above protective measures. These dose criteria were included in the 16/2000 Ministry of Health Decree [62] (until their removal in 2018) defining the intervention levels for specific protective actions expressed in mean avertable effective (or equivalent) dose for a suitably selected group of the population:

- Intervention level for sheltering: effective dose of 10 mSv, in a period of no more than 2 days
- Intervention level for evacuation: effective dose of 50 mSv, in a period of no more than 1 week
- Intervention level for iodine prophylaxis: committed absorbed dose in the thyroid gland of 100 mGy
- Intervention level for initiating temporary relocation: effective dose of 30 mSv/month
- Intervention level for terminating relocation: effective dose of 10 mSv/month
- Intervention level for initiating permanent relocation: effective dose of 1 Sv/lifetime

As this part of the decree is not in force any longer, the document that details the dose quantities connected to the countermeasures is the National Nuclear Emergency Response Plan (OBEIT) [63]. In the OBEIT, the reference levels are given as the projected dose without applying protective measures) in line with the IAEA generic criteria [54]. The reference levels defined as effective dose:

- for urgent protective actions (that can be connected to point 3a.2.4.0700 a) of the Nuclear Safety Codes) is 100 mSv effective dose for the first 7 days;

- for protective actions in the late phase (that can be connected to point 3a.2.4.0700 c) of the Nuclear Safety Codes) is 20 mSv/year effective dose (in the first year, excluding the first 7 days);
- for restrictions of food and drinking water (that can be connected to point 3a.2.4.0700 d) of the Nuclear Safety Codes) is 10 mSv/year effective dose (in the first year).

There are no reference levels defined in the OBEIT for temporary relocation (which could be connected to point 3a.2.4.0700 b) of the Nuclear Safety Codes). In addition to the effective dose, other reference levels are defined as equivalent dose for fetus and thyroid as well. These criteria aim to reduce the risk of stochastic effects, so their fulfillment also implies the minimization or avoidance of the deterministic effects which occur due to much higher radiation exposure.

2.3.3. Exposure pathways

The radiation exposure of the population due to radioactive release to the atmosphere from nuclear facilities can occur through various pathways. These pathways are

- cloudshine: external radiation from the radioactive plume,
- groundshine: external radiation from the radioactive material deposited on the ground from the plume,
- inhalation: internal radiation from inhaling the radioactive material from the plume directly or resuspended from the ground deposition,
- ingestion: internal exposure from ingesting radioactive material from foodstuff that was produced in a contaminated area (contamination due to direct deposition from the air onto the plant surface, intake from the soil, or contaminated feed for domestic animals),
- pathways of minor significance, e.g. skin contact dose or incorporation through wounds, etc.

Exposure from liquid emission is excluded because in most cases contribution to public doses is significantly lower with several orders of magnitude difference than the doses from atmospheric releases.

2.3.3.1. Cloudshine

The cloudshine is the external exposure due to the plume of the released radioactive material, which can be computed based on the concentration of activity of the plume in the vicinity of the receptor point as follows:

$$\Delta_i^{cl} = \left[\int_{t=0}^{\tau} \int_{t'=0}^{t} q_i \cdot \left(\frac{\chi}{Q}\right)_{i,cloud}^{V} \cdot \Gamma_{i,cloud}^{V} \, dt' dt \right] \cdot w_{i,cloud} \tag{15}$$

where:

Δ_i^{cl}: effective cloudshine dose from nuclide i [Sv],

q_i: rate of nuclide i [Bq/s],

$\left(\frac{\chi}{Q}\right)_{i,cloud}^{V}$: air activity concentration of nuclide i in the plume centreline for unit release [(Bq/m^3)/(Bq)],

$\Gamma_{i,cloud}^{V}$: dose factor for cloudshine [(Gy/s)/(Bq/m^3)],

t: exposure time [s],

τ: release time [s],

$w_{i,cloud}$: special radiation weight factor of nuclide i for unit absorbed dose due to the plume passage [Sv/Gy].

The unit of χ/Q is different from the generally used [(Bq/m^3)/(Bq/s)], because the time dependence of the source term can be taken into account by splitting the release duration into time periods as shown in Eq (4). If the release rate is constant throughout the entire duration of the discharge, the total released activity is:

$$Q_i = \int_0^{\tau} q_i(t)\mathrm{d}t = q_i \cdot \tau \tag{16}$$

The dose factor for cloudshine can be summed for the energy lines of the nuclide in question with consideration of linear attenuation of photons and build up in air:

$$\begin{aligned} \Gamma_{i,cloud}^{V} &= \sum_j K(E_j) \cdot \int_V F_j^V(R)\, dV \\ &= \sum_j K(E_j) \cdot \int_V \frac{e^{-\mu_j R}}{4\pi R^2} \cdot B_j(\mu R) \cdot f_j \cdot \left(1 \frac{\mathrm{Bq}}{\mathrm{m}^3}\right) dV \end{aligned} \tag{17}$$

where

j: is the number of energy lines for a given nuclide,

$K(E_j)$: absorbed dose per fluent for photon with energy E_j [Gy·m^2],

$F_j^V(R)$: volume fluent of photon with E_j energy from dV volume at distance R in air per unit air activity concentration [(1/ m^2)/(Bq/m^3)]

μ_j: linear attenuation factor for E_j in air [1/m],

R: is the distance of dV from the receptor point [m],

$B_j(R)$: build-up factor for E_j energy in air [-],

f_j : is the probability of emission of photon with E_j energy [-].

The unit air activity concentration [Bq/m^3] can be translated to the release of 1 photon/sec in a unit of air volume, thus the unit of the fluent can be considered to have a unit of (1 photon/m^2)/(1/s/m^3). The fluent in Eq. (17) can be precomputed based on a semi-infinite cloud model [63][65] assuming that the activity concentration in air around the receptor point is uniform and equal to the values at the receptor point. The semi-infinite cloud model – in some cases supplemented with correction factors – is applied in many consequence assessment codes, including MACCS [66], PC-COSYMA [13] as well as SINAC [16] and CARC [33]. In the CARC software these fluents are determined for a range of energies (from 30 keV to 15 MeV) by considering a large 5 km high cylinder with 20 km radius containing uniform 1 Bq/m^3 activity concentration of the nuclide in question. The receptor point was defined in the middle of the cylinder at 1m height and the numerical integration of the cylinder was started from a radius of 25 cm. The steps of the spatial integration and the size of the cylinder was chosen so that making the resolution denser or the size larger does not cause more difference in the resulting fluent than 1%. The dose factor for cloudshine was computed for each energy line of the radionuclides with interpolation of the precomputed fluent values multiplied with the appropriate absorbed dose factor. The absorbed dose per fluent for photon values are taken from the ICRP Publication 116 [49]. The energy lines and the attenuation factors were taken from widely used online databases [67][68].

The semi-infinite cloud model significantly simplifies the actual characteristics, however with this assumption, the dose from the cloud can be computed with a simple multiplication of a dose factor and the local activity concentration. This simplification is more valid further from the discharge point where the spatial change in air and ground activity concentration is slower around the receptor point.

2.3.3.2. Groundshine

The groundshine dose is the external exposure from the radioactive material deposited on the ground from the plume which can be computed based on the ground activity concentration as follows:

$$\Delta_i^{gr} = \left[\int_{t=0}^{\tau} \int_{t'=0}^{t} q_i \cdot \left(\frac{\chi}{Q}\right)_{i,ground}^{A} \cdot \Gamma_{i,ground}^{A} \, dt' dt \right] \cdot w_{i,ground} \tag{18}$$

where:

Δ_i^{gr}: groundshine dose from nuclide i [Sv],

q_i: release rate of nuclide i [Bq/s],

$\left(\frac{\chi}{Q}\right)_{i,ground}^{A}$: is the ground activity concentration of nuclide i for unit release [(Bq/m^2)/(Bq)],

$\Gamma_{i,ground}^{A}$: dose factor for groundshine [(Gy/s)/(Bq/m^2)],

t: exposure time [s],

τ: release time [s],

$w_{i,ground}$: is the special radiation weight factor of nuclide i for unit absorbed dose due to deposited activity [Sv/Gy].

Again the unit of χ/Q is different from the generally used [(Bq/m^2)/(Bq/s)], as the source term is integrated for different time periods as shown in Eq (4). Similarly to the cloudshine, the dose factor for groundshine can be summed for each energy line of the nuclide in question with consideration of linear attenuation of photons and build up in air:

$$\Gamma_{i,ground}^{A} = \sum_j K(E_j) \cdot \int_A F_j^A(R)\, dA = \sum_j K(E_j) \cdot \int_A \frac{e^{-\mu_j R}}{4\pi R^2} \cdot B_j(\mu R) \cdot f_j \cdot \left(1\frac{\mathrm{Bq}}{\mathrm{m}^2}\right) dA \tag{19}$$

where

j: is the number of energy lines for a given nuclide,

$K(E_j)$: absorbed dose per fluence for photon with energy E_j [Gy·m^2],

$F_j^A(R)$: surface fluence of photon with E_j energy from dA surface at distance R in air per unit ground activity concentration [(1/ m^2)/(Bq/m^2)]

μ_j: linear attenuation factor for E_j in air [1/m],

R: is the distance of dV from the receptor point [m],

$B_j(R)$: build-up factor for E_j energy in air [-],

f_j : is the probability of emission of photon with $E_j$energy [-].

Based on the infinite plane model [69] the fluence in Eq. (19) can be computed based on an infinite plane model assuming that the activity concentration on the ground around the receptor point is uniform and equal to the values at the receptor point. Such a model is applied in several consequence assessment codes, such as in MACCS [66], NUDOS [70] as well as SINAC [16] and CARC [33]. In the CARC software these "surface" fluences were determined for a range of energies (from 30 keV to 15 MeV) by considering a large circular plane with 20 km radius at ground level with 1 Bq/m^2 surface activity representing the ground contamination. The receptor point was defined at 1 m height. The steps of the spatial integration and the size of the plane was chosen so that making the resolution denser or the size larger does not cause more difference in the resulting fluence than 1%. The dose factor for groundshine is computed for each energy line of the radionuclides available in the software with interpolation of the precomputed fluence values multiplied with the appropriate absorbed dose factor. The absorbed dose per fluence for photon values are taken from the ICRP Publication 116 [49].

The infinite-plane model is again a significant simplification of the actual characteristics of the activity, but with this assumption, the ground dose is a simple multiple of a dose factor and the ground activity concentration.

2.3.3.3. Inhalation

Internal exposure due to the inhalation of radioactive material is computed with the multiplication of the incorporated activity and the pertinent dose conversion factor:

$$\Delta_i^{inh} = \int_{t=0}^{\tau} \int_{t'=0}^{t} q_i \cdot \left(\frac{\chi}{Q}\right)_{i,\,inhal}^{V} \cdot c_{inhal} \cdot \Gamma_{i,inhal}\, dt' dt \qquad (20)$$

where:

Δ_i^{inh}: committed effective inhalation dose from nuclide i, [Sv], (absorbed inhalation dose for thyroid [Gy])

q_i: release rate of nuclide i [Bq/s],

$\left(\frac{\chi}{Q}\right)_{i,inhal}^{V}$: air activity concentration of nuclide i, at 1 m height for unit release [(Bq/m^3)/(Bq)],

$\Gamma_{i,inhal}$: committed effective dose for unit inhaled activity [Sv/Bq] (or the absorbed dose for unit inhaled activity to the thyroid [Gy/Bq]),

t: exposure time [s],

τ: release time [s],

c_{inhal}: breathing rate [m^3/s].

The source term can be integrated for the release duration and released in periods as shown in Eq (4), thus the unit of χ/Q is different from the generally used [(Bq/m^3)/(Bq/s)]. The dose conversion factors for inhalation can be taken from literature, the most recent is the IAEA General Safety Requirements Part 3 [53]where the values are included for fast absorption for two age groups (infants and adults). The breathing rate which is connected to the activity intensities can be found in the U.S. Environmental Protection Agency Exposure Handbook [71] as average values for different age groups.

2.3.3.4. Ingestion

The internal exposure from ingestion due the consumption of radioactive material through the terrestrial food chain can be computed as follows:

$$\Delta_{i,f}^{ing} = \int_{t=0}^{\tau} \int_{t'=0}^{T} q_i \cdot \left[\left(\frac{\chi}{Q}\right)_{i,ground}^{A} \cdot K_f^A(t') + \left(\frac{\chi}{Q}\right)_{i,cloud}^{V} \cdot K_f^V(t') \right] \cdot m_f \cdot \Gamma_{i,ingest}\, dt dt' \tag{21}$$

where:

$\Delta_{i,f}^{ing}$: committed ingestion dose from nuclide i, from the consumption of foodstuff f [Sv],

q_i: release of nuclide i [Bq/s],

$\left(\frac{\chi}{Q}\right)_{i,ground}^{A}$: deposited activity concentration of nuclide i on the ground for unit release [(Bq/m^2)/(Bq)],

$\left(\frac{\chi}{Q}\right)_{i,cloud}^{V}$: air activity concentration of nuclide i in the plume centreline for unit release [(Bq/m^3)/(Bq],

$K_f^A(t')$: activity of nuclide i accumulated in foodstuff f for unit ground deposition at the receptorpoint on a given day after the release [(Bq/kg)/(Bq/m^2)/day],

$K_f^V(t')$: activity of nuclide i accumulated in foodstuff f for unit air activity concentration on a given day after the release [(Bq/kg)/(Bq/m^3)/day],

$\Gamma_{i,ingest}$: committed dose for unit ingested activity [Sv/Bq], in case of thyroid dose [Gy/Bq],

τ: release time [s],

T: intake time [days],

m_f: overall consumed mass of the foodstuff f [kg/days].

Inhalation of livestock leading to human ingestion is usually not taken into consideration by food chain models, thus this type of contribution from contaminated air to the activity in foodstuff can be omitted ($K_f^V(t') \cong 0$). The relative concentration in air and on the ground has a different unit than the generally used one as the released activity is considered to be time integrated for the release duration as shown in Eq (4). The committed effective ingestion dose can be computed with the consideration of dose conversion factors from the IAEA General Safety Requirements Part 3 [53], taken for five age groups (four groups for children, one for adults), with commitment time of 50 years for adults and 70 years for children. The intake time is usually considered from the beginning of the release as a conservative estimate. Due to the fixed commitment times of the dose conversion factors (DCFs), the ingestion dose is over estimated as the dose from intake decades after the release is also computed via 50 and 70 years commitment times not considering the ageing of the representative person above 18 years. The aging for children can be considered with shifting the age group of the used DCF.

The time dependent activity concentration in different foodstuff can be computed via a dynamic terrestrial food chain model as it is in the CARC [33]. In the framework of my Master's thesis [72], I developed this foodcahin model based on the ECOSYS model [73] of the PC-COSYMA program [13] and the Food Chain and Dose Module for Terrestrial Pathways (FDMT) [74] of the JRODOS [43]. The developed model is capable of computing the accumulation and dilution of activity in 18 plants and 16 animal products.

There are several parameters that effect the activity concentration in plants such as translocation (activity migrating from the surface to the edible part of the plant), root uptake (activity absorbed by the plant roots from the soil), resuspension (activity from the top soil layer resuspended to the surface of the plant). The activity concentration in plants depend also on the level of development of the plant, as it effects how much activity can be deposited on the surface of the plant (mostly the leaves) and on the ground below the canopy.

The activity concentration in the plants can be computed with the following expression:

$$C_{i,pl}(\Delta t) = B_{i,pl} \cdot TR_{i,pl}(\Delta t) \cdot \mathrm{e}^{-\lambda_{i,pl}\Delta t} + (TF_{i,pl} + TF_{resus}) \cdot B_{i,S} \cdot \mathrm{e}^{-\lambda_{i,S}\Delta t} \quad (22)$$

where:

$C_{i,pl}(\Delta t)$ activity concentration in plant indexed pl per unit mass at Δt days after the release [Bq/kg],

Δt is the duration between deposition and harvest [day],

$B_{i,pl} = A_{i,pl}/Y_{pl}$ [Bq/kg], activity concentration in plant due to surface deposition, $A_{i,pl}$ is the activity deposited onto the plant surface per unit surface deposition [Bq/m^2], Y_{pl} is the plant yield [kg/m^2],

$TR_{i,pl}(\Delta t)$ is the translocation factor characterizing the ratio of activity that reaches the edible part of the plant during Δt time [-],

$\lambda_{i,pl} = \lambda_t + \lambda_g + \lambda_w + \lambda_{i,r}$ time coefficient of activity decrease in plant due to translocation (λ_t), growth (λ_g), weathering (λ_w) and radioactive decay ($\lambda_{i,r}$) [1/day],

$B_{i,S} = A_{i,s}/(L_{pl} \cdot \delta)$ activity concentration in the root zone per unit mass of soil after the deposition [Bq/kg], $A_{i,s}$ is the activity deposited onto the soil (under canopy) per unit surface deposition [Bq/m^2], L_{pl} depth of root zone [m], δ soil density [kg/m^3],

$TF_{i,pl}$ is the soil-to-plant transfer factor which is the ratio of activity concentration in the edible part of the plant and the soil [(Bq/kg)/(Bq/kg)],

TF_{resus} is the transfer factor of resuspension, which is the ratio of activity concentration on the plant surface and the resuspended soil [(Bq/kg)/(Bq/kg)],

$\lambda_{i,s} = \lambda_{i,m} + \lambda_{i,f} + \lambda_{i,r}$ time coefficient of absorbable activity decrease in soil due to migration ($\lambda_{i,m}$), fixation ($\lambda_{i,f}$), and radioactive decay ($\lambda_{i,r}$) [1/day], The activity concentration is animal products can be computed as follows:

$$C_{i,an}(t) = TF_{i,an} \sum_{j=1}^{2} a_{i,j}^{bio} \, \lambda_{i,j}^{bio} \int_{0}^{t} I_{i,pl}(\tau) \cdot exp(-(\lambda_{i,j}^{bio} + \lambda_{i,r})(t-\tau))d\tau \qquad (23)$$

where:

$C_{i,an}(t)$ is the activity concentration at time t in animal product indexed an per unit mass [Bq/kg] or in case of liquid product per unit volume [Bq/dm^3],

$TF_{i,an}$ is the feed-to-animal transfer factor which is the ratio of activity concentration in the animal product and in the feed [day/kg] or [day/dm^3],

$a_{i,j}^{bio}$ fraction of biological transfer of j component [-],

$\lambda_{i,j}^{bio}$ time coefficient of biological transfer of j component [1/day],

$I_{i,pl} = C_{i,pl}(t) \cdot V_{pl}$ is the daily activity intake from feed indexed pl, [Bq/day], $C_{i,pl}(t)$ is the activity concentration in feed pl at time t [Bq/kg], V_{pl} is the feed intake rate [kg/day],

$\lambda_{i,r}$ is the time coefficient of radioactive decay [1/day].

The biological transfer in animals can be described via a slower and a faster process, which are noted with index j. The slower and faster process are characterized with a larger and smaller half-life corresponding to the time coefficient of the biological transfer ($T_{i,j}^{bio} = \ln(2)/\lambda_{i,j}^{bio}$). The activity of feed can be computed based on Eq. (22), with the consideration of different time periods, such as time of harvest, time of feeding, and time of processing. The processing of food products can be calculated as follows:

$$C_{i,f}^{proc}(t) = p_f \cdot e^{-\lambda_{i,r} \cdot \Delta t_f^{proc}} \cdot C_{i,f}(t - \Delta t_f^{proc}) \qquad (24)$$

where:

$C_{i,f}^{proc}(t)$ is the activity concentration in processed food product f [Bq/kg] or [Bq/dm^3] for liquids,

p_f is the processing dilution factor [-],

$\lambda_{i,r}$ is the time coefficient of radioactive decay [1/day].

Δt_f^{proc} is the processing time for food product f [day],

$C_{i,f}$ is the activity concentration in food product f before processing [Bq/kg] or [Bq/dm^3] for liquids.

Further details about the food chain model can be found in the model description of the new methodology (implemented in the CARC software) [33], the ECOSYS [73] and FDMT [74] modules and my Master's thesis [72].

Parameters used for the food chain model can be taken from literature. Regarding the CARC software, the characteristics of migration through root zone, plants and animals were based on parameters published in IAEA documents ([75], [76], [77]) model descriptions of other commercial programs ([73], [74], [78], [79]) and other journal articles ([80], [81], [82], [83]).

3. Validation and application of an improved method for deterministic safety assessment

Due to historical reasons, the national nuclear safety requirements concerning radioactive release from nuclear facilities vary considerably from country to country. High-level requirements to avoid accidents that could lead to large or early radioactive releases to the environment can be found in several national and international documents (which I described in Section 2.3.2), but the practical application of these requirements is not uniform. In order to achieve a full harmonisation of nuclear safety, and in particular of the safety levels for the release of radioactivity, a low level harmonisation is also needed, focusing on the practical application of the high level requirements, in order to provide better transparency and comparability of the results of the safety analyses. For the purpose of such harmonisation, an improved approach for the definition and calculation of the atmospheric release criteria has been established in the last decade by my colleagues working in my research group at the Centre for Energy Research. The compliance verification process and the terms and conditions of application were also developed (presented in more detail in Annex I.). The method is based on already existing formulae that were adopted and customized for practical implementation with additional assumptions and modifications. This methodology is primarily targeted for nuclear fission reactors, mainly NPP units. The improved approach is equipped to take into account the differences of unit design, site conditions and meteorological characteristics in the verification of criteria fulfillment. Thus, the methodology can be used in practice for existing and operating nuclear power plants as well as other nuclear facilities.

According to the improved methodology the dose representative of the radiation exposure at a given location (receptor point) can be computed from the source term of the release, the environmental transport and the exposure of the population, which can be separated and determined independently with appropriate boundary conditions. This separation makes it possible to distinguish the effect of the different contributing factors on the dose results, with the release source term being related to the safety of the nuclear installation, the transport dependent on the environmental conditions, and the exposure determined based on the characteristics of the site (population and habit data). The main advantage of this methodology is that the environmental transport and the exposure doesn't need to be computed for every assessment, they can be considered fixed for longer time periods (e.g. 10 years) because generally they do not change considerably for a specific location or site. This means that for a new source term, only very simple multiplication of three vectors representing the appropriate source term, transport and exposure is needed to determine the representative doses. It is important to note that the calculated representative dose has Sievert dimension, yet it does not provide an accurate estimate of the projected dose of a person in an actual radioactive release. Furthermore, the representative dose is not appropriate for comparison with the reference levels applied in emergency preparedness and response practice due to the difference in the computational methodologies and parameter values utilized in the calculations. The utilization of this method is solely justified for the purpose of confirming the fulfillment of release criteria during safety assessment. For similar reasons the calculated representative dose cannot be compared with operational intervention levels (OILs) [84] either.

With my participation, the improved methodology was implemented in the CARC software [33] which computes off-site consequences of radioactive atmospheric releases and is capable of confirming and determining release criteria for nuclear facilities. The primary application of the methodology is the verification of the fulfillment of existing emission limits but in addition, the methodology can also be used to set emission limits for new nuclear installation based on the site characteristics and considering the regulatory dose criteria. The development of the first version of the program was finished in 2017 and the current version (1.1) was completed in 2020. The program simulates the spread and dilution of short-term atmospheric radioactive emissions, as well as analyzes the public doses using site specific meteorological measurement data and habit data. I presented the atmospheric dispersion, deposition and dose calculation models of the CARC software in section 2. and describe the specific details of the application process in Annex I.

In section 3.1, I present the code-to-code comparisons between the dispersion and dose calculation modules of the improved methodology and commercially available similar software. In section 3.2 I show the application of the improved method throughout a hypothetical but realistic case study. In section 3.3 I present the results of investigating the sensitivity of the methodology to various parameters of the exposure calculation.

3.1. Code-to-code comparison of the improved methodology

Although the result obtained from the improved methodology is expressed in dose units [Sv], due to the use of different calculation methods and parameter, it is not directly comparable to the dose of person in an actual release or the dose values determined for emergency preparedness and response. Consequently, it is not possible to conduct the validation of the CARC model with measurements, which determines that the validation can only be performed by means of code-to-code comparisons. Thus, for the purpose of validation, I conducted evaluation of the computational modules of the CARC programme via comparing the step-by-step results with calculations made with widely used commercially available codes, PC-COSYMA [13] and Microshield [14].

The PC-COSYMA code [13] was developed through the MARIA (Methods for Assessing the Radiological Impact of Accident) project of the European Commission and is suitable for the analysis of consequences related to accidental radiological emissions. The program uses a Gaussian plume model for atmospheric dispersion calculations and the air and ground activity concentrations and doses can be evaluated in a radial coordinate system. Two types of results can be accessed in the PC-COSYMA, GRID values at specific radial distances and directional sectors (maximal resolution of sectors is 72), and MEAN values averaged over a given distance. From the dose quantities that can be determined by the PC-COSYMA program, the dose from cloud, ground and inhalation is computed for short and long term both as GRID and MEAN values, but ingestion doses are only available as MEAN values. The contribution of specific radionuclides that are specified by the user to the doses can only be shown by the program as percentages (rounded up to integer values).

The PC-COSYMA code was selected for comparison with CARC because of its widespread usage and extensive literature on calculation results, as well as due to the similarities of its models compared to the ones implemented in CARC. In addition, PC-COSYMA has been used in Hungary in the last decades for various dose calculations conducted for the Paks NPP. However, there are some limitations of this comparison as there is a lack of details in the documentation for some of the assumptions, functionalities of the PC-COSYMA are not flexible (some of the model parameters are fixed and cannot be modified to better fit different site characteristics), partial results of the computation chain cannot always be retrieved and the source code of the program is not available these arising questions cannot be clarified completely. These issues and limitations are discussed further in the summary of each comparison. In these aspects there is a difference in the level of transparency for the two codes, due to the lack of details in the documentation and the unavailability of the source code, the methods and their implementation of PC-COSYMA are not entirely traceable whereas the modules of the CARC code are completely known as I participated in its development.

The Microshield [14] program is validated and it is capable of computing external dose for a variety of radiological sources and shielding layers with different geometrical and material properties. There are different standard databases built into the program to be selected for the calculations, containing parameters for the radionuclides including half-life, attenuation, build-up and dose conversion factors. The radiation sources can be given either as radionuclide composition or by energy groups. Different photon energy grouping methods can be used, including user-defined ones which can be specified from 15 keV to 10 MeV. The program provides the computed results such as the fluence rate [MeV/cm^2/s], exposure rate [mR/h] and absorbed dose rate [mrad/h or mGy/h] with and without taking into account the buildup due to the scattering of photons. The MicroShield program was used to compare its absorbed dose rate results with those obtained from CARC to supplement the comparison conducted with PC-COSYMA.

The transport and exposure module of the CARC code was investigated separately, assessing the atmospheric dispersion and deposition model via the air and ground activity concentration due to unit release and analyzing the doses for different pathways computed for unit air and ground activity concentration for the investigation of the dose calculation. Based on similar code-to-code comparions, in my evaluation I defined the acceptable range of difference between the results obtained with the various codes to be between -50% and +150%. For reference, in benchmark comparisons of various codes the differences of the obtained results are in the one order of magnitude. As an example, in an international intercomparison of probabilistic consequence assessment software (including PC-COSYMA), the difference in the endpoints were even larger: the mean and the 99th percentile of the time-integrated Cs-137 activity concentration at ground level evaluated at 1 km showed 7 and 30 times difference between the participating codes [85]. In another benchmark conducted with various nuclear consequence assessment codes [86], the difference in the average yearly deposition values that were determined in various directions and distances ranged around 0.5 and 1.5.With regard to the doses, the mean adult bone marrow dose was computed at 1 km in the first day, and the contribution of different exposure pathways was determined for the various codes, which were ranging from 60% to 365% for cloudshine, from 14% to 354% for groundshine and from 14% to 722% for inhalation (for three codes) [86].

3.1.1. Assessment of atmospheric dispersion and deposition calculations

I evaluated the atmospheric dispersion module of the CARC software by comparing the time-integrated activity concentrations in the air [Bq s/m^3] and the surface concentration on the ground [Bq/m^2] computed by the PC-COSYMA program for various scenarios. The comparison is reasonable as both codes apply Gaussian plume model, the atmospheric stability is characterized with the same Pasquill parametrization and the deposition from the plume is computed with the identical methods (shown in Eq.(8) and Eq.(9)). The time integration of the air activity concentration was computed for the duration of the pume passage which was tha same in both PC-COSYMA and CARC. The released activity was 1E+16 Bq Cs-137 and 1E+16 Bq Xe-133 discharged at 50 m. The surface roughness was assumed to be smooth and the deposition velocity was set to 0.001 m/s in both codes.

The receptor points for the comparison were defined at 1 km, 3 km and 10 km along the wind direction. The environmental results from PC-COSYMA were obtained as "GRID" values. In addition to the meteorological cases presented in [P1], I used a wider range of weather characteristics for the comparison as shown in Table 2. The ID of a meteorological case contain the wind speed as first value, the Pasquill stability class as the second and the rain intensity as the last value.

Table 2. The values of meteorological parameters used for the comparison of CARC and PC-COSYMA activity concentrations [P1]

Meteorological case ID	Wind speed [m/s]	Pasquill class	Rain intensity [mm/h]
1 D 0	1	D	0
5 D 0	5	D	0
10 D 0	10	D	0
1 A 0	1	A	0
1 B 0	1	B	0
1 C 0	1	C	0
1 E 0	1	E	0
1 F 0	1	F	0
1 D 1	1	D	1
1 D 5	1	D	5
1 D 10	1	D	10

The results for the different wind speed values are shown in Table 3 for Xe-133 and in Table 4 for Cs-137. The differences obtained for the air and ground activity concentrations computed with the various codes are not negligible but are within the predefined acceptable range (from 5% to 23% for the considered distances) even considering that similar models and the same parameter values were used. As stated previously, a limitation of the PC-COSYMA is that some aspects of the computational chain are not clear and there may be differences in the implementation of the models which could cause the obtained differences.

Table 3. Comparison of CARC and PC-COSYMA time-integrated Xe-133 air activity concentrations for various wind speed values [P1]

Met. case ID	Distance of receptor point [km]	Time-integrated air activity concentration [Bq·s/m^3]		Ratio of time-integrated air activity concentrations [1]
		CARC	PC-COSYMA	CARC/ PC-COSYMA
1 D 0	1	3.43E+11	2.83E+11	1.21
	3	7.96E+10	7.58E+10	1.05
	10	1.40E+10	1.32E+10	1.06
5 D 0	1	6.87E+10	5.67E+10	1.21
	3	1.60E+10	1.51E+10	1.06
	10	2.84E+09	2.68E+09	1.06
10 D 0	1	3.43E+10	2.84E+10	1.21
	3	7.99E+09	7.55E+09	1.06
	10	1.42E+09	1.34E+09	1.06

Table 4. Comparison of CARC and PC-COSYMA time-integrated Cs-137 air activity concentrations and Cs-137 ground activity concentrations for various wind speed values [P1]

Met. case ID	Distance of receptor point [km]	Time-integrated air activity concentration [Bq·s/m^3]		Ratio of time-integrated air activity concentrations [1]	Ground activity concentration [Bq/m^2]		Ratio of ground activity concentration [1]
		CARC	PC-COSYMA	CARC/ PC-COSYMA	CARC	PC-COSYMA	CARC/ PC-COSYMA
1 D 0	1	3.43E+11	2.80E+11	1.23	3.43E+08	2.80E+08	1.23
	3	8.00E+10	7.41E+10	1.08	8.00E+07	7.41E+07	1.08
	10	1.43E+10	1.28E+10	1.12	1.43E+07	1.28E+07	1.12
5 D 0	1	6.87E+10	5.69E+10	1.21	6.87E+07	5.69E+07	1.21
	3	1.60E+10	1.51E+10	1.06	1.60E+07	1.51E+07	1.06
	10	2.85E+09	2.67E+09	1.07	2.85E+06	2.67E+06	1.07
10 D 0	1	3.43E+10	2.85E+10	1.21	3.43E+07	2.85E+07	1.21
	3	8.00E+09	7.57E+09	1.06	8.00E+06	7.57E+06	1.06
	10	1.43E+09	1.34E+09	1.06	1.43E+06	1.34E+06	1.06

As expected, increasing the wind speed, which causes more dilution along the x-axis leading to a decrease in the time-integrated air activity concentrations. For the noble gas Xe-133, no deposition from the plume occurs, but for the aerosol Cs-137, the same dry deposition scheme can be identified based on the ground activity concentrations obtained with the two codes. This is shown by the correspondence of the ratios of the air and ground activity concentrations with the 0.001 m/s deposition coefficient.

The differences between the two codes for various Pasquill stability classes are shown in Table 5. The values for inversion layer height used in the comparison were taken as the default values in PC-COSYMA connected to the Pasquill stability classes. Input coefficients for the horizontal and the vertical dispersion parameter were set to the same values in both codes (default PC-COSYMA values for smooth surface roughness) [87].

Table 5. Comparison of CARC and PC-COSYMA time-integrated Cs-137 air activity concentrations and Cs-137 ground activity concentrations for various Pasquill stability classes [P1]

Met. case ID	Distance of receptor point [km]	Time-integrated air activity concentration [Bq·s/m^3]		Ratio of time-integrated air activity concentrations [1]	Ground activity concentration [Bq/m^2]		Ratio of ground activity concentration [1]
		CARC	PC-COSYMA	CARC/ PC-COSYMA	CARC	PC-COSYMA	CARC/ PC-COSYMA
1 A 0	1	7.38E+10	6.80E+10	1.09	7.38E+07	6.80E+07	1.09
	3	1.45E+10	1.40E+10	1.04	1.45E+07	1.40E+07	1.04
	10	2.40E+09	2.24E+09	1.07	2.40E+06	2.24E+06	1.07
1 B 0	1	1.13E+11	1.04E+11	1.09	1.13E+08	1.04E+08	1.09
	3	2.30E+10	2.23E+10	1.03	2.30E+07	2.23E+07	1.03
	10	3.80E+09	3.57E+09	1.07	3.80E+06	3.57E+06	1.07
1 C 0	1	2.04E+11	1.77E+11	1.15	2.04E+08	1.77E+08	1.15
	3	4.34E+10	4.16E+10	1.04	4.34E+07	4.16E+07	1.04
	10	7.31E+09	6.85E+09	1.07	7.31E+06	6.85E+06	1.07
1 E 0	1	5.31E+11	4.18E+11	1.27	5.31E+08	4.18E+08	1.27
	3	1.47E+11	1.28E+11	1.14	1.47E+08	1.28E+08	1.14
	10	3.03E+10	2.50E+10	1.22	3.03E+07	2.50E+07	1.22
1 F 0	1	6.51E+11	5.25E+11	1.24	6.51E+08	5.25E+08	1.24
	3	2.17E+11	1.81E+11	1.20	2.17E+08	1.81E+08	1.20
	10	5.58E+10	4.85E+10	1.15	5.58E+07	4.85E+07	1.15

Similarly, to the effect of using different wind speed values, the change in atmospheric stability results in altering the extent of the plume. The more stable the atmosphere is the lower the horizontal and vertical spread of the plume is (along the y, and z axis), thus resulting in greater air and ground activity concentrations. Comparison of the CARC and PC-COSYMA results implies that there may be a difference in the dispersion calculation methods of the two codes related to the atmospheric stability. Changing the stability class from unstable to stable increases the difference between the air and ground activity concentrations, for the extremely unstable conditions (class A) the difference is maximum 9%, whereas for more stable conditions (class E and F) this value reaches 27%.

I investigated the CARC and PC-COSYMA results for different rain intensities (1 mm/h, 5 mm/h and 10 mm/h). The results are shown in Table 6. The comparison of the two codes in this respect is valid as both codes apply the same wet deposition scheme based on the exponential washout function in Eq.(9) with the same values for the coefficient parameters (α = 0.00008 and β = 0.8). To investigate only the effect of wet deposition, I neglected the dry deposition, by specifying the dry deposition parameter as 0 m/s. This omission was justified as dry deposition is usually several orders of magnitude lower than wet deposition if rain occurs. The ratio of the CARC/PC-COSYMA time-integrated air activity concentrations are within the range of previous results, whereas the differences between the ground activity concentrations are higher for wet deposition than for dry deposition reaching 50%. The difference in the time-integrated air activity concentration of CARC and PC-COSYMA is higher closer to the release point, thus resulting in more deposition in CARC. With the increase of the rain intensity this effect is more significant resulting in higher differences between the ground deposition results obtained with the two codes.

Table 6. Comparison of CARC and PC-COSYMA time-integrated Cs-137 air activity concentrations and Cs-137 ground activity concentrations for various rain intensity values [P1]

Met. case ID	Distance of receptor point [km]	Time-integrated air activity concentration [Bq·s/m³]		Ratio of time-integrated air activity concentrations [1]	Ground activity concentration [Bq/m²]		Ratio of ground activity concentration [1]
		CARC	PC-COSYMA	CARC/PC-COSYMA	CARC	PC-COSYMA	CARC/PC-COSYMA
1 D 1	1	3.17E+11	2.59E+11	1.23	3.20E+09	2.17E+09	1.47
	3	6.29E+10	5.83E+10	1.08	1.09E+09	9.70E+08	1.12
	10	6.41E+09	5.71E+09	1.12	2.31E+08	2.15E+08	1.07
1 D 5	1	2.57E+11	2.10E+11	1.23	8.73E+09	5.83E+09	1.50
	3	3.35E+10	3.10E+10	1.08	2.01E+09	1.79E+09	1.12
	10	7.85E+08	6.88E+08	1.14	1.01E+08	9.21E+07	1.10
1 D 10	1	2.07E+11	1.69E+11	1.22	1.21E+10	8.06E+09	1.50
	3	1.76E+10	1.62E+10	1.08	1.83E+09	1.62E+09	1.13
	10	9.16E+07	7.92E+07	1.16	2.04E+07	1.84E+07	1.11

I investigated in more detail the impact of changing the surface roughness, which parameter in the model accounts for the effect of the surface objects such as buildings or vegetation on the atmospheric dispersion. In PC-COSYMA there are two possible options to be set for surface roughness: smooth and rough, which are connected to different sets of diffusion coefficients used for atmospheric dispersion calculation. For rough surface there are various sets of diffusion coefficients in PC-COSYMA for different release heights (50 m, 100 m and 180 m), but for smooth surface the coefficients are independent from the height. For the comparison with rough surface, diffusion values corresponding to the considered release heights were defined in CARC to be as consistent as possible with PC-COSYMA. The results for rough surface roughness, when considering 50 m release height, 1 m/s wind speed, D Pasquill stability class and 0 mm/h rain intensity are shown in Table 7. Both in CARC and PC-COSYMA the time-integrated air activity concentration is about half of the ones for smooth surface, however the CARC/PC-COSYMA ratio is lower for distances of 1 km and 3 km, and higher for 10 km compared to the results for smooth surfaces.

Table 7. Comparison of CARC and PC-COSYMA time-integrated Xe-133 air activity concentrations for rough surface roughness

Distance of receptor point [km]	Time-integrated air activity concentration [Bq·s/m^3]		Ratio of time-integrated air activity concentrations [1]
	CARC	PC-COSYMA	CARC/ PC-COSYMA
1	1.99E+11	1.75E+11	1.14
3	3.56E+10	3.43E+10	1.04
10	8.98E+09	7.94E+09	1.13

In addition to the calculations published in [P1], I conducted comparison with the consideration of different effective release heights (energy of release considered to be 0 W). The results obtained for effective release heights of 20 m and 80 m are shown in Table 8 for Xe-133. The meteorological parameters were set as 1 m/s wind speed, D Pasquill stability class and 0 mm/h for rain intensity. For the 20 m release height, the ratio of the CARC and PC-COSYMA time-integrated air activity concentrations became more similar to those observed with 50 m release height as the distance increases, whereas for the 80 m release height, the ratios increase with distance. This suggests some unknown aspect of the calculation method related to the effective release height that may differ between the two codes.

Table 8. Comparison of CARC and PC-COSYMA time-integrated Xe-133 air activity concentrations for various effective release heights

Effective release height [m]	Distance of receptor point [km]	Time-integrated air activity concentration [Bq·s/m^3]		Ratio of time-integrated air activity concentrations [1]
		CARC	PC-COSYMA	CARC/ PC-COSYMA
20	1	4.23E+11	2.83E+11	1.49
	3	8.32E+10	7.58E+10	1.10
	10	1.41E+10	1.32E+10	1.07
80	1	2.32E+11	1.64E+11	1.41
	3	7.33E+10	4.19E+10	1.75
	10	1.39E+10	7.26E+09	1.92

Based on the considered parameters and receptor points the CARC method can be considered conservative as results were higher than those of PC-COSYMA. However, this may not generally hold true for all input data combination.

Overall, the results obtained with the perturbation of input parameters of the atmospheric dispersion calculation meteorological were within the predefined acceptable range with the diference being within -50% and +150%.

3.1.2. Assessment of dose calculations

I investigated the dose calculation modules of CARC via comparing external and internal dose quantities determined for unit air or ground activity concentration with the corresponding values obtained from MicroShield [14] and PC-COSYMA [13].

First, I compared the CARC external dose factor for cloudshine and groundshine that I calculated with semi-infinite model and infinite plane model respectively (see detailed descriptions in section 2.3.3.1. and section 2.3.3.2.) for a selected number of energies with the corresponding values determined with MicroShield. In case of the cloudshine a small difference between the geometry of CARC and MicroShield is that the gap in the middle of the considered cylinder was considered to be only 2 m high in MicroShield, whereas in CARC, the gap in the volume source reaches the top of the cylinder. It is anticipated that this small difference does not affect the results significantly. The geometry and the activity concentration of the source was set to the same value in the two codes, the yield for each energy was set to 100% in MicroShield. The quantity of MicroShield that was used in the comparison was the "Absorbed Dose Rate mGy/hr With Buildup" considered for unit volume (1 Bq/m^3) and surface (1 Bq/m^2) activity concentration. As the dose quantities computed by CARC are in Sievert unit, these were converted with effective dose per gamma fluence values for isotropic (ISO) geometry taken from ICRP 116 [49]. The results of the comparison are shown in Table 9.

Table 9. Comparison of CARC and MicroShield cloudshine and groundshine dose factors for various energies [P1]

Energy [MeV]	Cloudshine dose factor [$Gy/(Bq \cdot h/m^3)$]		Ratio of cloudshine dose factors	Groundshine dose factor [$(Gy/h)/(Bq/m^2)$]		Ratio of groundshine dose factors
	CARC	MicroShield	CARC/Microshield	CARC	MicroShield	CARC/Microshield
0.08	1.79E-11	1.86E-11	0.96	2.50E-13	2.63E-13	0.95
0.1	2.27E-11	2.31E-11	0.98	2.90E-13	2.99E-13	0.97
0.6	1.46E-10	1.40E-10	1.04	1.53E-12	1.36E-12	1.13
1	2.21E-10	2.33E-10	0.95	2.18E-12	2.11E-12	1.03
3	6.79E-10	6.97E-10	0.97	5.21E-12	5.03E-12	1.04
5	1.13E-09	1.15E-09	0.98	7.74E-12	7.42E-12	1.04
10	2.25E-09	2.25E-09	1.00	1.36E-11	1.28E-11	1.06

The values obtained by the two codes show acceptable agreement, the difference in the cloudshine and groundshine factors range between -5% and +13%. There is no visible dependency of the ratios on the energy.

In addition to analyzing the results for specific energies included in [P1], I conducted similar comparisons for a couple of nuclides with reasonably small number of energy lines taken from MicroShield's build in Grove Library. For the Gy to Sv unit conversion, the exact values of effective dose per gamma fluence were determined with linear interpolation of the values for available energies, used values shown in Table 10. In this case due to the larger number of energy lines, it was easier to convert MicroShield results Sv to be consistent with the quantity determined by CARC.

Table 10. External dose conversion factor for Xe-133, Cs-137 and Zn-65 determined on the basis of ICRP 116 for energy lines taken from MicroShield's Grove Library [14][49]

Nuclide	Energy [MeV]	Effective dose per air kerma free-in-air [Sv/Gy]
Xe-133	0.0043	1.63E-03
	0.0306	1.82E-01
	0.0310	1.90E-01
	0.0350	2.66E-01
	0.0796	7.72E-01
	0.0810	7.73E-01
	0.1777	6.99E-01
Cs-137 (+ Ba-137m)	0.0045	1.71E-03
	0.0318	2.05E-01
	0.0322	2.13E-01
	0.0364	2.93E-01
	0.6616	6.97E-01
Zn-65	0.0009	3.42E-04
	0.0080	3.04E-03
	0.0080	3.04E-03
	0.0089	3.38E-03
	0.5110	6.85E-01
	0.5577	6.89E-01
	1.1155	7.34E-01

The results of the comparison of cloudshine and groundshine factors for the three selected nuclides are shown in Table 11. The results show acceptable differences ranging between -11% and +3%.

Table 11. Comparison of CARC and MicroShield cloudshine and groundshine dose factors for various nuclides [P1]

Nuclide	Cloudshine dose factor [Sv/(Bq·h/m^3)]		Ratio of cloudshine dose factors	Groundshine dose factor [(Sv/h)/(Bq/m^2)]		Ratio of groundshine dose factors
	CARC	MicroShield	CARC/Microshield	CARC	MicroShield	CARC/Microshield
Xe-133	5.38E-12	6.038E-12	0.89			
Cs-137	8.69E-11	9.130E-11	0.95	9.02E-13	8.78E-13	1.03
Zn-65	9.20E-11	9.927E-11	0.93	8.89E-13	8.87E-13	1.00

The difference in the results obtained with CARC and MicroShield are within the predefined acceptable range considering that two different codes were used, even though the adjustable parameters in the programs were set to the same values, the codes could potentially have unknown differences in their calculation methods that are not described in the documentation in detail.

Concerning the internal dose calculation modules of CARC, I made comparisons of the inhalation and ingestion doses computed for unit air and ground activity concentrations with the corresponding values of PC-COSYMA determined for a hypothetical release scenario. Whereas CARC is capable of computing the dose factor for inhalation and ingestion without specifying the release characteristics, with PC-COSYMA, the needed quantity has to be determined from an entire calculation chain of release atmospheric dispersion and exposure. In the PC-COSYMA release scenario considered for the inhalation dose comparison the release source term was 1E+16 Bq Cs-137, 1E+16 Bq Sr-90 and 1E+16 Bq I-131 (100% aerosol form), effective release height was 50 m, meteorological parameters were set to be 1 m/s for wind speed, D Pasquill class, 0 mm/h for rain intensity and smooth surface roughness. The dose conversion factors for inhalation and ingestion (effective dose per unit incorporation) used in PC-COSYMA are taken from ICRP 56, 67 and 69 publications [88][89][90], whereas the same factors are taken from IAEA General Safety Requirements Part 3 [53].

The comparison of the CARC and PC-COSYMA inhalation does is reasonable as both codes compute the dose as the product of the same quantities: the time-integrated air activity concentration, the breathing rate and the dose per unit inhaled activity. Inhalation of resuspended material was not considered in the comparison, only the inhalation during the passage of the plume was taken into account. The value of the breathing rate was set to the same value in the two codes, to 15 m^3/day=0.625 m^3/h. In the comparison, the committed effective inhalation dose for 50 years commitment time were evaluated at 1 km. In PC-COSYMA only MEAN values can be retrieved separately for each nuclide and exposure pathway, thus this quantity divided by the MEAN air activity concentration was used in the comparison. The inhalation dose factors computed by CARC and determined from PC-COSYMA are shown in Table 12.

Table 12. Comparison of CARC and PC-COSYMA inhalation dose factors for various nuclides [P1]

Nuclide	Inhalation dose factor [Sv/(Bq·s/m^3)]		Ratio of inhalation dose factors
	CARC	PC-COSYMA	CARC/ PC-COSYMA
Cs-137	6.80E-13	6.76E-13	0.99
Sr-90	3.49E-12	3.52E-12	1.01
I-131	1.08E-12	1.09E-12	1.00

Results for the inhalation dose factor computed by CARC and PC-COSYMA show almost perfect accordance, within 1% differences, which can be attributed to the rounding error of the air activity concentration and inhalation dose that are only provided for 3 digits of PC-COSYMA.

For the evaluation of the food chain dose module of CARC, I compared the ingestion dose for 8 foodstuffs computed by the ECOSYS module of PC-COSYMA [73] with the corresponding values of CARC. Comparison of the CARC and PC-COSYMA ingestion doses is justified as both codes compute the dose as the product of the same quantities: the ground activity concentration, the concentration in food per unit deposition, the consumption rate and the dose per unit intake. In PC-COSYMA the season was set to summer to compute food chain doses and in CARC, the date of the deposition onto the vegetation was accordingly set to be 1st of July. The consumption rates of the various products were set to the same values in the two programs (exact values shown in Table 13), and processing times were set to zero days.

Table 13. Considered foodstuffs and consumption rates in the comparison of ingestion dose

Foodstuffs		Food consumption rate [kg/year]
CARC	PC-COSYMA	
milk	cow milk	115
beef bull	beef bull	25
pork	pork	50
spring wheat flour	grain products	95
potatoes	potatoes	70
leafy vegetables	leafy vegetables	20
fruit vegetables	non-leafy vegetables	25
root vegetables	root vegetables	15

To get the same ingestion dose factors from PC-COSYMA as the quantity determined by CARC, the long-term individual ingestion doses were evaluated at 1 km divided by the ground activity concentration. Similarly to the inhalation, only the MEAN values for various nuclides and exposure pathways can be retrieved from PC-COSYMA, thus the MEAN ground activity values were used for the division. In PC-COSYMA the dose conversion factors (dose-per-unit-intake) for the ingestion dose are available for different integration times and age groups [91]. The commitment time was considered to be 50 years (as for adults) and corresponding with the information in PC-COSYMA documentation [92] the consumption time of contaminated food is 50 years, thus this value was set for the integration time in CARC as well.

In the release scenario of PC-COSYMA considered for the ingestion dose comparison the release source term was 1E+16 Bq each for the following nuclides: Ba-140, Ce-141, Ce-144, Cs-134, Cs-136, Cs-137, I-129, I-131, I-133, Nb-95, Pu-238, Pu-239, Pu-240, Pu-241, Pu-242, Ru-103, Ru-106, Sr-89, Sr-90, Tc-99, Te-127m, Te-129m, Te-132, Zr-95 (extending the number of investigated nuclides from those that were considered in previous assessment [P1]). The effective release height was 50 m, meteorological parameters were set as the following 1 m/s wind speed, D Pasquill class, 0 mm/h rain intensity and smooth surface roughness. The ingestion dose factors computed by CARC and PC-COSYMA and their ratios are shown in Table 14. From the considered nuclides, I indicated with bold font those which typically have significant contribution to the ingestion dose due to an accidental release from a nuclear power plant.

Table 14. Comparison of CARC and PC-COSYMA ingestion dose factors for various nuclides

Nuclide	Ingestion dose factor [Sv/(Bq/m^3)]		Ratio of ingestion dose factors
	CARC	PC-COSYMA	CARC/PC-COSYMA
Ba-140	7.24E-10	7.55E-10	0.96
Ce-141	3.49E-10	2.65E-10	1.32
Ce-144	**5.01E-09**	**6.61E-09**	**0.76**
Cs-134	**4.97E-07**	**5.24E-07**	**0.95**
Cs-136	3.19E-09	2.02E-09	1.58
Cs-137	**4.01E-07**	**4.58E-07**	**0.87**
I-129	1.06E-06	2.41E-06	0.44
I-131	**9.44E-09**	**1.11E-08**	**0.85**
I-133	**1.54E-10**	**1.55E-10**	**1.00**
Nb-95	2.86E-10	2.67E-10	1.07
Pu-238	2.13E-07	2.44E-07	0.87
Pu-239	2.34E-07	2.70E-07	0.86
Pu-240	2.34E-07	2.70E-07	0.86
Pu-241	4.35E-09	4.97E-09	0.88
Pu-242	2.24E-07	2.56E-07	0.87
Ru-103	**4.04E-10**	**3.21E-10**	**1.26**
Ru-106	7.39E-09	1.02E-08	0.73
Sr-89	**2.31E-09**	**2.44E-09**	**0.94**
Sr-90	9.14E-08	1.36E-07	0.67
Tc-99	4.49E-09	1.45E-08	0.31
Te-127m	1.12E-08	1.20E-08	0.94
Te-129m	6.25E-09	3.26E-09	1.91
Te-132	3.95E-10	4.29E-10	0.92
Zr-95	**5.95E-10**	**6.17E-10**	**0.96**

The results for the ingestion dose factor computed by CARC and PC-COSYMA are in the same order of magnitude with difference ranging between -69% and +91%, thus for some nuclides the difference exceeds the predefined acceptable -50% and +150% range. However, looking at only those nuclides which typically contribute to the ingestion dose in case of an accidental release from a nuclear power plant (namely Ce-144, Cs-134, Cs-137, I-131, I-133, Ru-103, Sr-89 and Zr-95), the maximum difference between the values of CARC and PC-COSYMA is -24% and +26%, so within the predefined acceptable range.

To conclude, the results of the comparison of the doses for various exposure pathways show acceptable difference considering that similar comparisons provided such or even larger variation in the doses (e.g. in [86]).

3.2. Hypothetical case study with the improved methodology

I made calculations with CARC for a realistic but hypothetical release scenario to demonstrate the applicability of the code and the precision of the obtained results. The goal of the calculation is the verification of the acceptance criteria as described in Annex I. The source term and some characteristics of a DEC release scenario was taken from an international case study conducted throughout the European CONFIDENCE project [93]. The release (corresponding to the source term S in Annex I) was assumed to be instantaneous with the discharge of 8 nuclides with activities as described in Scenario 2 published in a project deliverable [op3](shown in Table 15). The release was considered with input parameter of 50 m effective release height, 0 MW energy content and 2/3 part of the iodine in elemental form and 1/3 portion in aerosol form.

Table 15. Release activity of the considered nuclides in the hypothetical DEC scenario [op3]

Nuclide	Released activity [Bq]
Ba-137m	2.37E+12
Cs-134	4.70E+12
Cs-136	1.77E+12
Cs-137	3.17E+12
I-131	5.42E+13
I-132	6.35E+14
Te-132	1.73E+13
Xe-133	6.91E+17

The meteorological input data used in the atmospheric dispersion calculation was a real-life 5 years-long measurement dataset with hourly time resolution obtained from the measurement of a meteorological tower (located at the site of the Paks NPP). Accordingly, the database contained 5×365×24=43800 data points.

The dose quantities computed in the study were chosen to be in line with the EUR criteria [21] described in section 2.3.2. Thus, the doses were calculated for the first 24 hours and 4 days. The committed effective dose included the pathways of cloudshine, groundshine and direct inhalation. To be consistent with the other similar assessments of this thesis, the receptor points were defined in 16 directions (differing from the ones selected in the previously published work [P1]) at distances of 800 m and 3 km according to the EUR DEC criteria as regards to the introduction of various countermeasures beyond the given distances.

The atmospheric dispersion and deposition calculation (determination of the transport factors T in Annex I) was performed for the 16 receptorpoints that were defined at the various angles at the given distances and the maximum from these were seleted for each meteorological data point. Then, these values were sorted in ascending order for all of the considered meteorological data, and the 95th percentile of the results were selected (in line with the method used in the EUR [21]).

No shielding or reduction was assumed for cloudshine, groundshine and inhalation, breathing rate was considered to be a mean daily long-term value from literature [71] 15 m^3/day=0.625 m^3/h.

The detailed results of the calculation are shown in Table 16 for 800 m distance and 24 hours after the start of the release and in Table 17 for 3 km and 4 days. (Due to the different number of considered directions, these results differ from those that were published previously in [P1].) The representative dose values (Δ_i) are the product of the appropriate S, T and E values according to the considered pathways as follows:

$$\Delta_i = S_i T_i^{cloud} E_i^{cloudshine} + S_i T_i^{ground} E_i^{groundshine} + S_i T_i^{cloud} E_i^{inhalation} \quad (25)$$

Table 16. The transport, exposure factors and the representative dose for various nuclides at 800 m distance and 24 hours after the start of the release

Nuclide (i)	T_i^{cloud}	T_i^{ground}	$E_i^{cloudshine}$	$E_i^{groundshine}$	$E_i^{inhalation}$	Δ_i
	(Bqs/m^3)/Bq	(Bq/m^2)/Bq	Sv/(Bqs/ m^3)	Sv/(Bq/ m^2)	Sv/(Bqs/ m^3)	Sv
Ba-137m	4.72E-06	4.69E-09	9.20E-15	9.55E-17	0.00E+00	1.03E-07
Cs-134	3.76E-05	3.75E-08	2.37E-14	2.45E-16	4.13E-13	7.70E-05
Cs-136	3.75E-05	3.74E-08	3.39E-14	3.40E-16	7.50E-14	7.23E-06
Cs-137	3.76E-05	3.75E-08	8.69E-15	9.02E-17	2.88E-13	3.53E-05
I-131	3.75E-05	3.74E-08	5.81E-15	6.42E-17	4.63E-13	3.17E-04
I-131e	3.75E-05	3.71E-07	5.81E-15	6.42E-17	4.63E-13	6.35E-04
I-132	3.27E-05	3.26E-08	3.53E-14	3.58E-16	5.88E-15	2.85E-04
I-132e	3.27E-05	3.22E-07	3.53E-14	3.58E-16	5.88E-15	5.70E-04
Te-132	3.75E-05	3.73E-08	3.19E-15	3.79E-17	1.13E-13	7.50E-05
Xe-133	3.76E-05	0.00E+00	5.38E-16	0.00E+00	0.00E+00	1.40E-02
SUM						1.60E-02

Table 17. The transport, exposure factors and the representative dose for various nuclides at 3 km distance and 4 days after the start of the release

Nuclide (i)	T_i^{cloud}	T_i^{ground}	$E_i^{cloudshine}$	$E_i^{groundshine}$	$E_i^{inhalation}$	Δ_i
	(Bqs/m³)/Bq	(Bq/m²)/Bq	Sv/(Bq s/m³)	Sv/(Bq/m²)	Sv/(Bq s/m³)	Sv
Ba-137m	2.20E-07	2.13E-10	9.20E-15	9.55E-17	0.00E+00	4.80E-09
Cs-134	6.09E-06	6.09E-09	2.37E-14	2.45E-16	4.13E-13	1.25E-05
Cs-136	6.06E-06	6.06E-09	3.39E-14	3.40E-16	7.50E-14	1.17E-06
Cs-137	6.09E-06	6.09E-09	8.69E-15	9.02E-17	2.88E-13	5.72E-06
I-131	6.03E-06	6.04E-09	5.81E-15	6.42E-17	4.63E-13	5.11E-05
I-131e	6.03E-06	5.98E-08	5.81E-15	6.42E-17	4.63E-13	1.02E-04
I-132	3.80E-06	3.79E-09	3.53E-14	3.58E-16	5.88E-15	3.31E-05
I-132e	3.80E-06	3.76E-08	3.53E-14	3.58E-16	5.88E-15	6.62E-05
Te-132	5.97E-06	5.99E-09	3.19E-15	3.79E-17	1.13E-13	1.19E-05
Xe-133	6.07E-06	0.00E+00	5.38E-16	0.00E+00	0.00E+00	2.26E-03
SUM						2.54E-03

Based on these results, the EUR criteria no. 1) of 50 mSv is fulfilled with the representative dose of $\Delta^{\mathrm{800m,24h}} = 16.0$ mSv, and the EUR criteria no. 2) of 30 mSv is also fulfilled with the representative dose of $\Delta^{\mathrm{3km,4d}} = 2.54$ mSv.

It is important to note that the results of the calculation have Sv unit, but it should not be confused with the projected dose or the reference levels or generic criteria of emergency preparedness and response assessment. This representative dose is a percentile of the committed effective dose distribution, its usage is only appropriate in safety assessment, for confirmation of fulfillment of release criteria.

3.3. Sensitivity of the improved methodology to habit data

The two main parts of the CARC calculations are the transport and the exposure calculation. The uncertainty of the calculation can be grouped into model uncertainty, model parameter uncertainty and input parameter uncertainty. In this section, the sensitivity to input parameters, namely the habit and consumption data of the exposure calculation of CARC are investigated providing insight on the influence of these data on the results of deterministic safety assessment.

A simple but realistic DEC release scenario was considered in the assessment. The source term of the released activity was taken from the international CONFIDENCE project [93], as shown in section 3.2 and Table 15. Additional release characteristics were: 50 m effective release height, 0 MW heat content, July 1st release date, and 100% aerosol chemical form of iodine. The receptor point was chosen to be in the plume centerline at 800 m distance from the release point according to the EUR criteria [21] no. 3) to avoid late phase countermeasures (relocation) beyond 800 m.

Regarding the meteorological conditions used for deterministic safety assessments, it is common practice to perform the calculations for a best estimate or conservative parameter set. For example, in Chapter 15.2 of the Final Safety Analysis Report (FSAR) of the Paks NPP [94], the environmental dispersion calculations are performed assuming a wind speed of 5 m/s and light precipitation (1 mm/h) and Pasquill D stability category, which is considered to be the most frequent for the plant site. In my analysis [P2], I have used these wind speed and atmospheric stability values but assumed a larger precipitation with 5 mm/h rain intensity. In addition to using one meteorological dataset I also assessed the effect of various habit and consumption parameters with a real one year-long hourly measurement database containing 8760 datapoints (from the meteorological tower located at the site of the Paks NPP) and the 95th percentile of the results.

To be able to include investigation of food consumption, the committed effective 50 years dose at the 1st year after the release was computed including cloudshine, groundshine, inhalation and ingestion dose for an adult representative person (so the time of exposure was 1 year but the commitment time was 50 years). The default dose conversion factors of CARC were used (taken from ICRP 116 [49] and IAEA GSR Part 3 [53]). In this calculation the effective dose from the different pathways was added and the percentile of the resulting total dose was computed as the final result.

The input parameters of the exposure calculation that I investigated in the sensitivity assessment [P2] are the following with default parameters marked by bold font:

- breathing rate (intensity of activity) taken as the average of the mean short-term value for age groups above 16 years from the US EPA Exposure Factor Handbook [71]
    - **0.735 m^3/h (light intensity)**
    - 1.59 m^3/h (moderate intensity)
    - 2.963 m^3/h (high intensity)
- time spent outdoors daily varied arbitrary:
    - **1 hour**
    - 2 hours
    - 4 hours
    - 6 hours
- shielding (building type) taken as the representative values of shielding factors for surface deposition from the IAEA TECDOC 1162 [95]:
    - **0.4 (wood frame house)**
    - 0.2 (block or brick house)
    - 0.05 (Three or four story structures 1st and 2nd floor)
    - 0.01 (Multi-story structures upper floors)
- food consumption data taken as the default values of the ECOSYS food chain model of PC-COSYMA [73]
    - **No contaminated food consumption**
    - Leafy vegetables: 20 kg/y

- Potatoes: 70 kg/y
- Root vegetables: 15 kg/y
- Fruit vegetables (corresponding to Non-leafy vegetables in Ecosys): 25 kg/y
- Milk: 115 kg/y
- Beef: 25 kg/y

In the analysis, I perturbed the parameters one by one separately. The plume passage was considered to occur while staying outside, thus the cloudshine dose is not affected by the time spent outdoors, and inhalation is only influenced by the intensity of activity connected to the breathing rate [P2].

The effective dose for the default case and the one meteorological data was 8.82 mSv. The results of perturbing separately the various input parameters are shown in Table 18. These values differe from the published results in [P2] due to the slightly modified meteorological parameters.

Table 18. The committed effective 50 year dose for 1 year exposure with perturbation of exposure parameters in case of using one meteorological parameter set

Exposure parameters		Committed effective 50 years dose for 1 year exposure	Ratio with default
Default case: Breathing rate: 0.735 m^3/h (light intensity) Time spent outdoors daily: 1 h Shielding factor: 0.4 (wood frame house) No contaminated food consumption		8.82 mSv	-
Breathing rate (intensity of the activity)	1.59 m^3/h (moderate intensity)	9.48 mSv	108%
	2.963 m^3/h (high intensity)	10.55 mSv	120%
Time spent outdoors daily	2 h	8.95 mSv	102%
	4 h	9.23 mSv	105%
	6 h	9.50 mSv	108%
Shielding factor (building type)	0.2 (block or brick house)	7.77mSv	88%
	0.05 (Three or four story structures 1st and 2nd floor)	6.99 mSv	79%
	0.01 (Multi-story structures upper floors)	6.78 mSv	77%
Consumption of contaminated foodstuff	Leafy vegetables: 20 kg/y	21.12 mSv	251%
	Potatoes: 70 kg/y	11.32 mSv	128%
	Root vegetables: 15 kg/y	10.11 mSv	115%
	Fruit vegetables): 25 kg/y	11.38 mSv	129%
	Milk: 115 kg/y	15.63 mSv	177%
	Beef: 25 kg/y	9.77 mSv	111%
	All foodstuff	36.23 mSv	411%

The 95th percentile of the committed effective dose for the default input parameters and considering a year-long meteorological database was also 8.82 mSv. This is the same value as obtained for the fixed meteorological data but only due to rounding, the exact values were different, 8.81963 mSv for the fixed meteorological data and 8.82407 mSv for the yearly meteorological data. Although the same exposure parameters were used for the two cases, the apparent correlation in the resulting dose is merely a coincidence. Considering the perturbation of the input parameters the results and ratios compared to the default case are shown in Table 19.

Table 19. The 95th percentile of the committed effective 50 year dose for 1 year exposure with perturbation of exposure parameters in case of using one year long meteorological measurement database [P2]

Exposure parameters		Committed effective 50 years dose for 1 year exposure	Ratio with default
Default case: Breathing rate: 0.735 m^3/h (light intensity) Time spent outdoors daily: 1 h Shielding factor: 0.4 (wood frame house) No contaminated food consumption		8.82 mSv	-
Breathing rate (intensity of activity)	1.59 m^3/h (moderate intensity)	9.67 mSv	110%
	2.963 m^3/h (high intensity)	11.10 mSv	126%
Time spent outdoors daily	2 h	8.85 mSv	100%
	4 h	8.89 mSv	101%
	6 h	8.94 mSv	101%
Shielding factor (building type)	0.2 (block or brick house)	8.61 mSv	98%
	0.05 (Three or four story structures 1st and 2nd floor)	8.47 mSv	96%
	0.01 (Multi-story structures upper floors)	8.43 mSv	96%
Consumption of contaminated foodstuff	Leafy vegetables: 20 kg/y	10.96 mSv	124%
	Potatoes: 70 kg/y	9.23 mSv	105%
	Root vegetables: 15 kg/y	9.00 mSv	102%
	Non-leafy vegetables (fruit vegetables): 25 kg/y	9.22 mSv	104%
	Milk: 115 kg/y	11.31 mSv	128%
	Beef: 25 kg/y	9.03 mSv	102%
	All foodstuff	15.41 mSv	175%

Overall, the results are in line with the expectation that considering long-term meteorological data and a higher percentile (but not the maximum) is more robust (i.e. resistant or shows lower variation) against changes in habit data compared to using a single one meteorological parameter set is used. An exception is observed in the inhalation, for which increasing the intensity resulted in a larger effect for the percentile compared to using a single one meteorological case.

The parameter with the lowest influence, both in single meteorological case and when using the year-long database was the time spent outside and the type of building. These factors only cause around a 10% difference in the effective dose. The low level of influence of these two parameters is partly due to the fact that these only affect the groundshine dose whose contribution to the total effective dose is around 20%. The intensity of outdoors activity and the consequent variation in breathing rate resulted in a more considerable difference, significantly affecting the committed effective dose despite the inhalation dose having a contribution of only around 7%. The consumption of contaminated foodstuff had the largest effect on the results computed for a single meteorological case. The ratios compared to the default values with no consumption ranged between 111-251% for different foodstuff. When consumption of all foodstuffs was considered, there was a more than fourfold increase in the effective dose.

Using a long meteorological measurement database and the 95th percentile resulted in lower influence of the time spent outside, the type of building and the consumption of contaminated foodstuff on the effective dose compared to the case of using a single meteorological data. The effective dose is more sensitive to the breathing rate and thus to the intensity of the activity when not only a single, but a long meteorological database is used in the calculation. This is partly due to the higher contribution of about 9% of inhalation to the total dose. Changing the time spent outside and the type of building only caused less than 5% difference in the 95th effective dose percentile, groundshine contribution to total dose being around 3%. The consumption of contaminated foodstuff resulted in a maximum of 75% difference compared to the case without consumption.

The effective 1-year dose did not exceed the proposed 20 mSv safety criteria with either perturbation of the habit parameters. However, if the result is closer to the safety criteria (computed for a different percentile or with a different meteorological dataset) variations in habit data can affect compliance.

My main conclusion is that in deterministic safety assessment using a long meteorological database and a relatively high percentile instead of just one meteorological parameter set chosen as a best estimate lead to an effective dose that is less sensitive to most of the considered exposure parameters, namely time spent outdoors, shielding factor, consumption of contaminated foodstuff (with the exception of breathing rate resulting in higher sensitivity due to higher contribution of inhalation to total dose). Thus, using a long meteorological database and a relatively high percentile in deterministic assessment produces more robust, i.e. less variant results.

The results can be compared to deterministic safety criteria, the value of which can differ from country to country. In Hungary, according to Hungarian Nuclear Safety Codes [59] and the current National Nuclear Emergency Response Plan (OBEIT) [63], the criterion for DEC for yearly exposure is 20 mSv. More specifically the criteria refer to the exposure during the first year excluding the first 7 days after the release. As my calculations were conducted for a hypothetical release case the comparison with the criteria just serves demonstrational purpose, I compare the total 1-year dose with the proposed 20 mSv safety criteria. Nevertheless, my results show that the criterion is exceeded only in case of using one meteorological parameter set with consumption of leafy vegetables or all considered contaminated foods.

The difference between these results and the case study demonstrating the application of the CARC methodology mainly arises from the difference in the orientation of the selected receptor points. Here, the result for one selected direction is used whereas in the previous case study (Section 3.2), the maximum value around 16 sectors was considered. The approach of selecting a receptor point at one direction is consistent with assessing residence at one fixed location, whereas computation of the maximum value for various directional sectors provides an overall analysis of the surroundings of a nuclear facility. When considering a fixed location with a real meteorological database, lower results are produced compared to those computed with the maximum around all directions. This is expected as the wind does not consistently blow in the selected direction, resulting in many zero values.

4. THE IMPACT OF USING DIFFERENT METEOROLOGICAL DATA FOR DETERMINISTIC SAFETY ASSESSMENT

In the case of the atmospheric release of radioactive material, the trajectory of the dispersion and the size of the contaminated area are determined by the weather conditions. The parameters that characterize the meteorological conditions and therefore are most commonly considered in atmospheric dispersion modelling for safety assessment which include the wind vector, atmospheric turbulence and precipitation.

For nuclear safety assessments, meteorological parameters need to be characteristic and representative of the location of the atmospheric release taking into account long-term changes to describe a wide range of possible events. As the resolution of available meteorological information is limited in both time and space, a measurement database for one location over an extended time period (at least one year) is usually utilized in such assessments. A common practice when such assessments were first conducted was to perform assessment with only one meteorological parameter set selected to be either conservative or a best estimate of local characteristics [10]. Alternatively, several meteorological conditions were conducted but with very simple dispersion models [17]. When only one meteorological parameter set is used, it is difficult to select one that best describes possible events and even more challenging to appoint a conservative one, as the more and more conservative conditions usually have a lower probability of occurrence and unrealistically higher level of consequences as a result. With the increase in computational capacity, it became feasible to perform a greater number of calculations with the consideration of different meteorological data better representing the wide range of possible consequences specific to a given site. The results of utilizing different meteorological conditions can be described with a selected statistical parameter, such as the mean, range, percentiles or a distribution derived by binning the results.

The main requirements for the calculation approach to be used for deterministic nuclear safety assessment and the meteorological input data to be considered

- to be informative so that accurately detailed information can be provided about the possible consequences to promote informed judgement of safety;
- to be robust, i.e. to be resistant to small changes in the input data so that the uncertainty of meteorological parameters does not significantly affect the final result and thus the decision on safety;
- to be optimized so that the required level of complexity can be ensured and to be practically feasible and efficient, balancing computational demands with the need for precise results

In my work I investigated different aspects of usage of meteorological databases for deterministic safety assessment and as a conclusion outlined a universal that can ensure that the requirements of informativeness, robustness and optimization are fulfilled. The methodology of my assessment is an optimal technique in terms of the computational burden that can be applied in safety assessments to compile the meteorological input. Another contribution of my analysis is that it provides insight into the uncertainties of dose assessments caused by the uncertainties of the meteorological input data. My methods also support the selection of a percentile for the verification of safety criteria, illustrating the range of possible candidates, only pertaining to specific input data and endpoints used, avoiding arguing in favor of a given percentile generally, ensuring the chosen percentile is relevant to the specific context of the assessment.

I used the CARC software for the investigation with a release scenario taken from literature according to the international case study of the CONFIDENCE project [P10]. The release duration was considered to be instantaneous with an effective release height of 120 m, 0 MW energy content and 100% aerosol chemical form. The exact released activity results are shown in Table 20.

Table 20. The release activity of the considered nuclides in the meteorological case study [P10]

Nuclide	Released activity [Bq]	Nuclide	Released activity [Bq]
Xe-133	3.90E+18	Cs-134	2.99E+15
I-131	2.50E+16	Cs-136	7.08E+14
I-132	3.16E+16	Cs-137	2.29E+15
Te-132	1.52E+16	Ba-137m	3.09E+14

The meteorological data that I used for the assessment was obtained from a real measurement station (from the meteorological tower located at the site of the Paks NPP) with data available at 10-minute resolution for five consecutive years from 2014 to 2018 at a measurement height of 120 m. The distance between the measurement station and the proposed discharge point is about 100 m. The surrounding area around the station is flat and the data can be considered representative of the local conditions.

The meteorological database contains the wind direction [°], wind speed [m/s] the Pasquill stability class and precipitation [mm] values with a 10-minute time resolution. The Pasquill stability classes were determined based on the horizontal fluctuation of the wind direction and were indicated with alphabetical letters which I converted into numbers for the purpose of averaging. Fixed inversion layer height values were used linked to the six Pasquill stability classes according to the following [85]:

- class A: 1600 m;
- class B: 1200 m;
- class C: 800 m;
- class D: 560 m;
- class E: 320 m;
- class F: 200 m.

In the following paragraphs, I present statistical information about the meteorological database. In Figure 3, I show the annual average and maximum wind speed and in Figure 4, I show the occurrence of various atmospheric stability conditions grouped based on their classification (unstable: A, B, C; neutral: D, stable: E, F). I determined the hourly precipitation intensity by summing the six consecutive 10-minute values. In

Table *21*, I summarize the annual total precipitation amount and the corresponding duration of the precipitation events, and the maximum and average precipitation intensity derived from the hourly precipitation values. When computing the average precipitation intensity, I did not take into account the zero values not to bias and underestimate the mean. The highest precipitation intensity was registered as 96.6 mm/h on 29 09 2014. The annual total precipitation was the highest in 2014. The lowest number of hours of precipitation was in 2017 and the total and average precipitation was lowest in 2018. In Figure *5*, I show the annual wind rose for 16 directions.

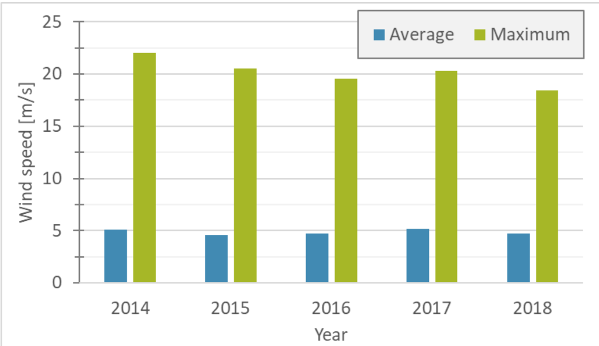

Figure 3. Annual wind speed (average and maximum) [P3]

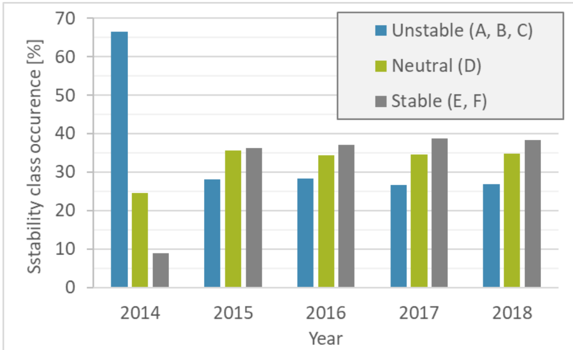

Figure 4. The occurrence of different Pasquill stability classes each year [P3]

Table 21. Annual statistics of the precipitation [P3]

Year	2014	2015	2016	2017	2018
Annual total precipitation [mm]	3298	621	662	606	496
Annual total precipitation duration [h] (% of the yearly weather)	575 (6.6%)	605 (6.9%)	674 (7.7%)	586 (6.7%)	625 (7.1%)
Maximum precipitation [mm/h]	96.60	28.20	21.10	13.80	10.90
Average precipitation [mm/h]	5.736	1.027	0.982	1.035	0.793

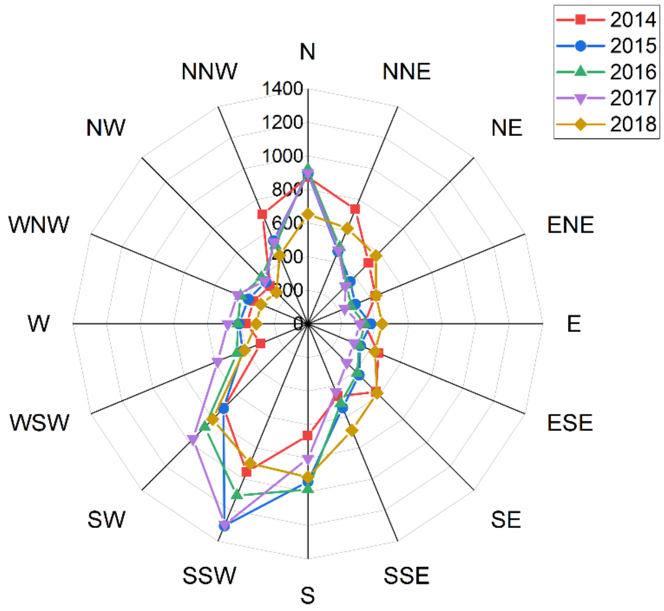

Figure 5. Annual wind rose for 16 directions [P3]

Most of these meteorological parameters show similar annual values (except for the stability groups and the annual total rainfall in 2014), which means that due to the insignificant variation in the values, a one-year dataset may be representative of the weather conditions of this location. Using less than one yearly data would not be optimal as the monthly variation in the meteorological parameter is usually much higher than the year-to-year variation. For example in 2015 the monthly average and maximum wind speed values (in Figure 6) and the monthly total precipitation values (in Figure 7) show a higher variation compared to the same yearly values. The precipitation shows the larger variance having a maximum of total rainfall of 140 mm/month in August and a minimum of around 0 mm/month in December. This aligns with the expectation, what we would expect, and this variation emphasizes the necessity of using at least 1 yearlong meteorological database for deterministic safety assessment calculations.

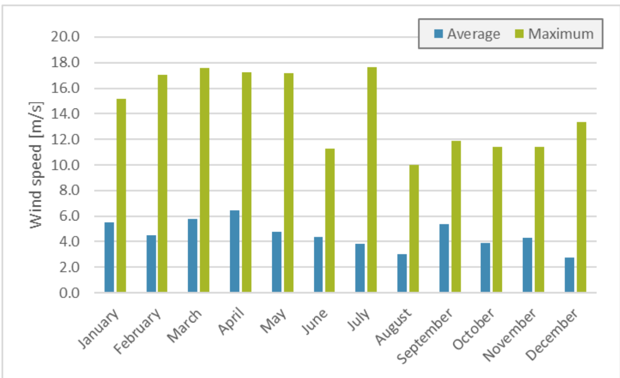

Figure 6. Monthly average and maximum wind speed in 2015 [P3]

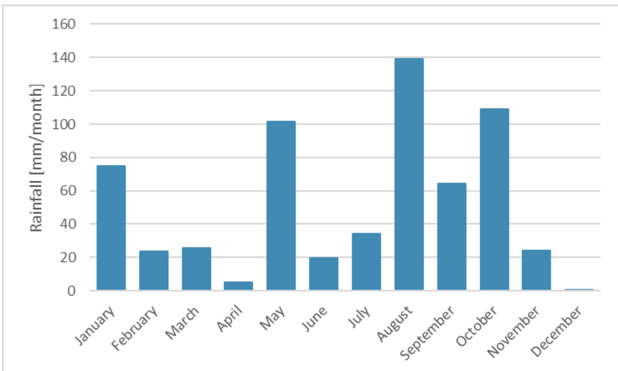

Figure 7. Monthly total precipitation in 2015 [P3]

An additional influential aspect of atmospheric dispersion modelling is the treatment of very low wind speed values. The measurement of these very low values, around or below 1 m/s is very uncertain, thus these wind speed and direction values have high uncertainty. In the dispersion calculation the horizontal dispersion parameter (see Eq. ((2)) in section 2.1.3) is expanded in case of very low wind direction values using the minimum threshold of the measurement system [38]. The minimum measurement threshold for the wind vane that was the source of the meteorological data was 0.5 m/s, so in the calculations I used this value. In the yearly meteorological data, the occurrence of wind speed measurement data below 0.5 m/s was around 4-7%.

The meteorological data was considered with separate simulations for each data point. The result I calculated for the assessment were the effective committed 7-day dose either at fixed locations or as maximum values in 16 directional sectors. The maximum along the 16 directions was determined by performing the atmospheric dispersion and deposition calculation for 16 receptorpoints that were defined at the various angles and the maximum from these were seleted for each meteorological data point. Then, these values were sorted in ascending order for all of the considered meteorological data, and the specific percentiles of the results were selected. I evaluated the results at the distances of 1 km, 3 km, 10 km and 30 km. The results at fixed points correspond with the requirements of DBC while the maximum in all directions is in accordance with the requirement of DEC. The cloudshine, groundshine and inhalation pathways were included in the dose assessment, where exposure of 7 days and commitment of 50 years was taken. In deterministic safety analysis, the goal is to calculate a scenario that can be considered to cover all the possible consequences above a specific probability of occurrence. In practice, a high percentile value such as the 95th or the 99.5th percentile is used for such a scenario. Using the maximum would be overly conservative and representing a case with very low probability of occurrence. On the contrary, using a lower percentile, such as the median, would not provide information on the more severe consequences. In the following, I present my results in histograms as dose distributions and as selected percentiles ranging from the 80th to the 100th. As the actual dose values of the calculations are of no importance in this assessment, I show my results normalized to the maximum dose or as ratio of two dose values obtained with the consideration of different meteorological input.

I evaluated the variability of the meteorological measurement database and the effect it can have on the dose calculation for safety assessment. My methodology and conclusions are general even though the exact results of my calculations are only valid for the location and time interval of the selected meteorological database.

4.1. Meteorological "Worst case"

Even though advanced computational capacity allows to conduct deterministic safety assessment for a large number of different meteorological conditions there are regulatory requirements to perform one deterministic nuclear safety assessments with only a couple of meteorological situations.

It is also a common practice to compute the consequences of a meteorological worst-case scenario that is chosen based on expert judgment. In some cases, this meteorological parameter set is fixed for decades to enable the atmospheric calculations and thus the dose estimations to be performed on the same basis, using the same meteorological parameters. The selection of the worst case meteorological conditions it not straightforward because it depends on the distances and the endpoints being considered. In addition, it would be unrealistic to consider the worst characteristics for every meteorological parameter and location. The dose analysis for safety assessment is performed differently for DBC and DEC. For DBC, the dose calculation is carried out for a specific place and person (representative person), which may not be located in the prevailing wind direction, whereas for DEC, the doses are computed independently from the wind direction. To be appropriate for both DBC and DEC, I computed the effective 7-day dose at 1 km either in a fixed direction (at 0°) assuming that at the residence of the representative person and at 16 directions selecting the maximum value from the results.

In my assessment I selected the proposed worst case meteorological parameters on the basis of the ones used in Chapter 15.2 of the Final Safety Analysis Report of the Paks NPP [94]. However, because those parameters were considered to be the most frequent for the plant site, I chose more conservative values to better represent a proposed worst case. Instead of Pasquill D atmospheric stability class, I utilized the Pasquill F class, which describes a more stable atmosphere with a smaller plume spread and therefore a higher air activity concentration (consistently with calculation conducted for the FSAR of the Paks NPP prior to 2012). For the wind speed, I considered the value of 2 m/s instead of 5 m/s, which results in a smaller spread along the x-axis of the plume and consequently a higher air activity concentration. Regarding the rain intensity, I considered the same 1 mm/h value as in the FSAR of the Paks NPP [94].

I computed the effective dose for this proposed meteorology and for all the data points in the 5-year long database. My goal with these calclations was to demonstrate that the utilisation of a meteorological measurement database yields dse results that are less variant than those obtained from a single predetermined meteorological parameter set selected without the consideration of the actual meteorological characteristics. In order to show the difference in the two types of calculations, I derived the ratio of the dose results obtained from the proposed worst case scenario and for the meteorological inputs leading to the actual worst consequences for each year of the database as shown in Table 22. I summarize the meteorological condition of the cases which yielded the highest values of the effective 7-day dose computed at 1 km distance for every considered year in Table 23. The relative variation of the maximum effective 7-day dose at 1 km distance and 0° direction and within 16 sectors for each year is 71% and 197%, respectively.

These results illustrate that in the case of using only a single meteorological condition chosen based on expert judgement or selected according to a measurement database, there can be a large difference in the computed doses. My results also indicate that in a large meteorological database, the actual worst case can be too conservative and describe conditions with a very low probability of occurrence and thus not be representative of the location. I note, that I obtained these ratios of the effective doses computed at 1 km, but the values could be different at other distances.

Table 22. The ratio of the actual and proposed worst case scenario regarding the effective 7-day dose at 1 km for each year [P3]

Year	Ratio of effective 7-day dose [%]
2014	4 900%
2015	2 470%
2016	2 000%
2017	479%
2018	1 660%

Table 23. The meteorological conditions yielding the highest effective 7-day doses at 1 km for each year [P3]

Year	Wind speed [m/s]	Wind direction [°]	Pasquill category	Precipitation [mm/h]
2014	0.16	61.3	B	2.5
2015	0.15	17.8	C	0.3
2016	0.52	10.4	E	1.3
2017	0.57	357.6	C	0
2018	0.19	288.1	B	0.8

In Table 24, I present the ratios of the effective 7-day doses computed as the maximum value of the 16 directional sectors at 1 km distance and the preselected worst case meteorology (wind speed: 2 m/s, Pasquill class F, precipitation intensity: 1 mm/h). As I mentioned before the maxium along 16 sectors was determined by performing the atmospheric dispersion and deposition calculation for 16 receptorpoints (defined at the various angles) and the maximum from these were seleted for each meteorological data point. These values were then sorted in ascending order for all of the considered meteorological data, and the specific percentiles of the results were selected, in this case the 100th percentile.

Table 24. The ratio of the actual and proposed worst case scenario regarding the maximum effective 7-day dose at 1 km within 16 sectors for each year.

Year	Ratio of the maximum effective 7-day dose within 16 sectors [%]
2014	11 100%
2015	69 880%
2016	4 020%
2017	1 140%
2018	3 030%

This method corresponds to the DEC assessment when the doses are determined independently from the wind direction. Here I obtained higher ratios than with the fixed direction, the reason of which is that when considering every direction, there is no constraint on the meteorological database thus yielding more conservative results.

These results illustrate that there could be several order of magnitude difference in the computed doses when applying different methods for selecting the worst case meteorological scenarios. The results also show that there is a wide range of possible consequences but without containing any information about the frequency of occurrence of these doses, which is of paramount importance to enable differentiation between consequences that have extremely low or reasonably high probability of occurrence. Thus, it is imperative to take into account many meteorological occurrences to get information about the frequency of the possible outcomes. Concerning the three expectations of being informativeness, robustness and optimization about the method of using meteorological data for deterministic safety assessment, this approach of using a proposed or actual worst-case scenario is somewhat informative, it is definitely not robust but requires minimal computational capacity therefore it can be considered as optimized.

4.2. Usage of dose percentile

When using a long-term meteorological database for deterministic safety assessment, the question arises of how long the considered database should be to cover the local characteristics well, while not requiring unnecessarily high computational resources for an established site or allowing a sufficient time for the otherwise time-consuming establishment of an adequately comprehensive meteorological database for a new site. If meteorological data is not available for a site location for a long time period, it would be possible to use a correction factor to be multiplied by the dose percentile computed with meteorological data for the shorter period. This multiplication factor, with values larger than 1, would represent the inherent variability of meteorological parameters, which might not be accounted for with fewer meteorological data. This factor is hard to quantify without extensive knowledge about the weather characteristics of a given site. In my work I provide examples of what values this multiplication factor could take based on the available 5-year long data and demonstrate how it could be used. But for a real new site, this factor should be determined according to pre-estimating the variability of the meteorological conditions and the evaluation of how this will propagate throughout the dose calculation. Usually, at least one year-long meteorological database is used, but if data is available for a longer time period it could be also used. Another decision related to using several meteorological data points instead of a single one is the value of the percentile to be used as the final result of the assessment when comparing with a regulatory limit. Based on literature, there are two candidates that are commonly mentioned and utilized 1) the 99.5th percentile described in the US.NRC Regulatory Guide 1.145 [17]; and 2) the 95th percentile chosen in the determination of the release coefficients for acceptance criteria published in the European Utility Requirements [21]. With my assessments I aim to verify that for this specific case (release and site characteristics, meteorological database and computed quantities), the 95th percentile would be an appropriate choice to use as the final result of the safety assessment.

First, to investigate if it is sufficient to use meteorological data measured corresponding to a shorter time period so that computing intensity can be decreased while maintaining the aimed precision of results, I conducted the assessment using different 3-month periods from the 2014 data so that the effect of the seasonal variation on the dose results can also be evaluated. In Figure 8, I show the normalized 7-day effective doses calculated at a fixed location in a histogram for the various time periods (covering different 3-month and the entire 5-year durations). As the number of meteorological data points differ for the various durations, I normalized the number of simulations to the total value and show their percentage in each range. The shape of the histograms for the 3-month periods seem more or less in accordance with those of the 5-year-long results, but there is definite difference between the values for the various 3 months, particularly for the higher doses. In Figure 9, I show the ratio of the 7-day effective doses calculated from the 3-month to the 5-year meteorological data series for variant percentiles ranging from the 80^{th} to the 100^{th}. The ratios cover 4 orders of magnitude with the lowest result of 0.04% obtained for October-December 2014 and the highest of 1107% for April-June 2014. This demonstrates that due to the large variability, it would not be optimal to apply a multiplication factor for the 3-month meteorological measurement data. To guarantee the conservatism of the calculation the multiplication factor shall be based on the largest predicted variance of the result. If a multiplication factor were used in this case, its value would be 2500 based on the largest difference, in this case the lowest ratio, which is 0.04%. This would result in an overestimation of 27500 times for the 80^{th} percentile of the April-June 2014 result compared with the one obtained with the 5-year-long meteorological data.

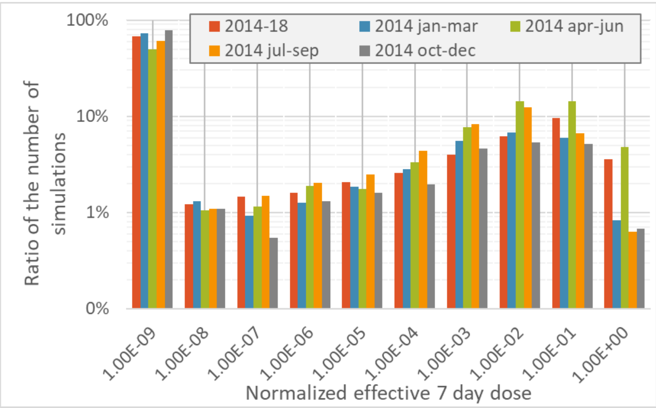

Figure 8. Histograms of the normalized effective 7-day dose at 30 km distance in 0° direction for 3 months and 5 years of meteorological data [P3]

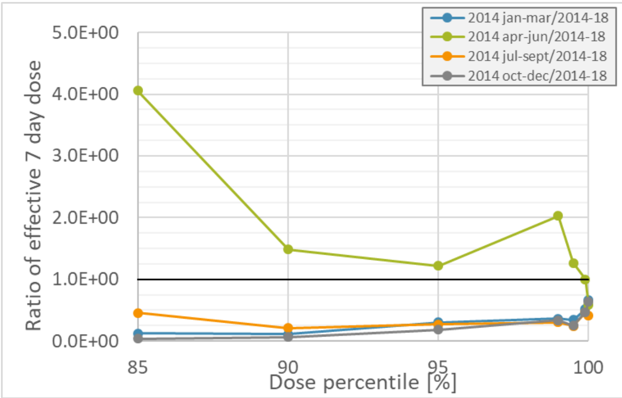

Figure 9. The ratio of dose percentiles at 30 km distance in 0° direction for 3 months and 5 years of meteorological data [P3]

Looking at the yearly meteorological data, I calculated the dose values at 0° direction and as the maximum along 16 directional sectors. The histograms and the ratio of percentiles for the fixed direction are shown in Figure 10 and Figure 11, and for the 16 sectors in Figure 12 and in Figure 13, respectively. I evaluated the doses at various distances but as the results were similar I only show the ones for 30 km distance as an example.

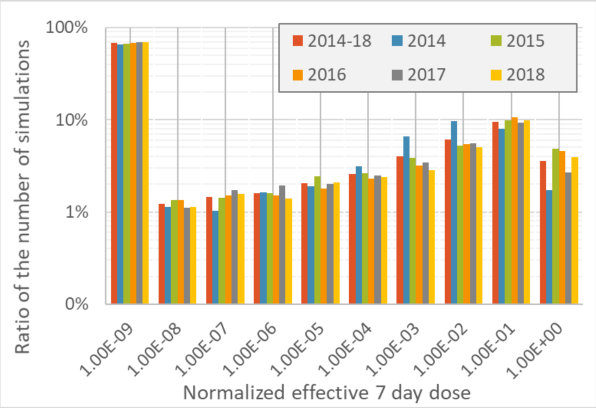

Figure 10. Histograms of the normalized effective 7-day dose at 30 km distance in 0° direction for 1 and 5 years of meteorological data [P3]

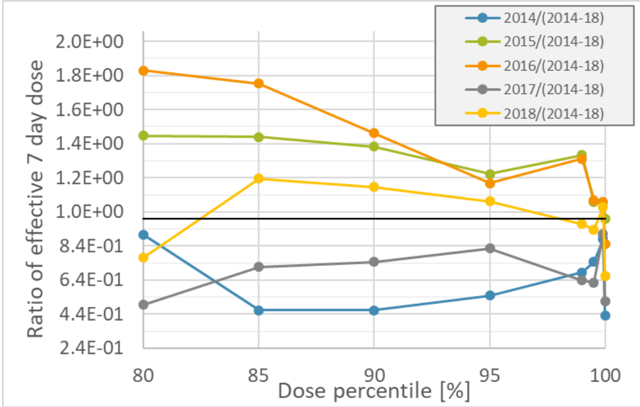

Figure 11. The ratio of dose percentiles at 30 km distance in 0° direction for 1 and 5 years of meteorological data [P3]

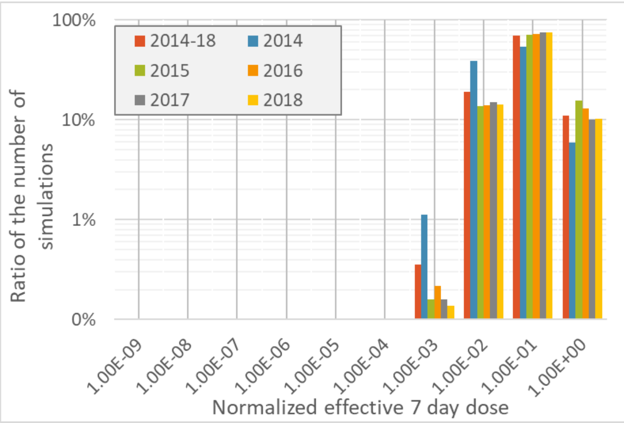

Figure 12. Histograms of the maximum normalized effective 7-day dose along 16 directions at 30 km distance in for 1 and 5 years of meteorological data [P3]

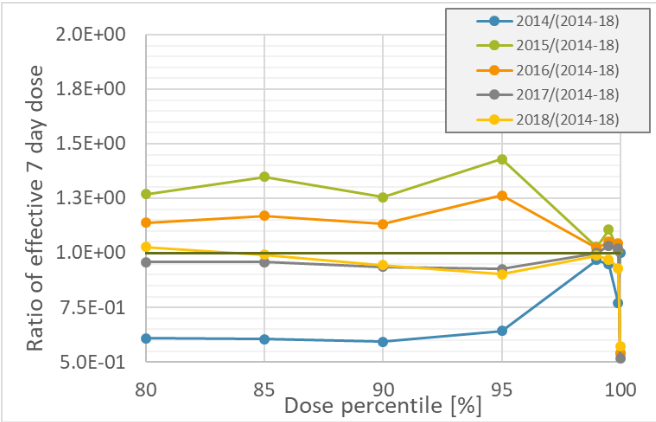

Figure 13. The ratio of the maximum normalized effective 7-day dose percentiles along 16 directions at 30 km distance in for 1 and 5 years of meteorological data [P3]

As expected the variability of the percentiles is lower for the 1-year and the 5-year meteorological data with the ratios ranging between 41% to 353% in the 0° direction and between 33% to 215% for the maximum along the 16 directions. The nature of the curves for the various years look relatively similar except for the year 2014 which is explained by the different meteorological conditions in that year. As shown before, the total precipitation in 2014 was about 5-6 times higher than in the other years and regarding the atmospheric stability, unstable conditions occurred about twice as often in 2014 than in the other years. This also demonstrates that these meteorological parameters can significantly influence the atmospheric dispersion calculations and thus the resulting doses.

If only one year of meteorological data is available, it is not definitely predictable how the next year will relate to it and how it would affect the dose results. The multiplication factor can be used in this case with conservative assumptions, selected on the basis of the worst ratios (which represent the largest difference between the used meteorological databases). For the computations at 0° direction, these ratios for the 90th, 95th and 99th percentiles were 41%, 72% and 63%, and for the maximum along 16 sectors were 76%, 67% and 88%, respectively. According to the reciprocal values of these ratios, the multiplication factor to be used in the safety assessment for this specific type of calculations (release and site characteristics, meteorological data computed quantities) and for the 90th, 95th, and 99th dose percentiles should be 2.41, 1.39 and 1.58 at fixed direction and 1.32, 1.50 and 1.13 for the maximum along 16 directions. Thus, the resulting doses of the calculations should be multiplied and corrected with these values to account for the variability in the meteorological data. The multiplication factor should be determined based on an acceptable length of meteorological data which length can be different for various locations. Nevertheless, it would not be optimal to use a database less than 1 year long as the seasonal variability of the meteorological conditions could be significant. Similarly, using incomplete years for example two summers and two winters would potentially distort the results. When there is 1-year-long or even longer meteorological data with hourly time resolution, the decision to use a multiplication factor or not should be based on the variability of the available data. The multiplication factor could also be determined based on meteorological data for a different location but with similar characteristics to the actual release point. I note that variability of the meteorological conditions on a longer term (e.g.10-20 years) should also be taken into account which would be expectedly higher due to the changes in the climate, but the investigation of long-term changes in meteorological conditions is out of the scope of my work.

To compare the actual worst consequences and the results obtained with the preselected worst case meteorology chosen a conservative parameter set based on expert judgement, I show in Table 25 the ratio of the highest 7-day effective dose for each year and the proposed worst case scenario with wind speed of 2 m/s, wind direction of 0°, Pasquill F class and precipitation of 1 mm/h for selected percentiles (the results for the 100th percentile are already shown in Table 22). For the various years the ratios for the 95th percentile range from 38% to 64%, for the lower percentiles the ratios are less than 25% and for the higher percentiles, the ratios are larger than 148%. The ratios range between 1-437% for the 5 years meteorology.

Table 25. Ratio of the 7-days effective dose percentiles and the proposed worst case result at 1 km for various lengths of meteorological data [P3]

Percentiles	Ratio of effective 7-day dose percentiles for different meteorological data and the dose results of the proposed worst case					
	2014	2015	2016	2017	2018	2014-2018
80th	4.92%	1.35%	1.41%	0.40%	0.75%	1.47%
85th	10.30%	4.91%	5.30%	2.16%	4.28%	5.18%
90th	24.7%	20.1%	21.3%	7.36%	14.2%	17.7%
95th	51.7%	64.0%	60.8%	38.0%	50.5%	52.7%

99th	281%	277%	251%	148%	181%	234%
99.5th	335%	332%	320%	264%	281%	317%
99.9th	1550%	454%	444%	369%	423%	437%

Using the previously determined multiplication factor, the ratio of the 95th percentiles and the proposed worst case would be between 53-89%, for the 90th and 99th percentile this range would be 18-60% and around 200-500%, respectively. This demonstrates that depending on the chosen percentile and the endpoint (e.g. distance from the release point) the optimal multiplication factor varies. Thus for a safety assessment of a real NPP, these should be defined in specific guidelines based on which the multiplication factor could be more precisely determined.

Concerning the expectations about the method of using meteorological data for deterministic safety assessment, this approach of using a higher percentile e.g. the 90th, the 95th or the 99th based on a one year long database is more robust than using one selected meteorological conditions, but requires a little more computational capacity. Regarding the aspect of being informative, using a higher percentile such as the 95th or the 99th achieves the expectation of conservativism, but is not as overly conservative as the actual worst case (the 100th percentile), which may be an outlier with very low frequency of occurrence. The objective of my assessments was not to argue in favour of using a particular percentile, but to demonstrate the appropriateness and robustness of the 95th percentile applied in the EUR [21]. However, based on my results the 99th percentile could be acceptable as well, because it also meets the requirement of robustness but does not take into account the highest 1% of the results describe very rare and extreme conditions.

4.3. Imperfections of meteorological databases

In this section I investigate how the deficiencies in the meteorological database can influence the results of the assessment to quantify the effect of different amount of missing data points on the effective dose percentiles using 1 year long meteorological data.

When prolonged meteorological measurements are gathered, the problem with missing data usually arises due to a failure of the equipment or from a planned shutdown. In literature, the studies that are related to how the missing meteorological data could be substituted are mostly in the field of climatology or agriculture (e.g., [96], [97]). However, the same issues arise in radiological assessments when such meteorological databases are applied with the expectation of appropriate representation of the weather characteristics. In general, the raw data of meteorological databases are not accessible (usually only the hourly or daily averages or sums are available without knowing how many data points were taken into account in their computation) so the evaluation of the completeness is not always possible. In various applications however, there are completeness requirements specified by guidelines, for example in air quality modelling 90% of the database required to be available [98], or in climatological calculations 80% or the data is needed [99]. There can be differences in the reliability of the meteorological measurements obtained from various weather stations as shown in a research article [100], where the completeness of the meteorological parameters is evaluated for several stations, with values of the completeness ranging between 59.3% and 99.8% for wind speed and between 36.4% and 99.0% for precipitation.

In order to assess the influence of using such incomplete databases, I made calculations with different amounts of missing data from the hourly meteorological data. I computed the dose percentiles with the consideration of the full and incomplete meteorological database for 2015, where I artificially generated incomplete data sets using various methods: I considered occasional errors in the measurements with omitting sporadically scattered data points and simulated a prolonged failure of the system by leaving out longer periods of data consecutively.

4.3.1. Scattered omission of meteorological data

With the omission of sporadical values from the 2015 meteorological database, I first computed the doses at a fixed 0° direction. I omitted the meteorological measurements jointly, meaning that for a given time step, I skipped all parameters as if the entire weather station experienced a temporary error. I selected the utilized subset of the meteorological database randomly by stepping through the data points randomly until the targeted number of points was obtained.

In Figure 14, I show the normalized effective 7-day dose histograms for different meteorological subsets. I normalized the number of simulations in each category with the total number to show the results on the same basis. Most of the dose results obtained with the calculations were very low, and there were relatively higher bin numbers at around 0.1-1% of the maximum.

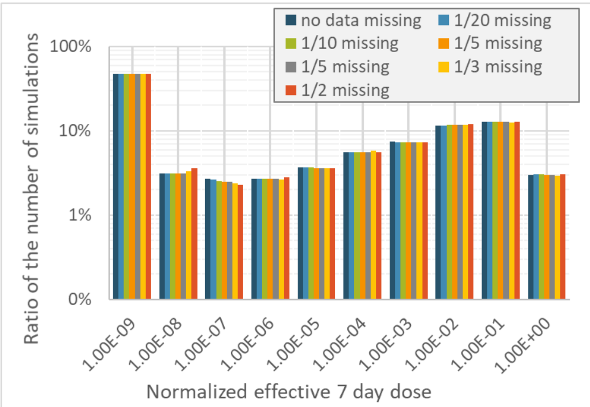

Figure 14. Histograms of the normalized effective 7-day dose at 1 km distance in 0° direction for different amount of 2015 meteorological data missing (sporadically) [P3]

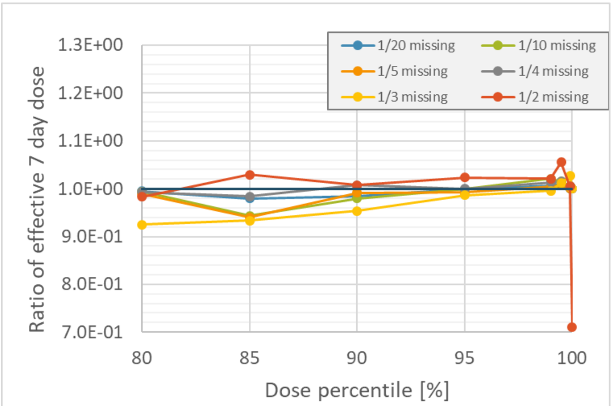

Figure 15. The ratio of dose percentiles at 1 km distance in 0° direction for different amount of meteorological data missing (sporadically) divided by the results obtained with the 2015 annual database [P3]

I show the ratio of the dose percentiles computed with different amount of missing data with the ones obtained with the entire year-long database at 1 km distance and in the 0° direction in Figure 15. The curves produced for the other distance were very similar. The difference between the dose percentiles is not substantial, the ratios range between 92% and 106% for the percentiles from the 80th to the 99.9th. However, regarding the 100th percentile, there can be significant difference in the final dose, if exactly those meteorological conditions are missing which result in the highest dose. The lower the amount of missing data points there is less probability that in the random selection, the scenario resulting in the highest dose is selected. I present the ratios of the 100th dose percentile obtained with the incomplete and full database in Table 26.

Table 26. The ratio of the 100th dose percentile for the incomplete and full meteorological data of 2015 (data missing sporadically) [P3]

Amount of missing meteorological data	Ratios of the 100th effective 7-day dose percentiles for various distances			
	1 km	3 km	10 km	30 km
1/20	100.0%	100.0%	100.0%	100.0%
1/10	100.0%	100.0%	100.0%	100.0%
1/5	100.0%	100.0%	100.0%	100.0%
1/4	100.0%	100.0%	100.0%	100.0%
1/3	100.0%	100.0%	100.0%	100.0%
1/2	71.1%	50.0%	56.9%	100.0%

The only difference in the 100th percentile was obtained for half of the meteorological data missing, but with a significant deviation. This suggests that even with a third of the data missing, the worst case was still in the considered subset of meteorological data. The most robust percentile (excluding the 100th as too conservative based on the findings of the precious sections) with the smallest variations due to the missing meteorological data was the 95th with a maximum difference of 4%. I summarize these ratios for the 95th percentile for the considered distances in Table 27. Some of the other percentiles such as the 80th, 85th, 90th and 99th also showed considerably low variability with difference ranging from -8% to +24% for the considered cases.

Table 27. The ratio of the 95th dose percentile for the incomplete and full meteorological data of 2015 [P3]

Amount of missing meteorological data	Ratios of the 95th effective 7-day dose percentiles for various distances			
	1 km	3 km	10 km	30 km
1/20	99.9%	100.0%	99.6%	99.8%
1/10	99.9%	99.7%	99.1%	98.6%
1/5	99.2%	99.4%	99.1%	97.8%
1/4	100.0%	100.0%	99.2%	97.6%
1/3	98.6%	99.3%	96.8%	95.6%
1/2	102.0%	104.0%	102.0%	100.0%

I made further calculations with more complete databases, with only a small amount of missing data (e.g. 1/200, 1/100 and 1/50). As expected, the obtained dose percentiles were very close, with less than a 5% difference, which deviation is insignificant considering the other types of uncertainties in atmospheric dispersion modelling and dose assessment.

4.3.2. Consecutive periods omitted from the meteorological data

Considering prolonged failure or shutdown of the meteorological measurement system I conducted dose calculations leaving out consecutive periods, i.e. specific months from the 2015 meteorological data. I chose to omit the wettest months as precipitation is shown to significantly influence atmospheric dispersion and dose calculation [P5]. I summarize the total monthly precipitation values in 2015 in Table 28. The months with the highest total rainfall are August, October, May, January and September in decreasing order. In my calculations I omitted these months (not just the precipitation values but all of the meteorological parameters) one after the other from the considered meteorological data.

Table 28. The total monthly precipitation in 2015 (wettest months indicated with bold font) [P3]

Month	**Jan**	Feb	Mar	Apr	**May**	Jun
Rainfall [mm/month]	**74.7**	23.6	25.6	4.9	**101.7**	19.5
Month	Jul	**Aug**	**Sep**	**Oct**	Nov	Dec
Rainfall [mm/month]	34.2	**139.1**	**64.2**	**109.1**	24.4	0.2

In Figure 16, I preset the histograms of the normalized effective 7-day dose at 1 km distance in 0° direction for different months of meteorological data missing. The histograms look very similar but show a little shift to the lower values with increasing the number of missing months. The ratio of dose percentiles at 1 km distance in 0° direction is shown in Figure 17 for different months of meteorological data missing divided by the results obtained with the 2015 annual database. The ratios above the 90th percentile are between 40%-101%.

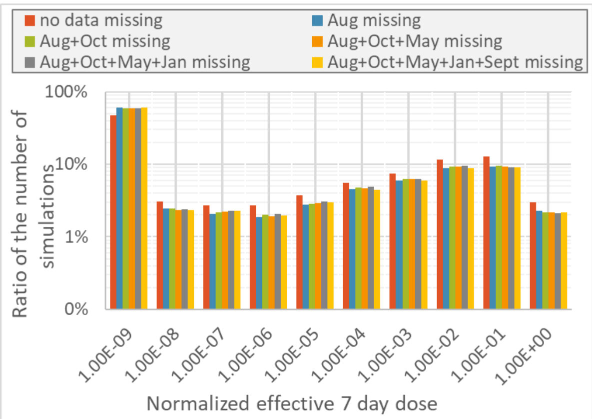

Figure 16. Histograms of the normalized effective 7-day dose at 1 km distance in 0° direction for different months of the 2015 meteorological data missing [P3]

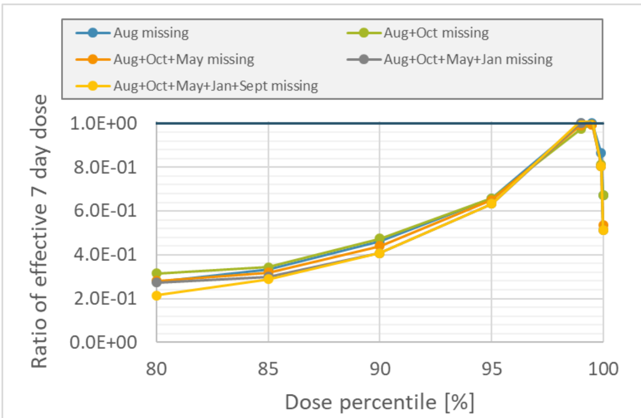

Figure 17. The ratio of dose percentiles at 1 km distance in 0° direction for different months of meteorological data missing divided by the results obtained with the 2015 annual database [P3]

While with the scattered omission of meteorological data the 95th percentile showed the smallest deviation, in this assessment the lowest variation (maximum 11%) was obtained for the 99.5th percentile. I present the ratio of the 99.5th dose percentile for the incomplete and full meteorological data of 2015 in Table 29. Having the lowest variability makes this percentile a good candidate for using it as the final result of safety assessment while ensuring that excessive conservatism is avoided. For the 100th percentile, the ratio of the results obtained with various months missing from the database range between 45-97% due to the meteorological conditions which cause the highest dose occurs in August which is omitted in all cases.

Table 29. The ratio of the 99.5th dose percentile for the incomplete and full meteorological data of 2015 (data missing consecutively).

Months of meteorological data missing	Ratios of the 99.5th effective 7-day dose percentiles for various distances			
	1 km	3 km	10 km	30 km
Aug	1.00E+00	9.75E-01	9.72E-01	9.22E-01
Aug+Oct	9.96E-01	9.60E-01	9.63E-01	9.22E-01
Aug+Oct+May	9.96E-01	9.60E-01	9.72E-01	9.22E-01
Aug+Oct+May+Jan	1.01E+00	9.60E-01	9.63E-01	8.93E-01
Aug+Oct+May+Jan+Sept	1.01E+00	9.75E-01	9.63E-01	8.95E-01

According to my calculations with various incomplete meteorological data the most robust percentiles are the 95th and the 99.5th showing the lowest deviation from the result obtained with the full database. In addition, the surrounding percentiles also show relatively low variance with the ratios between 90th-99th percentiles ranging between -37% to +24% compared to the full database for the considered distances.

To conclude, the differences between the dose percentiles larger than the 90th obtained with various missing data from a yearlong meteorological database are not significantly high (the difference ranging between -59% and +24%), with the exception of the 100th percentile which showed considerable differences in some cases. This indicates that it would not be optimal to use the maximum dose value for the verification of fulfillment of regulatory criteria because depending on the considered meteorological conditions it can significantly vary. My evaluations verify that for this specific scenario (release and site characteristics), using the 95th percentile is appropriate as it robust in case of changes (e.g. incompleteness) in the meteorological data that is taken into account in the assessment and it also allows to avoid the too conservative options.

5. DIFFERENT METHODS OF PUFF PROPAGATION IN ATMOSPHERIC DISPERSION MODELLING FOR DECISION SUPPORT

The other field of calculations that apply atmospheric dispersion models to estimate the dose consequences of radioactive releases and which I investigate in my thesis and are performed with decision support systems. Decision support systems are used in case of nuclear accidents to calculate the off-site public effects of the accident as precisely as possible and to provide information to the decision makers about the possible extent, geographical distribution and the severity of the consequences via the simulation results.

The course of a nuclear or radiological emergency situation is separated into three phases, according to the temporal progress and the various protective actions or recovery options that can be introduced.

- The ***urgent response phase*** starts from the recognition of possible emergency situation and a potential radioactive release to the first few hours or days of the release. During this phase the precautionary and urgent protective actions are introduced which are predetermined based on observables and conditions at a facility. The protective actions include evacuation, short-term sheltering, Iodine thyroid blocking, decontamination of individuals and restriction of food and water.
- The ***early response phase*** spans from the first few days after the release up to weeks, when the major release has occurred but the dispersion and deposition of the released radioactive material in the environment (atmosphere, ground, water bodies) is still intensive. At this stage the early protective actions can be introduced which include temporary relocation, bans on food, milk and drinking water, restrictions on land use or contaminated animal feed.
- The ***transition phase*** is a longer time period of several months or years, it commences after the radioactive release has stopped or is under control and when the characterization of environmental radiation fields have been measured to provide sufficient information for the necessary remedial and recovery actions which include permanent relocation, agricultural actions, interdiction or restrictions on grazing, consumption of drinking water, radiological waste management [101].

In the early phase of the accident, when environmental measurements are not or just limitedly available, predefined actions based on the plant conditions need to be implemented. Atmospheric dispersion and dose calculations can also be used to provide information about the possible contamination levels and projected doses of the population based on the available source term and meteorological data from weather prediction models. These data can help justify the introduction of protective measures connected to pre-established intervention levels (dose limits) aimed at the protection of the public.

The aim of the atmospheric dispersion and dose calculations by decision support systems is to simulate the actual events as detailed as possible to provide reliable information of the consequences. The uncertainty of the calculations has to be evaluated in these types of calculations as well, given that the magnitude of uncertainty associated with the computational results may have an impact on the outcome of the decision-making.

The three main expectation towards the result of a calculation for decision support are to be:

- reliable, providing information about the uncertainty,
- profound, conducted with well-established and robust methodology,
- available in time, the computations made quickly (i.e. with the time of simulation and determination of recommendations made in less than an hour).

In this section I investigate the model uncertainty of different propagation methods part of the dispersion calculation conducted with Gaussian puff model of the SINAC decision support system [16]. The purpose of my assessment is to evaluate various puff propagation approaches and to compare their precision against their running time. The dose consequences of a radioactive release are calculated from the air and ground activity concentrations, so in order to provide accurate results, the activity concentration need to be computed precisely. In a decision support system, the calculations needs to be fast to be able to provide timely recommendations for emergency response[P4].

5.1. Puff propagation methods

In addition to the basic equations of the puff modell which I already presented in Section 2.1.4, I show the details of the different puff propagation methods that are implemented in the SINAC software. The puffs are released from the discharge point with certain time steps and the puffs propagate according to the prevailing wind direction at the given location. The time step is computed as the ratio of the step distance of the puff propagation and the absolute value of the effective wind velocity vector:

$$\Delta t = \frac{\Delta s}{|\vec{u}|} = \frac{\Delta s}{\sqrt{u_{eff}^2 + v_{eff}^2}} \tag{26}$$

The different methods of the puff propagations pertain to the computation of the step distance which can be determined as a fixed value or can be defined by a variable. The time step determines the frequency and locations of the puff being evaluated and added, thus the consideration of different time steps can result in different activity concentrations at certain points. The most precise activity concentrations would be obtained with infinitely small step size the description of which, however is not mathematically feasible in a calculation. An acceptable compromise is to select a relatively small step size and approximation suitable to provide precise results. In this assessment, I consider the very small step size of 1 m to be the appropriate for the required precision.

In my investigation I consider the following three types of puff propagation methods:

1. Constant step size;
2. Variant step size based on the value of the horizontal dispersion parameter;
3. Variant step size based on the increment of the vertical dispersion parameter.

Method I: constant step size

In the constant step size method, the distance of a puff propagation step is constant so the time step only depends on the wind speed. If the wind speed is considered to be constant in space, then the puff centers are at the same distance from each other. In Figure 18, I present an illustration on the propagation of the constant step size of one puff (represented by circles with σ_r radius) moving in time with the assumption of fixed meteorological parameters. The figure shows that at the beginning of the release the puff states are smaller and farther from each other but as the puffs propagate and expand, they start to overlap.

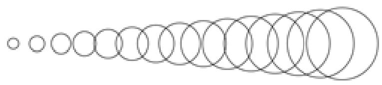

Figure 18. An illustration of puff states using the constant step size method of puff propagation with fixed meteorology

With this method, it can be expected that closer to the release point the inprecision of the activity concentration will be higher. Another aspect is that at greater distance the overlapping puff states require unnecessary computations increasing the simulations time.

Method II: variant step size based on the value of the horizontal dispersion parameter

In the first variant step size method the step size is computed according to the horizontal dispersion parameter (σ_r: [m]) multiplied with a factor (m_0 [1]) as follows:

$$\Delta s = m_0 \cdot \sigma_r \tag{27}$$

In Figure 19, I present the illustration on the propagation of one puff (represented by circles with σ_r radius) moving in time with the assumption of fixed meteorological parameters and $m_0 = 2$ when using the variant step size method. In this case the step size will be the same as the diameter of the expanding circles of the puff states.

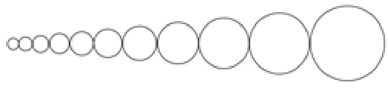

Figure 19. An illustration of puff states using the variant step size method of puff propagation with fixed meteorology

Method III: variant step size based on the increment of the vertical dispersion parameter

According to the Gaussian puff model, the vertical dispersion parameter is proportional to the dth power of the distance (show in Eq. (3)) with d being a constant parameter with values lower than 1. Therefore, the dispersion parameter quickly increases with the distance close to the release point but the change slows down farther away. To achieve greater precision in the beginning of the release and to follow the small changes in the dispersion parameter, the second type of variant method adjusts the puff propagation step size to the increment of the vertical dispersion parameter. The step size is determined by creating virtual release distances assuming constant atmospheric stability for the entire propagation for the dispersion parameter as follows:

$$\Delta s = r(M_0 \cdot \sigma_z) - r(\sigma_z) \tag{28}$$

where r is the virtual release distance calculated for the given stability [m]; M_0 is the step multiplying factor [1] and σ_z: is the vertical dispersion parameter [m].

5.2. Comparison of different puff propagation methods

To compare the different puff propagation methods, I considered a simple discharge scenario with only one released puff at 100 m effective release height (no heat content) with 100 s release interval. In this scenario only one nuclide, Cs-137 is being released with 1E+10 Bq total activity. The meteorological conditions were considered both temporally and spatially constant with the following parameter values characterizing a calm wether situation: 1 m/s wind speed, Pasquill D class, and 0 mm/h rain intensity. In addition to the results included in previous publication [P4] for the distance of 1 km, I defined two additional receptor points along the wind direction at 5 km and 10 km distances, at 1m height from the ground. I computed the instantaneous and time-integrated air activity concentrations at each receptor point based on the puff propagation with different time resolutions: 10 s for 1 km, 50 s for 5 km and 100 s for 10 km distance (due to the 1 m/s wind speed, these time resolutions allow the same number of endpoints to be used to show the passage of the puffs above the receptor points at the various distances). Although this release case is unrealistic in terms of the nuclide composition and the released activity, it is adequate for the demonstration of the puff propagation schemes.

In my investigation, I considered several cases with the various puff propagation methods which are shown in Table 30. In the evaluations, I regarded the I.a. case as the baseline and compared all the other methods to this.

Table 30. The considered cases of the puff propagation methods [P4]

Case id	Puff propagation method
I.a	Constant step size (Δs = 1 m)
I.b	Constant step size (Δs = 30 m)
I.c	Constant step size (Δs = 500 m)
II.a	Variant step size based on σ_r (m_0 =0.5)

II.b	Variant step size based on σ_r ($m_0 = 2$)
III.a	Variant step size based on the increment of σ_z ($M_0 = 1.001$)
III.b	Variant step size based on the increment of σ_z ($M_0 = 1.005$)

The endpoints that I compared in the assessments were the instantaneous and time-integrated air activity concentrations at various distances. The time integration of the activity was computed from the beginning of the release until the considered timestep. In Figure 20 and Figure 21 the results at 1 km distance from the release point are presented. The most precise results were obtained for cases III.a and III.b, which provided almost identical results to that of the I.a. baseline case. As expected, the results for the larger constant step sizes (case I.b with Δs=30 m, and case I.c with Δs=500 m) do not follow closely the Gaussian function of the puff passing. Results for I.b, I.c, II.a and II.b look like step functions, because the resolution of the summation at the receptor points is denser than the steps of the puff propagation, so the same puff contributes to several consecutive activity concentration values at the receptor point resulting in the same values. The summation of the puff states is considered when the time step and the distance of the puff coincide with the time step of the receptor point, cut-off of the puff extent is considered at $5 \cdot \sigma^2$. The results for I.c with Δs=500 m show that there is only one puff state that contributes to the air activity, which stays at 1 km for one time step which is 500 s due to the 1m/s wind speed. Similarly for case II.b (variant step size method based on σ_r with $m_0 = 2$) about 5 puff states contribute to the computation of the air activity concentration at 1 km starting from starting from the one at 680 s to the one at 1210 s (from which only 4 is visible in Figure 20).

I evaluated the ratios of the air activity concentrations compared to the I.a. case at the peak of the puff passage, where the center of the puff is exactly above the receptor point which are 98% for case I.b, 0 % for case I.c, 91 % for case II.a, 93 % for case II.b, 99 % for case III.a, and 99 % for case III.b.

Regarding the time integral, for almost all cases the activity concentrations are higher than the baseline I.a. values before the puff arrives at the receptor point. Results for case II.a and II.b show underestimation by about 2-7% after the puff passes over the receptor point. Results for case I.b, III.a and III.b show that after the puff passed over the receptor point, the time-integrated activity is equal to the baseline I.a. case. The precision of the time-integrated air activity concentrations after the puff passed depends on how well the instantaneous values track the values of the baseline case.

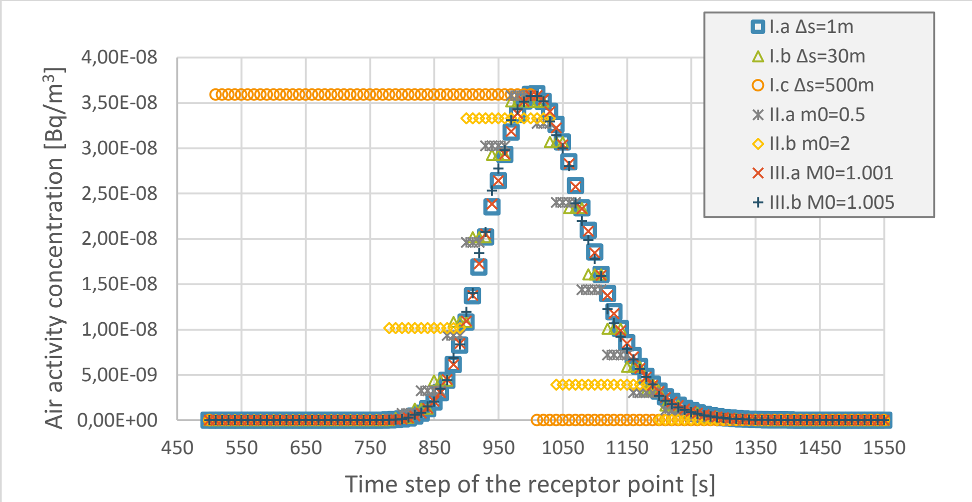

Figure 20. The instantaneous air activity concentrations calculated at 1 km [P4]

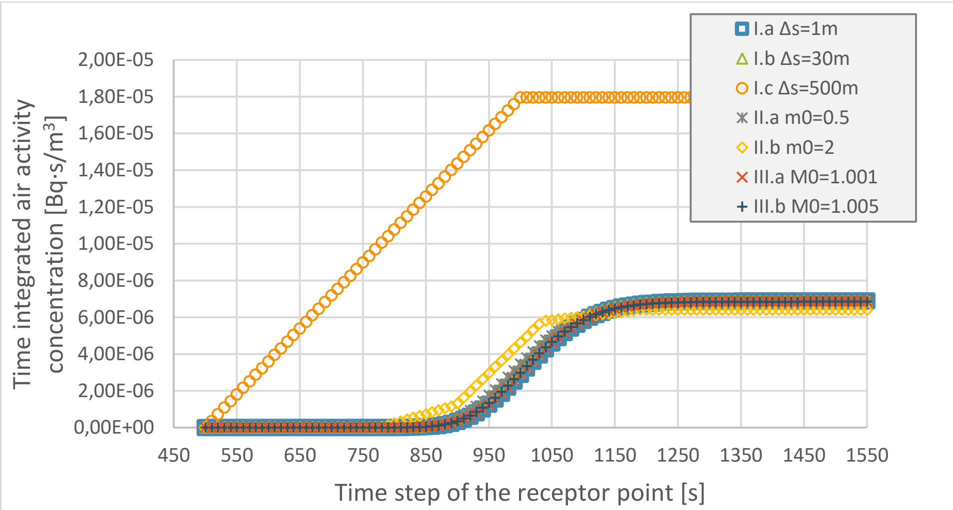

Figure 21. The time-integrated air activity concentrations calculated at 1 km [P4]

The results obtained at 5 km distance are shown in Figure 22 and Figure 23. It can be seen that the time during which the puff passes over the receptor point is greater here, than at 1 km which is due to the larger extent of the puff (as the wind speed is constant at 1 m/s, and does not affect it). The half-width of this puff passage is about 800 s (±50 s) whereas the same value was about 190 s (±10 s) at 1 km. The half-width is the difference of the time steps where the function values reach half of the peak value. The uncertainty of the half-width values is based on the time resolution of the results. It is also apparent that the longer the puff passage occurs above a receptor point the less effect the puff propagation method has on the results. In the case of I.c with Δs=500 m step size, the air activity concentration curve covers the actual process better than at 1 km with about five steps. This better coverage of the air activity concentration results in better precision for the time-integrated air activity concentration. The overestimation of the time-integrated air activity concentration when the puff center reaches the receptor point is 4%, 66%, 20%, 28% 1% and 5% for cases I.b, I.c, II.a, II.b, III.a, and III.b, respectively. After the puff passed the time-integrated air activity results show almost perfect accordance with the baseline case, with less than 2% difference.

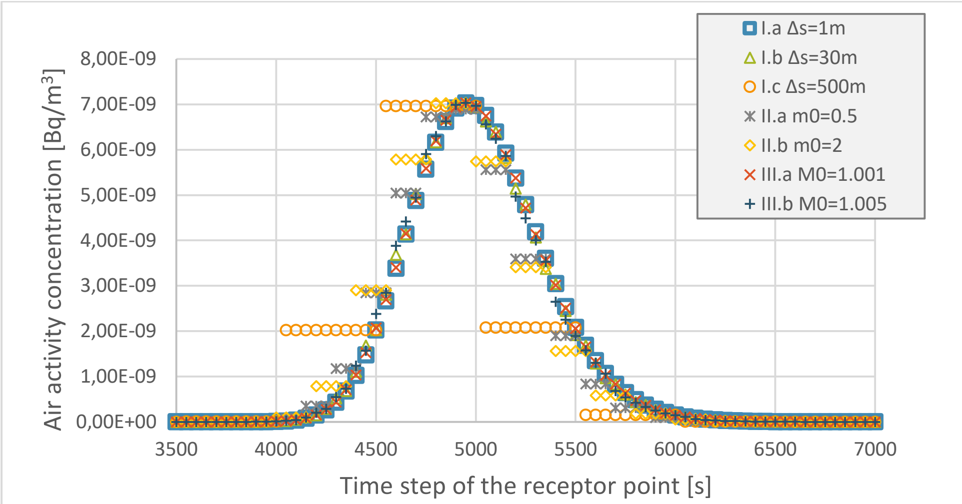

Figure 22. The instantaneous air activity concentrations calculated at 5 km

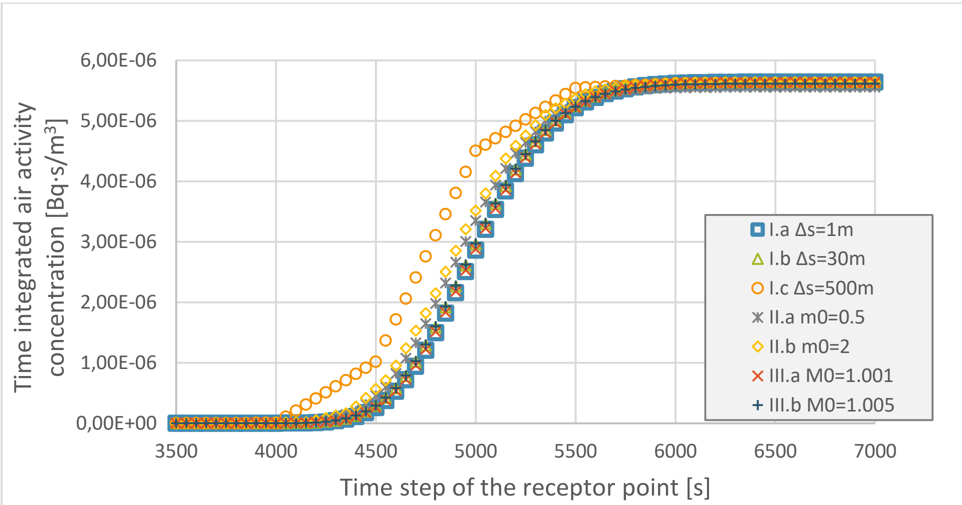

Figure 23. The time-integrated air activity concentrations calculated at 5 km

The instantaneous and time-integrated air activity concentrations calculated at 10 km are shown in Figure 24 and Figure 25. At an even larger distance the passage of the puff is even longer here with a half-width of the activity concentration function of about 1500 s (±100 s). With a longer passage the results for the various puff propagations do not differ considerably, even the case I.c with the large fix Δs=500 m step size covers quite well the air activity concentration function. This is also visible in the time-integrated air activity concentration overestimating the baseline concentration at the time when the puff center reaches the receptor point by 2%, 36%, 15%, 15%, 1% and 5% for cases I.b, I.c, II.a, II.b, III.a, and III.b, respectively. The difference of the time-integrated air activity concentration after puff passage is less than 0.5%.

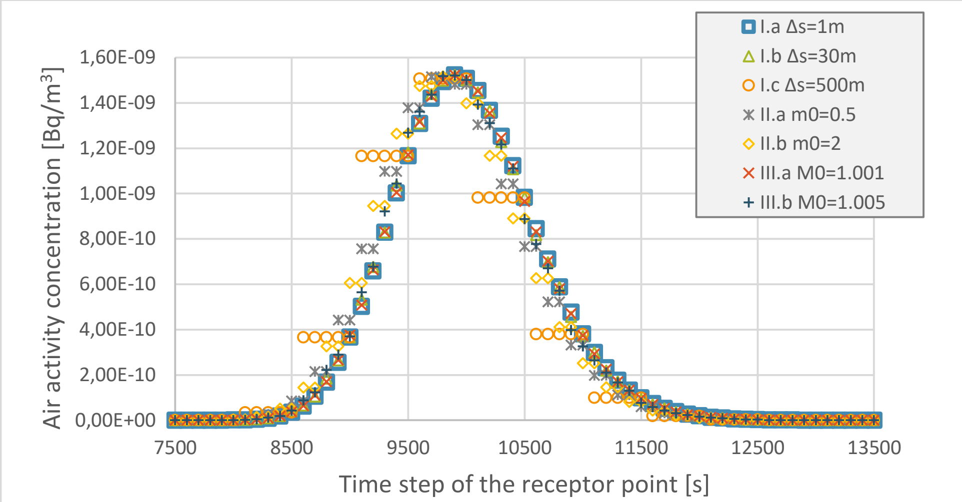

Figure 24. The instantaneous air activity concentrations calculated at 10 km

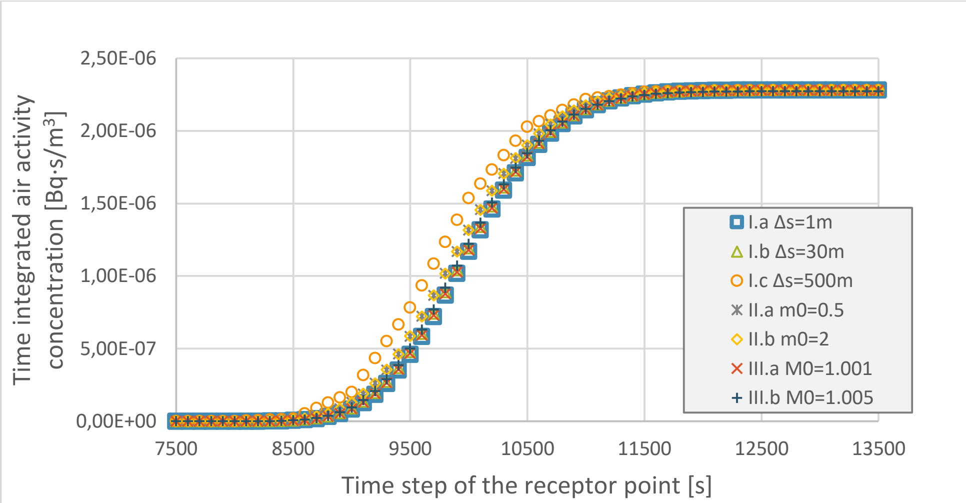

Figure 25. The time-integrated air activity concentrations calculated at 10 km

As the results for the various puff propagation methods depend highly on the atmospheric stability, which affects the extent of the puff, I repeated the assessments at 1 km distance with Pasquill F class resulting in a lower spread of the released puff. The instantaneous and time-integrated air activity concentrations are shown in Figure 26 and Figure 27 with the same legend as for the results with Pasquill D class. In this case where the spread of the puff is lower than for Pasquill D class, the results for the large fix Δs=500 m step size and case II.b with the larger m_0 value look similar to the results obtained for Pasquill D class. However, the difference of time-integrated air activity concentration values compared to the baseline after puff passage are larger here for cases I.b, I.c, II.a, II.b, namely 37%, 1027%, 20%, 58% respectively.

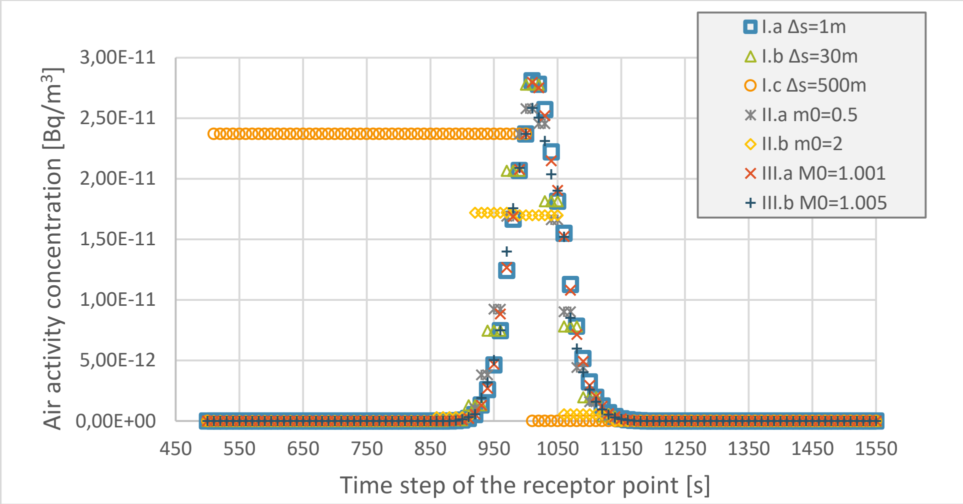

Figure 26. The instantaneous air activity concentrations calculated at 1 km for Pasquill F stability class

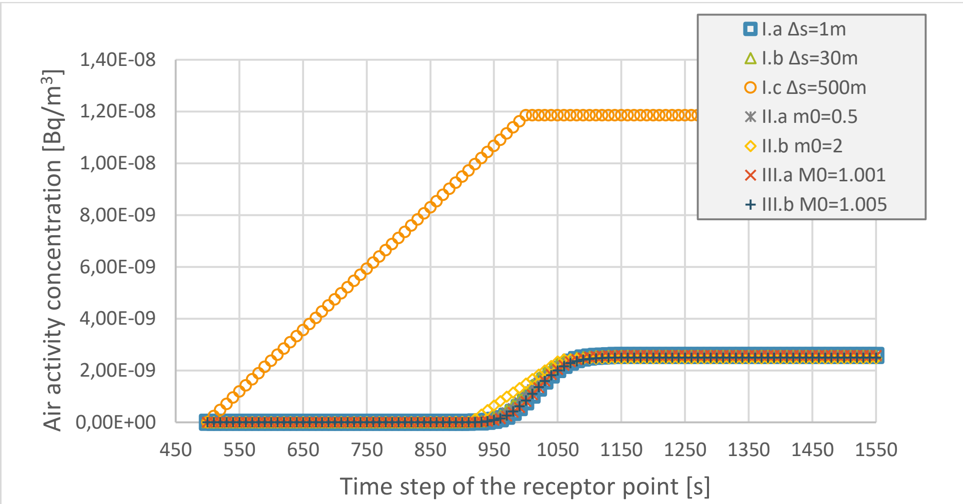

Figure 27. The time-integrated air activity concentrations calculated at 1 km for Pasquill F stability class

To compare the computational time for the different puff propagation methods I evaluated the running times for each case, including the time needed for the dispersion calculation and the determination and saving of the results, while omitting the time for initialization which was the same for all cases, therefore independent of the puff propagation method. In Table 31, I summarize the running times for the various cases (averaged over three runs). As expected, the constant step size method with the very small step size required the longest time while the majority of the other running times are in the same order of magnitude, except for case III.a requiring longer running time. I note that these simulations times are much shorter than those needed for actual emergency preparedness calculations due to the more complicated release scenarios, meteorological data and much greater number of considered nuclides and receptor points.

Table 31. The running times for the considered cases [P4]

Case id	Puff propagation method	Running time [s]
I.a	Constant step size (Δs = 1 m)	28.05
I.b	Constant step size (Δs = 30 m)	1.16
I.c	Constant step size (Δs = 500 m)	0.72
II.a	Variant step size based on σ_r (m_0 =0.5)	0.81
II.b	Variant step size based on σ_r (m_0 = 2)	0.73
III.a	Variant step size based on the increment of σ_z (M_0 = 1.001)	3.73
III.b	Variant step size based on the increment of σ_z (M_0 = 1.005)	1.06

In conclusion, I demonstrated the level of difference in the air activity concentration that can occur due to using different methods of puff propagation. I showed that for the air activity concentration the values closest to the baseline I.a. case using a very small constant step size of 1 m was obtained with method III, the variant step size based on the increment of σ_z. Regarding the time-integrated air activity concentration, the same cases produced the best results with a maximum difference of 1% for D Pasquill class and less than 3% for F Pasquill class compared to the results of the baseline case I.a. The level of difference obtained with the various methods decreased with increasing the distance of the receptor point, expectedly as the extent of the puff gets larger with distance. My results also highlight that the precision of the various methods depends on the atmospheric stability, which determines the spread of the radioactive puffs. Based on the air activity concentrations the best model to use would be method III with the lowest reasonable M_0 parameter. However, the time of calculation is of high importance for a decision support system, which provides recommendations in case of a real emergency situation. Regarding this aspect, the running times were greater for these cases than for method II, the variant step size method based on σ_r. So, when it is imperative to have quick simulations, it would be best to use method II, which produces acceptable time-integrated air activity concentration results and requires less time for the simulation than method III.

6. UNCERTAINTY OF METEOROLOGICAL DATA IN DECISION SUPPORT SYSTEMS

In this section I investigate the consequences of the uncertainty of meteorological data in the SINAC decision support system used for nuclear emergency response in case of a real event.

I took part in the work of the 1st Work Package (WP1) of the international H2020 CONFIDENCE[1] (COping with uNcertainties For Improved modelling and DEcision making in Nuclear emergenCiEs) project, the goal of which was to investigate uncertainties in the pre- and early release phase of a radiological accident. Our tasks included the identification and ranking the main sources of uncertainties, characterization of their effect on the simulation results (e.g. activity concentrations, dose assessment, reference levels) and making a proposal of practical solutions to better take into account these uncertainties in an emergency response context. Participant of the WP1 additional to me and my colleagues form the Centre for Energy Research (CER) were the Institut de radioprotection et de sûreté nucléaire (IRSN) in France, the Met Office and the Public Health England (PHE) in the UK, the Bundesamt für Strahlenschutz (BfS) in Germany, the RIVM: National Institute for Public Health and the Environment in The Netherlands, the Technical University of Denmark (DTU) in Denmark and the Greek Atomic Energy Commission (EEAE) in Greece.

We investigated the range of uncertainties of atmospheric dispersion modelling in case of emergencies which included uncertainties from source term and release characteristics, and "intrinsic uncertainty" of the model along with the uncertainties associated with meteorological data. Our goal was to identify which variable might introduce the largest uncertainties in the results and rank the identified input parameters based on the influence of their uncertainty on the outputs of atmospheric dispersion modelling. The method of investigation was reviewing the existing relevant literature. Based on the review of a significant number of publications we found that quantitative ranking of the impact of parameters was not feasible due to the large variability of parameters, models and scenarios available in the literature. Instead, we found that certain parameters can be grouped into categories having similar impact their uncertainties can have on the results. Thus, we grouped the different parameters into 7 categories (ranked in decreasing influence from Category 1 to 7) based on their effect on the results of the atmospheric dispersion calculation as shown in Table 32. This categorization only approximates the influence of the parameters and cannot be treated as an exact ranking, as the effects of the uncertainty of the parameters can depend on the considered scenario as well.

[1] Disclaimer: This project has received funding from the Euratom research and training programme 2014-2018 under grant agreement No 662287. This publication reflects only the author's view. Responsibility for the information and views expressed therein lies entirely with the authors. The European Commission is not responsible for any use that may be made of the information it contains.

Table 32. Ranking of parameters used in atmospheric dispersion modelling based on their influence on the uncertainty on the outputs [P9][op1]

Ranking	Description	Parameters
Category 1	Most influential parameters	Source term, wind direction
Category 2	Often (but not always) influential; capable of having a large influence in some circumstances	Plume rise, release height, wind speed, release timing (or time shift)
Category 3	Sometimes not relevant at all, but can be very influential in some circumstances	Precipitation, scavenging coefficients, dry deposition velocity, surface resistance, particle size distribution
Category 4	Often have some influence, but usually only a moderate one	Release duration, atmospheric stability class, mixing height, vertical diffusion parameters, horizontal diffusion parameters
Category 5	Generally not found to be particularly influential in the studies reviewed (possibly with a few exceptions), but which could have some influence in certain circumstances	Terrain modelling, ambient temperature, surface roughness, vertical source profile, time step, grid cell size
Category 6	Found to be influential in one or more of the studies reviewed, but where it seems unlikely that such influence would apply in situations that are of interest to CONFIDENCE WP1	Cross-wind entrainment parameter, multi-energy index for flammable gas, uncertainty in regional background ozone, boundary conditions
Category 7	Not found to be influential in any of the studies reviewed	Effectively includes an unlimited number of parameters, but for example: time of day, solar radiation, cloud cover, building downwash

In a complex model, the influence of the uncertainty of input parameters cannot be considered separately but needs to be assessed together. A solution to consider the uncertainties of parameters collectively is to use ensemble data. The usage of meteorological ensemble data has become more and more widespread to characterize the uncertainties of atmospheric dispersion models [102][103][104].

Meteorological ensembles are produced by numerical weather prediction models having uncertainties due to stochastic quality of the described phenomena and the approximating nature of modelling. To describe these uncertainties, the deterministic numerical weather prediction models are run several times with slightly different initial conditions. It is also possible to produce ensemble data by perturbing not only the initial conditions but also the parametrization or even the models used [26]. The results of the different runs are considered the various members of the ensemble data. The ensemble data can be characterized with statistical quantities like mean, variance or root mean square error. The difference between the various ensemble members cover the range of uncertainties of the parameters [28]. This ensemble approach made it possible for WP1 of the CONFIDENCE project to investigate the effect of the uncertainty of the source term and meteorological data on the results of atmospheric dispersion modelling.

The participants of WP1 carried out ensemble simulations with their own atmospheric dispersion models with the same input data set computing the agreed upon output quantities to be compared and assessed. I participated in the REM case study in which two hypothetical release scenarios were considered with a meteorological data sequence with the first part having small meteorological variability and the second part describing a more variant weather conditions. With this meteorological ensemble sequence (having 10 ensemble members) a total of three cases were considered, with two short releases considering the first and second part of the meteorological data separately and a third long release with the entire meteorological sequence. The release was assumed to be from the geographical location of the Borssele Nuclear Power Plant in the Netherlands, the source term was scaled to a 900 MWe PWR reactor [P10].

I developed a new method in the SINAC DSS software to consider ensemble meteorological input and modified the input function to be able to handle the format of the input data provided for the REM case study.

In the following subsections, first I look at the parameter uncertainty of different meteorological input data through a sensitivity assessment. In section 6.1., I present my results of this sensitivity assessment that I conducted with the SINAC DSS and illustrate the effect of perturbing the time-integrated air activity concentration and the ground activity concentration [28][P5][op1][op1][op1][op1].

Secondly I considered assessments with the usage of ensemble meteorological data for a simple release scenario with meteorological input provided by the Hungarian National Weather service [P6][P7] and through the REM case studies of the CONFIDENCE project [P8][P9][P10] [op2][op3][op4] to illustrate and visualize the application. I show these results in Section 6.2.

Lastly, I conducted analysis to identify different ways of optimizing the computationally expensive ensemble calculations, in which the usage of a number of ensemble members significantly increases the running time of the simulation, as in case of a real emergency, the simulations have to be made quickly to provide information to decision makers in time [P11][P12][op5]. I present my results in section 6.3.

6.1. Sensitivity analysis for meteorological parameters in SINAC

To investigate the effect of using different type of meteorological data (regular measured and ensemble) in atmospheric dispersion calculations conducted for emergency response and to identify the parameters of higher importance, I conducted sensitivity assessment of the SINAC DSS with the perturbation of different parameters. I quantified the impact of changing values of meteorological parameters on the time-integrated air activity concentration of selected nuclides.

First, I conducted sensitivity assessment for the meteorological parameters, with default and perturbed values shown in Table 33. The assessment continues the investigation that has been conducted by Tamás Velenyák in his MSc thesis [105] with the previous version of the SINAC software. To supplement the qualitative conclusions of these previous assessments in the Master's thesis of Tamás Velenyák, I conducted the analysis with a wider range of perturbations. The selected meteorological parameters also differ slightly from those considered in a previous publication [P5]. The release scenario that I considered also differs slightly from the previous analysis to be in line with the investigations of the international CONFIDENCE project.

In the assessment I considered the 4-hours long release of 1e10 Bq of Cs-137 and1e10 Bq of Xe-133 at 50 m height. The activity was released uniformly in 16 puffs. I evaluated the time-integrated air activity concentration for 24 hours after the beginning of the release at different distances along the 0°wind direction from 500 m to 30 km distances. During this period the meteorological parameters were considered constant both temporally and spatially. As the speed of the simulation wasn't a critical element to be optimized in the sensitivity analysis, I used the puff propagation method with a fixed step size of 10 m. (see details in Section 5.1.)

Table 33. Default and perturbed meteorological parameters used in the sensitivity assessment of SINAC [28]

Meteorological variable	Default value	Perturbed values
Wind velocity [m/s]	1	2, 5, 10, 20
Wind direction [°]	0	1, 2, 5, 10, 15
Pasquill stability category	D	A, B, C, E, F
Precipitation intensity [mm/h]	0	1, 5, 10, 15

6.1.1. Wind speed

I investigated the effect of changing the wind speed (according to Table 33 ranging from 1 m/s to 20 m/s) with fixed wind direction (0°), stability (Pasquill class D) and no rainfall (0 mm/h), thus I neglected the correlation between the wind speed and the atmospheric stability. I evaluated the time-integrated air activity concentration at 1 m height at the receptor point and at various distances from the release point, as shown in Figure 28 for Xe-133. As the activity concentration is inversely proportional to the wind speed, the unit air concentration values decrease with higher wind speed, as the same amount of contaminant is dispersed in a larger volume along the x-axis. Slight deviation from exact proportionality is due to the plume depletion via dry deposition (and decay in case of nuclides with short half-life). Results show that up to about 20 km, increasing the wind speed from 1 m/s to 10 m/s resulted in around one order of magnitude difference. It is also visible from the Figure that with 1 m/s wind speed the contaminant does not reach as far as with higher wind speeds, there is a steeper decrease of activity concentration for the 1 m/s results after about 20 km. Wind speed also effects the time period it takes a puff to pass over a location and the time when the first puff reaches a receptor point. I compare the time dependence of the ground activity concentration for the different wind speeds at 5 km distance in Figure 29. With wind speed of 1 m/s, 2 m/s and 5 m/s, the deposition starts around 60 min, 30 min and 10 min after the start of the release respectively, when the puffs arrive at the receptor point. This demonstrates that the first puff arrives at 5 km at different times. Wind speed also influences the amount of deposition on the ground as the lower the wind speed, the higher the concentration of a unit air volume is, and the longer time that the puffs spend above a given unit of surface results in higher deposition.

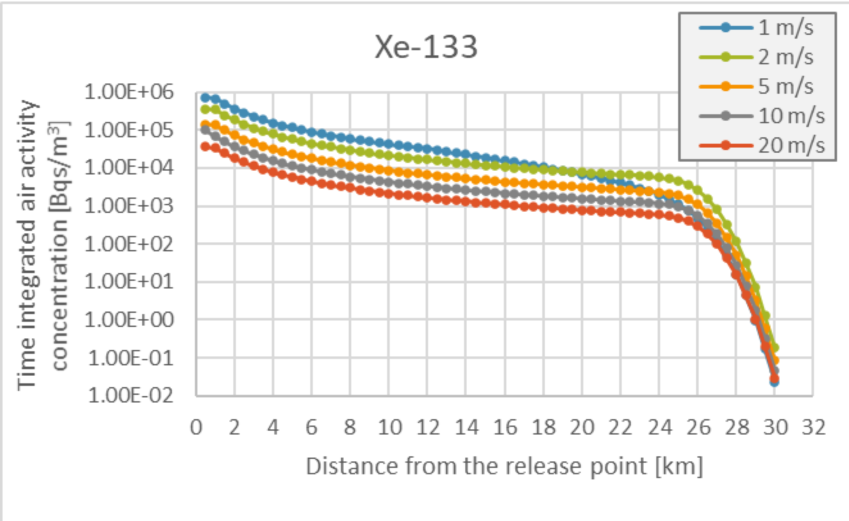

Figure 28. Time-integrated air activity concentration of Xe-133 for different wind speed values along the plume centerline (logscale) [28]

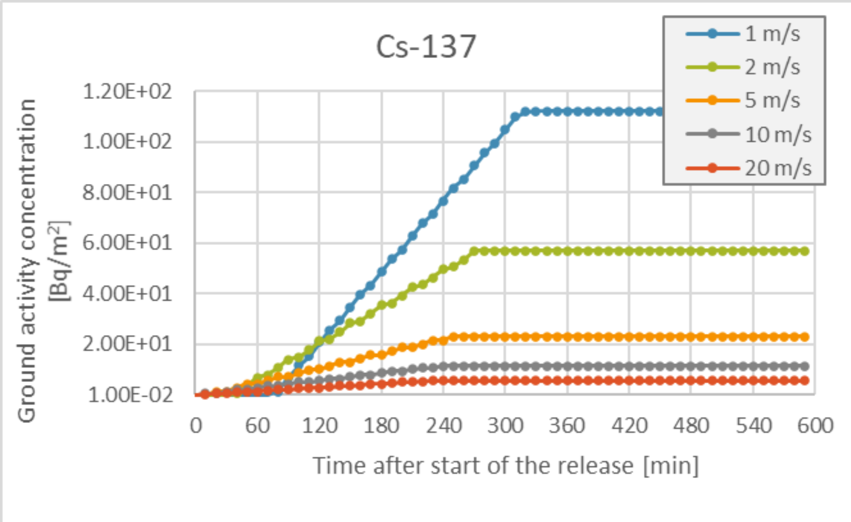

Figure 29. Time dependence of the ground activity concentration of Cs-137 for different wind speed values at 5 km distance [28]

6.1.2. Wind direction

I studied the effect of changing wind direction (according to Table 33 ranging from 0° to 15°) for the default case with fixed wind speed (1 m/s), stability (Pasquill class D) and no rainfall (0 mm/h), results of the time-integrated air activity concentration of Xe-133 is shown in Figure 30. As expected, the activity concentration decreases along the original plume centerline with increasing the angular range of the wind. Changing the wind direction from 0° to 5°, caused about 80-90% decrease in the time-integrated centerline air activity concentration, even larger angle changes from 0°to 10° resulted in 2-4 orders of magnitude difference. Looking at the cross section of the activity concentration shown in Figure 31, the maximum value shifts as the direction of the wind changes. Depending on the distance from the release point, the width of the plume and the angle of the wind direction, there can be 1-2 orders of magnitude difference in the activity concentrations at the centerline. The time-integrated air activity concentration results at 5 km distance show a ratio of 93.0%, 80.5%, 21.8% and 0.5% for angles 1°, 2°, 5° and 10° respectively, compared results for 0°.]

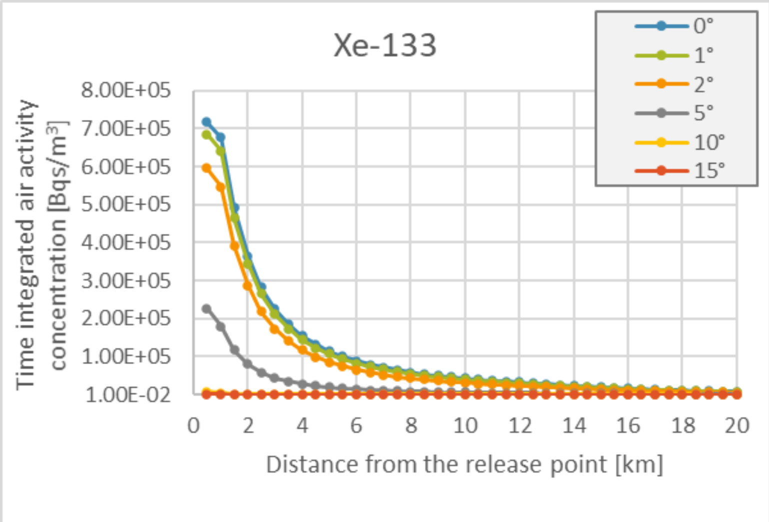

Figure 30. Time-integrated air activity concentration of Xe-133 for different wind directions along the plume centerline [28]

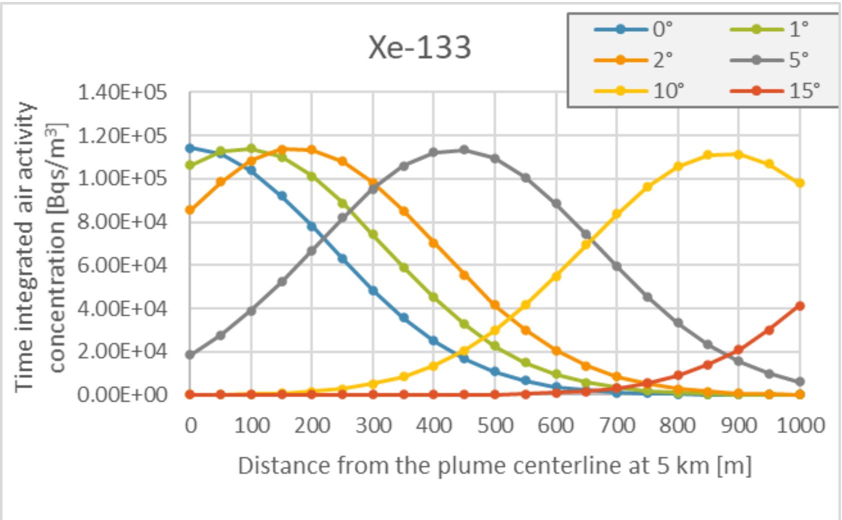

Figure 31. Time-integrated air activity concentration of Xe-133 for different wind directions perpendicular to the plume centerline at 5 km distance [28]

6.1.3. Pasquill stability

I investigated the activity concentrations for different Pasquill stability classes (according to Table 33 ranging from class A to F) with other meteorological parameters fixed on the default values (0°wind direction at and 0 mm/h rain intensity). The ranges of wind speeds that can occur in reality for various atmospheric stability classes differ, thus I considered the wind speed of 3 m/s fixed through this part of the study, because all of the Pasquill classes can occur with this wind speed value. The stability of the atmosphere determines the spread of the plume independent from the wind in the y and z axes via influencing the horizontal and vertical dispersion parameters (σ_y,

σ_z). The spread of the plume (or puff) influences the maximum activity concentration as in a smaller volume the same amount of activity causes higher concentration.

The time-integrated air activity concentration of Xe-133 is shown in Figure 32 for different Pasquill stability classes along the plume centerline. Results show that for more unstable atmosphere (characterized by Pasquill classes A, B and C) the activity disperses in a larger volume thus the activity concentration is lower. This is always true at the release height, but on ground level close to the release point, more stable classes (Pasquill classes D, E and F) provide lower activity concentration values than unstable ones. This phenomenon occurs because in the case of stable atmosphere and consequently slim plume, none or only a small part of the contaminant may reach the ground level close to the release. In these cases, with increasing distance from the release point first there is an increase in the time-integrated air activity concentration until the entire puff (or plume) reaches ground level, and then comes a gradual decrease as the spread of the puffs get larger and the activity dilutes. Whereas one class change in the Pasquill stability usually only causes less than one order of magnitude difference in the time-integrated air activity concentration, further from the release point, this difference can increase (e.g. further than 15 km the average ratio of results with Pasquill classes A and B is 6%).

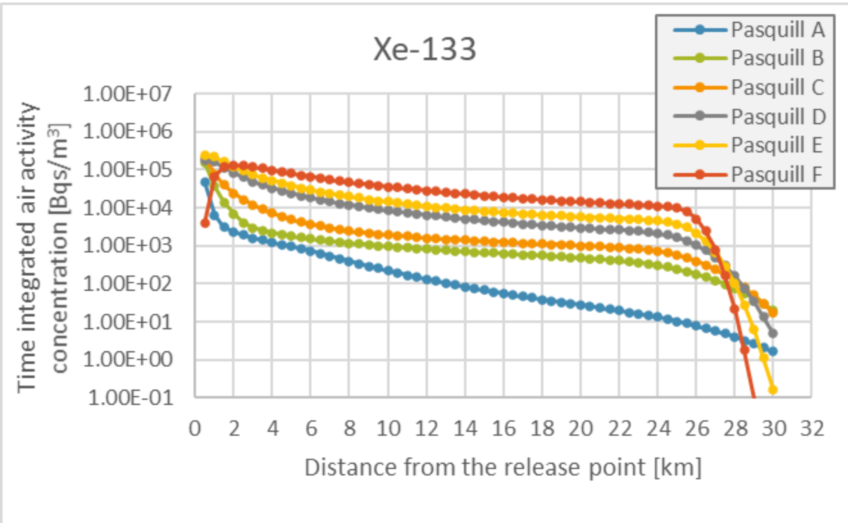

Figure 32. Time-integrated air activity concentration of Xe-133 for different Pasquill stability classes along the plume centerline (logscale) [28]

Showing the cross section of the plume in Figure 33, the expected results are visible, namely that for more stable atmosphere (Pasquill classes D, E and F) the plume is denser with higher air activity concentration, and with more unstable atmosphere (Pasquill class A, B and C) the plume is spreading wider with lower concentrations. Closer to the release point, for example at 1 km distance, the results for Pasquill F category would differ from this, illustrated by Figure 33, it would have a lower maximum than results for Pasquill classes E, D, C and so on due to puffs not reaching ground level yet.

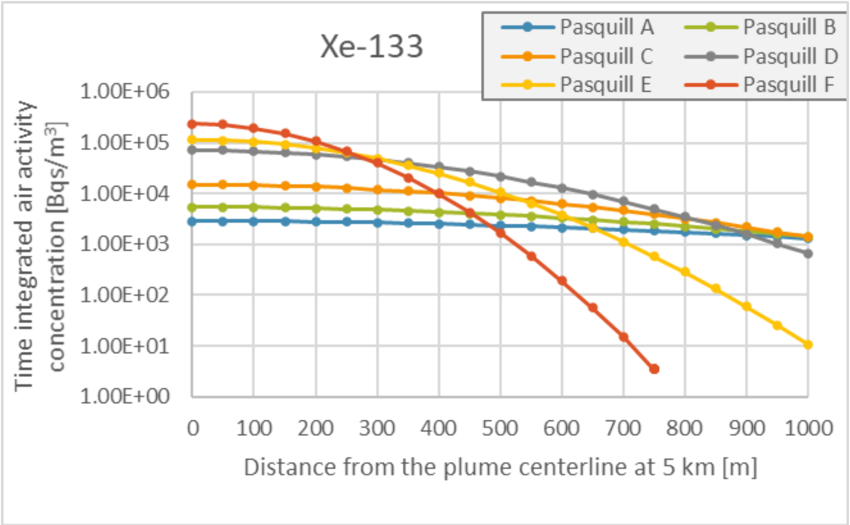

Figure 33. Time-integrated air activity concentration of Xe-133 for different Pasquill stability classes perpendicular to the plume centerline at 5 km distance (logscale) [28]

6.1.4. Rain intensity

I investigated the effect of rain intensity (according to Table 33 ranging from 0 mm/h to 15 mm/h) with the default meteorological case (wind speed 1 m/s, wind direction 0°, and Pasquill stability class D), compared to the default scenario with no rainfall (0 mm/h. The rainfall is proposed to be constant both spatially and temporally. In reality, the probability of occurrence for such a constant rainfall for a large region is unlikely, but for the purpose of demonstrating the effect of rainfall on the results the scenario is appropriate.

As noble gases do not get deposited, I evaluated the time-integrated air activity concentration and the ground deposition results only for Cs-137. The air activity concentration is shown in Figure 34, and the deposition in Figure 35. As expected with increased rain intensity, contaminants are washed from the air to the ground resulting in progressively lower air activity concentrations. This difference gets more pronounced farther from the receptor point because with higher rain intensity more contaminants are washed out from the plume at shorter distances, resulting in lower concentration reaching farther points, from which, less activity can be washed out. The deposition of Cs-137 correspondingly shows that compared to no rainfall, the activity concentration on the ground is the highest close to the release point and decreases more rapidly with higher rain intensities. Thus, at a receptor point around 10-20km from the release point, lower rain intensity values result in higher deposition.

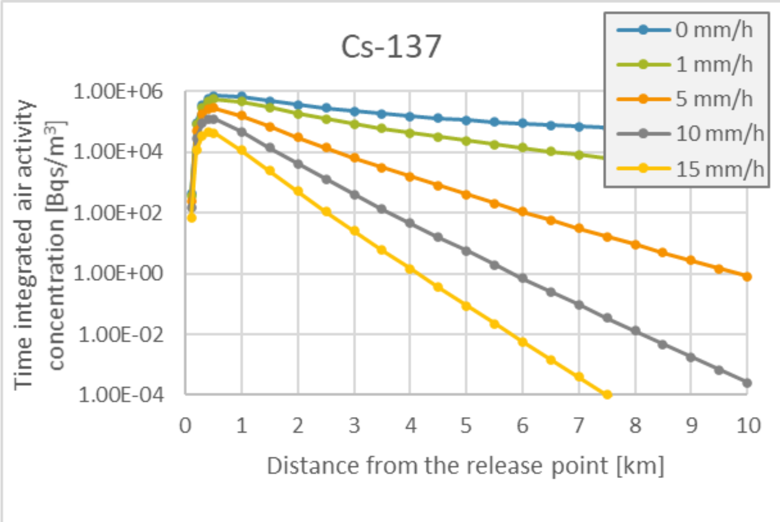

Figure 34. Time-integrated air activity concentration of Cs-137 for different rain intensities along the plume centerline (logscale) [28]

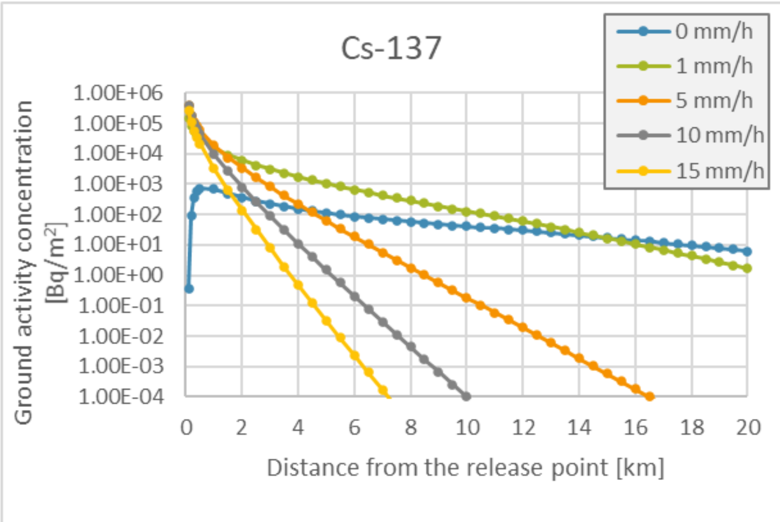

Figure 35. Ground activity concentration of Cs-137 for different rain intensities along the plume centerline (logscale) [28]

6.1.5. Ranking of the considered meteorological parameters

Overall, the meteorological parameter can have significant effect on the results of the atmospheric dispersion modelling depending on the range of variation for a given parameter and the choice of the not perturbed values of the other meteorological parameters. However, to compare the sensitivity of these meteorological parameters, I selected a realistic perturbation for each parameter that corresponds best with the uncertainty of the meteorological data from different sources. Meteorological data can be obtained from measurements and observations or from numerical weather prediction (NWP) models. The uncertainty of the obtained meteorological data depends on the measurement system or the exact NWP model, so for my evaluation I considered the expected accuracy of the meteorological data based on recommendations and general requirements made by the World Meteorological Organization concerning the measurements and observations [106] and the forecasting systems [107]. It is important to regard both sources because in case of an emergency (for which a decision support system like SINAC can be used) neither the meteorological measurements and observation nor the results from NWP models may be available at the required time and location, or with the necessary spatial and temporal resolution. I show the accepted accuracy of the meteorological parameters in Table 34.

Table 34. The maximum accepted uncertainty of meteorological parameters from measurements and observations or from NWP models [P5]

Meteorological parameter	Maximum accepted uncertainty	
	Measurements and observation	Numerical weather prediction models (regional)
Wind speed	± 0,5 m/s for values ≤ 5 m/s ± 10% for values > 5 m/s	± 2 m/s for troposphere ± 3 m/s for stratosphere
Wind direction	± 5°	n.a.
Precipitation intensity	± 1 mm/h for values 0.2 – 2 mm/h ± 5% for values > 2 mm/h	± 0.1 mm/h

As the Pasquill stability class is not measured implicitly but can be derived from other meteorological parameter (e.g. the surface wind speed, level of insulation, temperature gradient, wind direction fluctuation), there is no uncertainty requirement for them. In my comparison of the sensitivities to the meteorological parameters I considered one class difference for the Pasquill stability parameter.

To evaluate the sensitivity of the atmospheric dispersion model concerning the meteorological parameters, I determined the maximum ratio of the time-integrated air activity concentration for the selected alteration in the input data, as shown in Table 35. To make the comparison easier to follow, I present the ratios as values above 1 (1.00E+00). The effect of the perturbations is shown for three different ranges of release distances. For some of the parameters, I considered the assessment of more than one perturbation to cover a wider range of results.

Table 35 The maximum ratio of the time-integrated air activity concentration for different perturbations of the meteorological parameters at various distance ranges

Meteorological parameter	Perturbation (change of value)	Distance ranges from the release point		
		0 km - 10 km	10 km - 20 km	20 km - 30 km
		Maximum ratio of the time-integrated air activity concentration		
Wind speed	+1 m/s (1→2 m/s)	2.00E+00	1.98E+00	7.74E+00
	+3 m/s (2→5 m/s)	2.50E+00	2.49E+00	2.48E+00
Wind direction	+5° (0°→5°)	7.98E+00	1.08E+01	2.10E+01
	+5° (5°→10°)	4.76E+02	1.20E+03	5.01E+03
Pasquill stability class	1 class (A→B)	5.75E+00	1.75E+01	2.32E+01
	1 class (B→C)	4.01E+00	2.09E+00	2.39E+00
	1 class (C→D)	5.00E+00	4.32E+00	3.57E+00
	1 class (D→E)	1.67E+00	1.92E+00	3.05E+01
	1 class (E→F)	6.09E+01	2.57E+00	7.09E+01
Precipitation intensity	+1 mm/h (0→1 mm/h)	1.99E+01	3.46E+02	1.97E+03

According to my results the following ranking of the considered meteorological parameters can be established, showcasing their influence on the results of atmospheric dispersion modeling of radioactive materials:

- 1^{st}: wind direction (based on the results of 5°→10°);
- 2^{nd}: precipitation intensity;
- 3^{rd}: Pasquill category (based on the average of the five perturbations);
- 4^{th}: wind speed (based on any of the perturbations in Table 35).

Compared with the parameter ranking derived from the literature review [op1], my results show general alignment. Both my assessments and the literature-based ranking identify the wind direction as the most influential parameter in the atmospheric dispersion of radioactive materials. Precipitation intensity, identified as the second most influential parameter in my assessments, is grouped in Category 3 in the literature-based ranking, indicating its varying relevance depending on specific cases. The third parameter in my calculations is the Pasquill stability class, grouped in Category 4 in the literature-based ranking, often having influence but usually only moderate. The most significant discrepancy between my assessments and the literature-based ranking concerns the effect of wind speed. While the literature-based ranking categorizes wind speed in Category 2 as being frequently influential with a capability of having a significant influence in some cases, my calculations indicate that the wind speed is the least influential parameter among the other meteorological parameters.

6.2. Usage of ensemble meteorological data

As mentioned before, ensemble meteorological datasets can be produced by running deterministic numerical weather prediction models multiple times with slightly different initial conditions or parameterization schemes [26]. The software that produce ensemble meteorological data set are abbreviated as EPS (Ensemble Prediction System). In addition to perturbing the initial conditions or the used the parameterization scheme (multi-physics EPS), various weather prediction models can also be used to produce the ensemble data (multi-model EPS) [108]. For example the PEARP model, used by the Météo-France, applies ten different parametrization schemes to produce the ensemble meteorological data [109], and the first ensemble of the widely used ECMWF (European Center for Medium-range Weather Forecasts) was created by perturbing the initial conditions that cause the fastest growing errors [110]. These perturbations can also be combined such as in the meteorological ensemble that we used in the WP1 of the CONFIDENCE project. The meteorological ensemble was produced by the Harmonie-AROME using two meteorological models, various turbulent schemes and combining successive forecasts to create a dataset which accurately represents the possible spread of the meteorological condition and that corresponds with the format of the input data necessary for the atmospheric dispersion models [111].

In the following, I present the details of my research using ensemble meteorological data. In Section 6.2.1, I introduce a simple case study using the SINAC DSS with ensemble meteorological data provided by the Hungarian Meteorological Service (OMSZ) to demonstrate the applicability of the newly developed ensemble module. In Section 6.2.2, I describe the results of the REM case study of the CONFIDENCE 1st work package in which I took part with my calculations made with the SINAC DSS.

6.2.1. Case study with Hungarian ensemble weather data

To enable SINAC to consider ensemble meteorological data, I developed the SINAC Decision Support System, in which I created a module that could read the ensemble meteorological data provided by OMSZ and modified the existing code so that several meteorological sequences can be computed, and the result quantities determined. I conducted a simple case study [P6][P7] to demonstrate the application of the newly developed module with real meteorological ensemble data provided for two-time period of the Hungarian Paks NPP site.

Meteorological data I used for the assessment was provided by the AROME [112] and the ALADIN-EPS [113] numerical weather prediction models used by the Hungarian Meteorological Service. The ALADIN-EPS is the system that runs operationally at the service with 11 members and having a horizontal resolution of 8 km. In this case study, the goal with the AROME-EPS was to generate meteorological ensembles according to the input of the SINAC software that is produced operationally with the deterministic AROME. The available 9 members of meteorological ensemble data from ALADIN-EPS was converted from a coarser resolution of the model runs to the AROME resolution covering the Carpathian Basin, is summarized in Table 36.

Table 36. Spatial and temporal characteristics of the ALADIN-EPS meteorological data [P6] [op2]

	Horizontal	Vertical	Temporal
Model coordinates	Lambert	sigma-pressure hybrid	-
Output coordinates	Latitude-Longitude	in pressure and height levels	-
Forecast length	-	-	36 h
Resolution	~2.5 km	60 model levels, 12 planetary boundary layer height-level and 32 pressure-levels	1 h

As the goal of my work was only the demonstration of the ensemble module, I considered a simple fictional 12 hours long release of 1E+16 Bq of Cs-137 and 1E+16 Bq of Xe-133 distributed uniformly in 360 puffs (with a puff release time resolution of 2 minutes). It was assumed that the discharge originated from the Paks NPP in Hungary, with an effective release height of 120 meters. Two meteorological datasets were considered: one representing a winter period beginning at 18:00 on 21 January 2017, and the other representing a summer period beginning at 18:00 on 14 August 2018. The release characteristics were identical for both the winter and summer cases, with the exception of the time of release, which was set as the starting time of each meteorological dataset. The modelling domain selected for the atmospheric dispersion calculation was a 600 km ×600 km Cartesian-grid with the release point in the center, located at the Paks NPP. The output quantities were the time-integrated air activity concentration [Bq·s/m^3] and the ground activity concentration [Bq/m^2] with hourly time resolution and 3 km spatial resolution within the modelling grid. The simulation was conducted for a 24-hour period following the start of the release.

The results are presented in two ways: firstly, as contours, and secondly, as overlapping plots. The contours (outlines) illustrate the extent of the affected area where the presented quantity exceeds a specified threshold value, which is related to the reference levels of emergency response actions (e.g. 10 kBq/m^2 deposition of Cs-137). The overlapping plots (filled in areas) demonstrate the number of ensemble members that have a result exceeding the selected limit value. This type of visualization is analogous to the presentation of percentiles; for instance, the 66th percentile corresponds with the area where six or more members from the total nine overlap.

As a deterministic calculation, the results are initially presented solely for the first member of the meteorological ensemble. Figure 36, illustrates the areas where the time-integrated Xe-133 air activity concentration at 12 hours and the Cs-137 deposition at 24 hours exceeds the zero value. The same contours are shown in Figure 37, considering all nine members of the meteorological ensemble. Different colors are used to indicate the results for the various members. While there are slight discrepancies in the direction of the plumes obtained for the various members, the overall shape and extent of the covered areas appear to be similar for the majority of members, indicating a moderate degree of variability within the meteorological ensemble. Figure 38 shows the overlap plots for the aforementioned two quantities, considering all nine meteorological members. The time-integrated Xe-133 air activity concentration at 12 hours, displayed on the left, reveals that no area exhibits results above zero across all meteorological members. However, on the right-hand side, there is a small area where the Cs-137 deposition at 24 hours is higher than the selected limit (which is zero in this case) for all nine members. When higher exceedance limits are selected, the impacted areas are separated and show less overlap, indicating a reduced level of confidence in the impacted areas.

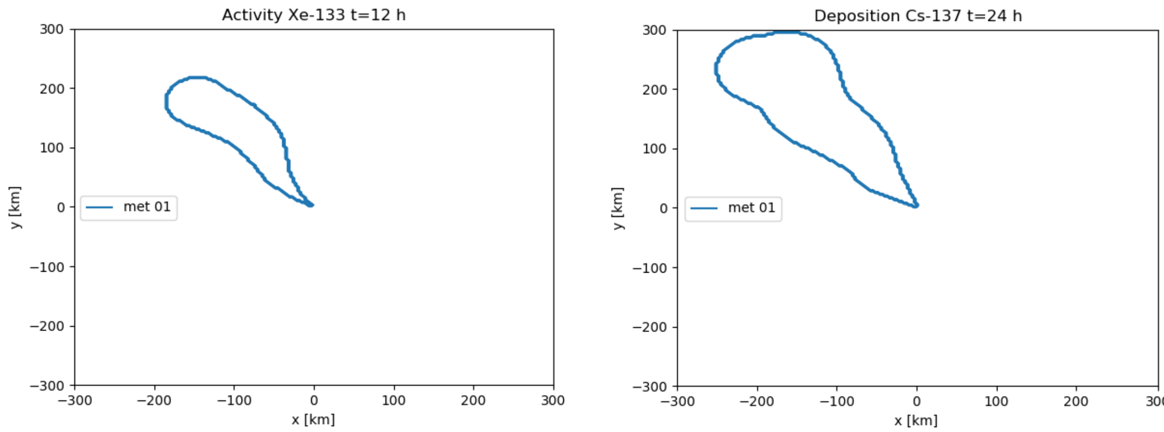

Figure 36. The contours of the time-integrated Xe-133 activity concentration [Bq·s/m³] at 12h and the Cs-137 deposition [Bq/m²] at 24 h for the 1st meteorological member in the winter case [P6]

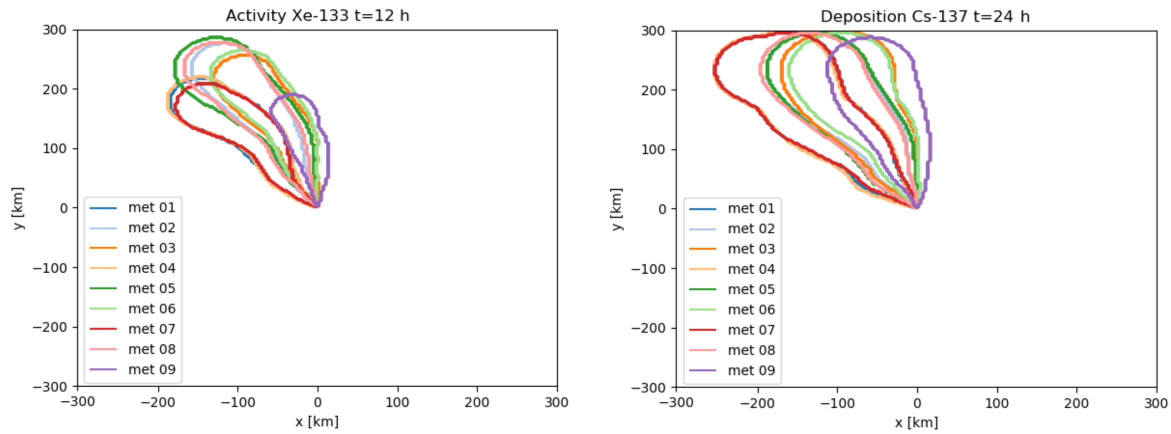

Figure 37. The contours of the time-integrated Xe-133 activity concentration [Bq·s/m³] at 12 h and the Cs-137 deposition [Bq/m²] at 24 h for all 9 meteorological members in the winter case [P6]

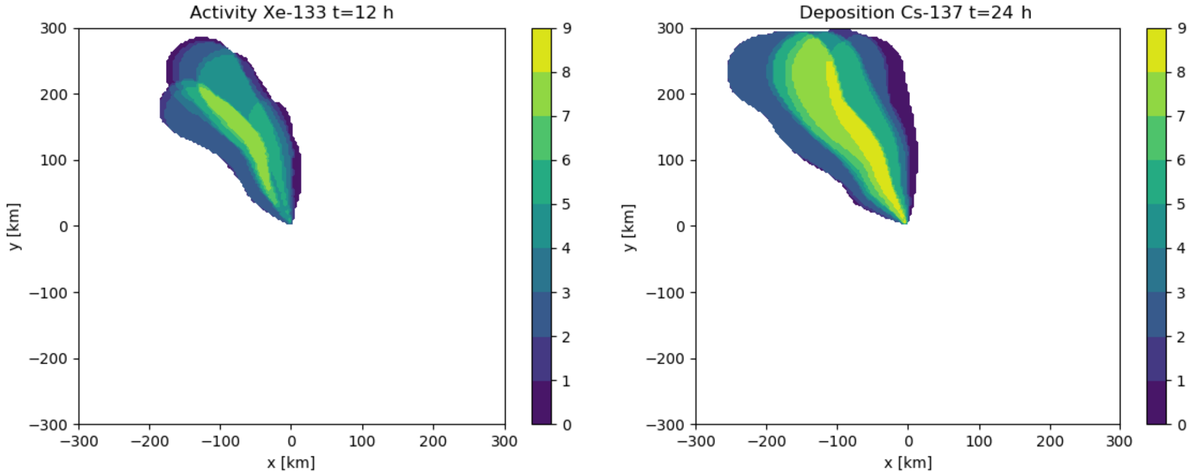

Figure 38. The overlap plots of the time-integrated Xe-133 activity concentration [Bq·s/m³] at 12h and the Cs-137 deposition [Bq/m²] at 24 h for all 9 meteorological members in the winter case [P6]

In the summer case, the meteorological parameters exhibit greater variability than in the winter case, reflecting the more dynamic weather scenario. Figure 39 illustrates the outcomes of the deterministic run utilizing only the first meteorological member, which exhibits a relatively slower wind speed and less variable wind direction compared to some of the other members (depicted in Figure 40). For a few meteorological members, there is a notable shift in wind direction, accompanied by an increase in wind speed, which results in a more dispersed plume and a larger impacted area. Figure 41 shows the probability of activity occurrence in specific locations, with higher probability in areas where multiple members overlap.

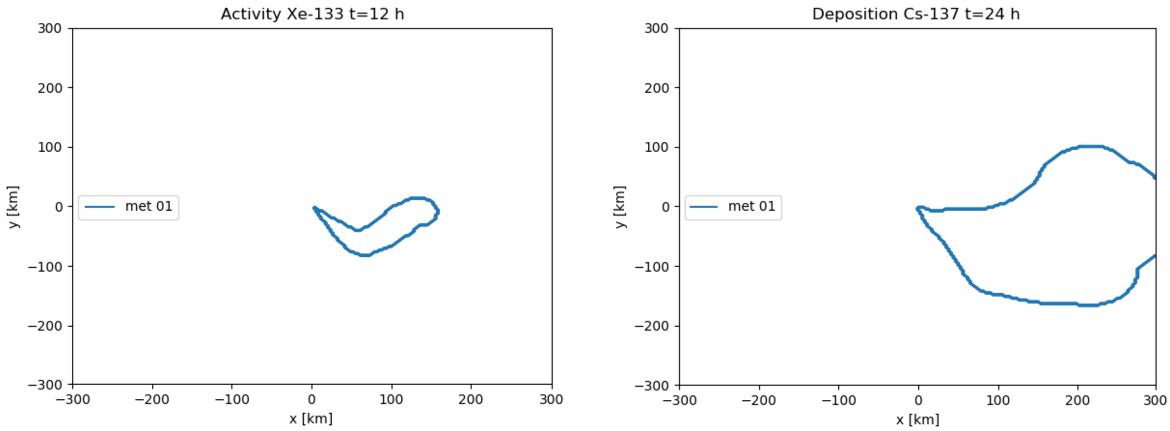

Figure 39. The contours of the time-integrated Xe-133 activity concentration [Bq·s/m³] at 12h and the Cs-137 deposition [Bq/m²] at 24 h for the 1st meteorological member in the summer case [P6]

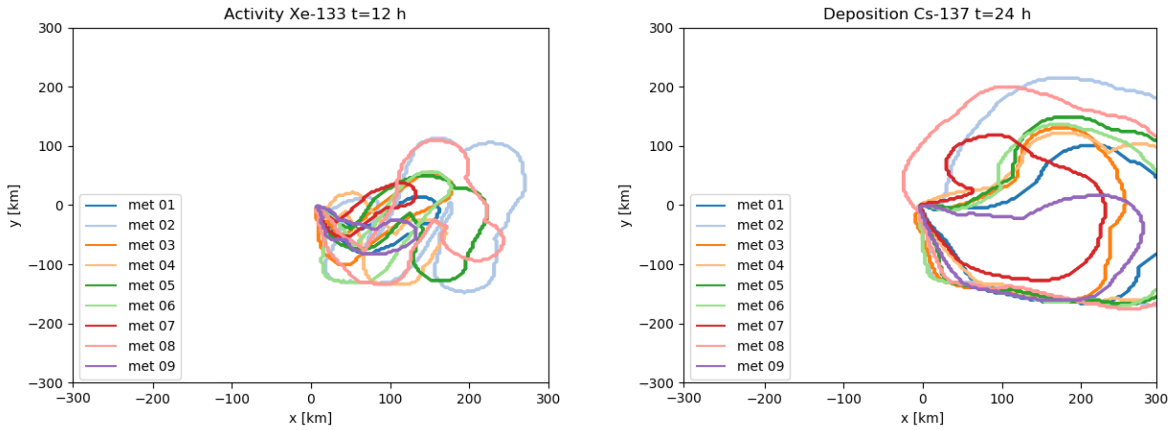

Figure 40. The contours of the time-integrated Xe-133 activity concentration [Bq·s/m^3] at 12 h and the Cs-137 deposition [Bq/m^2] at 24 h for all 9 meteorological members in the summer case [P6]

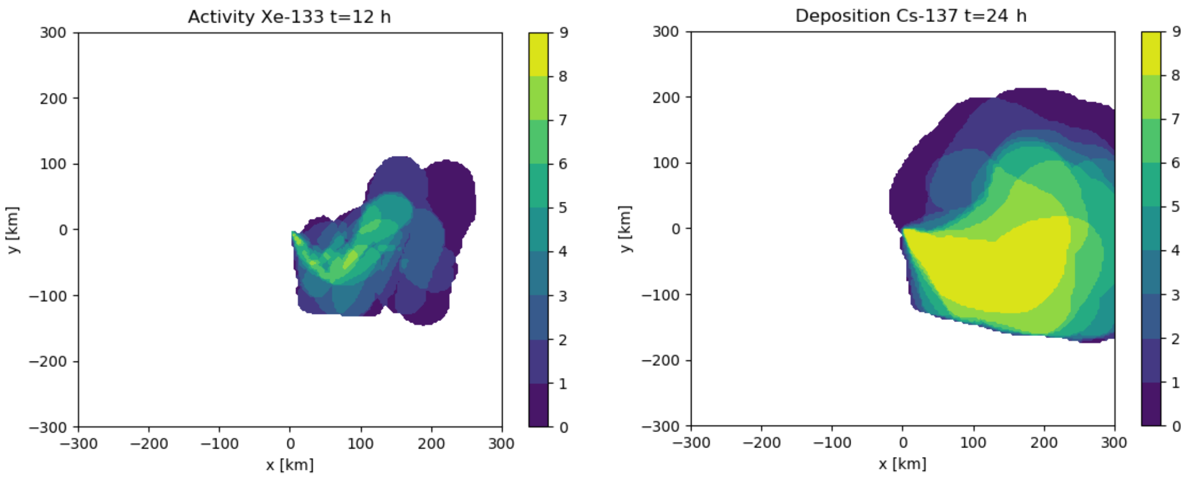

Figure 41. The overlap plots of the time-integrated Xe-133 activity concentration [Bq·s/m^3] at 12h and the Cs-137 deposition [Bq/m^2] at 24 h for all 9 meteorological members in the summer case [P6]

Overall, I have presented a series of visual representations of the results of several ensemble calculations, with the aim of demonstrating the impact of meteorological uncertainty on the atmospheric dispersion calculation.

6.2.2. Case study of the CONFIDENCE project

I developed the SINAC program to be able to handle the input data from the CONFIDENCE project, which included the modification of the module responsible for reading the meteorological input data from NetCDF format. Originally the SINAC software was developed to read the NetCDF meteorological data from OMSZ, as the program is used in the Hungarian Atomic Energy Authority's Centre for Emergency Response, Training and Analysis. In contrast, however, the meteorological data file provided for the CONFIDENCE project contained different variables with different file structure. Concerning the source term data which was provided in the International Radiological Information Exchange (IRIX) format, I developed an external code to produce time dependent source term input files that can be read by the SINAC software.

In the REM case study [P10], a total of three release scenarios were assessed with the proposed discharge occurring from the geographical location of the Borssele Nuclear Power Plant in the Netherlands. The REM1 case was considered to be a short release with a release duration of 4 hours scaled to a 900 MWe nuclear power plant. The released activities for this case are shown in Table 37 for the eight nuclides that were considered in the simulations. The chemical form of iodine was considered to be 1/3 particulate (aerosol) and 2/3 elemental (vapor). The uncertainties of the release characteristics were taken into account by varying the time of the release by ±6 hours; the effective release height was considered to be 50 m± 50 m, and the released activity was scaled with the multiplication factor of 1/3 and 3. Two periods of the meteorological data was used for the short release, the first one covering an interval with small meteorological variability and well-established wind direction on the 11th of January2017 (REM1), and the second one representative of large variations with turning wind directions and high precipitation on the 12th of January 2017 (REM2) [111]. The third case was a long release with duration of 72 hours (REM-L). The source term for this long release was taken from a database of the European project FASTNET using the ASTEC severe accident code [114] containing 10 ensemble members representing the uncertainties in the released quantities and timing for a 3-inches break Loss of Coolant Accident (LOCA) scenario. The median and the maximum of the released activity for this source term is shown in Table 37. The meteorological data for this release covered the time between 11th and 13th of January, 2017 [111]. The meteorological data used in the assessment was provided by the Dutch national weather service, The Royal Netherlands Meteorological Institute (KNMI) generated by the HARMONIE-AROME high-resolution meteorological model and contained 10 ensemble members covering the uncertainties of the meteorological parameters.

Table 37. The total released activity of the hypothetical scenarios for the REM case study [op4]

Scenario	**Short release (REM-1, REM-2)** **Borssele NPP scaled to 900 MWe**	**Long release (REM-L)** **FASTNET 3-inches break LOCA scenario**
Nuclide	**Total released activity [Bq]**	**Median (Maximum) total released activity**
Xe-133	3.51E+18	4.97E+18 (5.25E+18)
I-131	2.25E+16	1.08E+15 (1.972E+16)
I-132	2.84E+16	1.23E+15 (2.21E+16)
Te-132	1.37E+16	6.58E+13 (2.41E+14)
Cs-134	2.69E+15	1.30E+13 (6.02E+13)
Cs-136	6.37E+14	4.90E+12 (2.22E+13)
Cs-137	2.06E+15	8.80E+12 (4.06E+13)
Ba-137m	2.78E+14	1.37E+13 (8.45E+13)

The participants chose which cases and perturbations they wanted to consider depending on their computational capabilities as the consideration of the perturbations resulted in the maximum of 650 simulations. The participants, the used atmospheric dispersion models and the number of perturbations considered are shown in Table 38.

Table 38. Participants, atmospheric dispersion models used, and the number of simulations applied in the REM case study of the CONFIDENCE project [P8]

Participant (Country)	Atmospheric dispersion	Number of simulations
IRSN (France)	ldX – Eulerian	100
Met Office/ PHE (UK)	NAME – Lagrangian	90
BfS (Germany)	RIMPUFF – Gaussian puff	150
RIVM (The Netherlands)	NPK-puff – Gaussian puff	650
CER (Hungary)	**SINAC – Gaussian puff**	**150 (REM-1) + 90 (REM-2)**
DTU (Denmark)	RIMPUFF – Gaussian puff	10 (REM-1) + 50 (REM-2)
EEAE (Greece)	DIPCOT – Lagrangian	50

The participants used various codes for the assessment, each implementing different models, with distinct model parameters and assumptions. Thus, the discrepancies in the assessment results can be attributed to these differences.

The following outputs were computed throughout the simulations and compared in the case study:

- time integrated air activity concentration at 1 m above ground [Bqs/m^3],
- total deposition and wet deposition [Bq/m^2],
- gamma dose rate [Gy/s],
- effective dose for a 1-year-old child [Sv] (including cloudshine, groundshine and inhalation doses),
- inhalation thyroid dose for a 1-year-old child [Sv].

Most participants computed all quantities, but some only provided air and ground activity concentrations from which IRSN produced the required effective dose and dose rate values.

The ensemble results were visualized using statistical values (e.g. median) and on maps of probability of exceedance, indicating the impacted area where a given ratio of the ensemble simulations yield values exceeding the reference level [op3]. The reference levels for the threshold exceedance maps were:

- 37 kBq/m^2 of Cs-137 deposition (Chernobyl reference level),
- 10 kBq/m^2 deposition for Cs-137 and I-131,
- 10 mSv effective dose for 1-year old child,
- 50 mSv effective dose for 1-year old (French reference level for evacuation),
- 10 mSv inhalation thyroid dose for 1-year old child,

- 50 mSv inhalation thyroid dose for 1-year old child (IAEA reference level for iodine intake [115]).

The threshold exceedance maps show the area where the different results are in agreement, values of 100% indicate that all considered ensemble members are above the given threshold, while 0% means that none of the ensembles exceeded the threshold. The maximum distance of exceedance was also computed by the participants for the reference levels, defined as the distance to the farthest grid point where the reference value is exceeded [op4].

6.2.2.1. Short release with small meteorological variability (REM-1)

To highlight the differences of the assessments made by the various participants, the median of the Cs-137 deposition 24 hours after the start of the release is shown in Figure 42, taking into account only the meteorological uncertainties via the 10 ensemble members of the meteorological data. These outcomes illustrate shows that even with identical input data the results obtained by different codes can vary considerably due to different types of atmospheric dispersion models, dry and wet deposition schemes, modelling domain and interpolation methods. Even for the identical dispersion model (RIMPUFF) used by BfS and DTU, the difference of the results is substantial presumably due to the distinct assumptions made in the calculations. It is also visible from the Figure that the modelling domain for some participants is lower than for others which can affect the compared quantities e.g. the maximum distance of threshold exceedance or the probability maps of threshold exceedance.

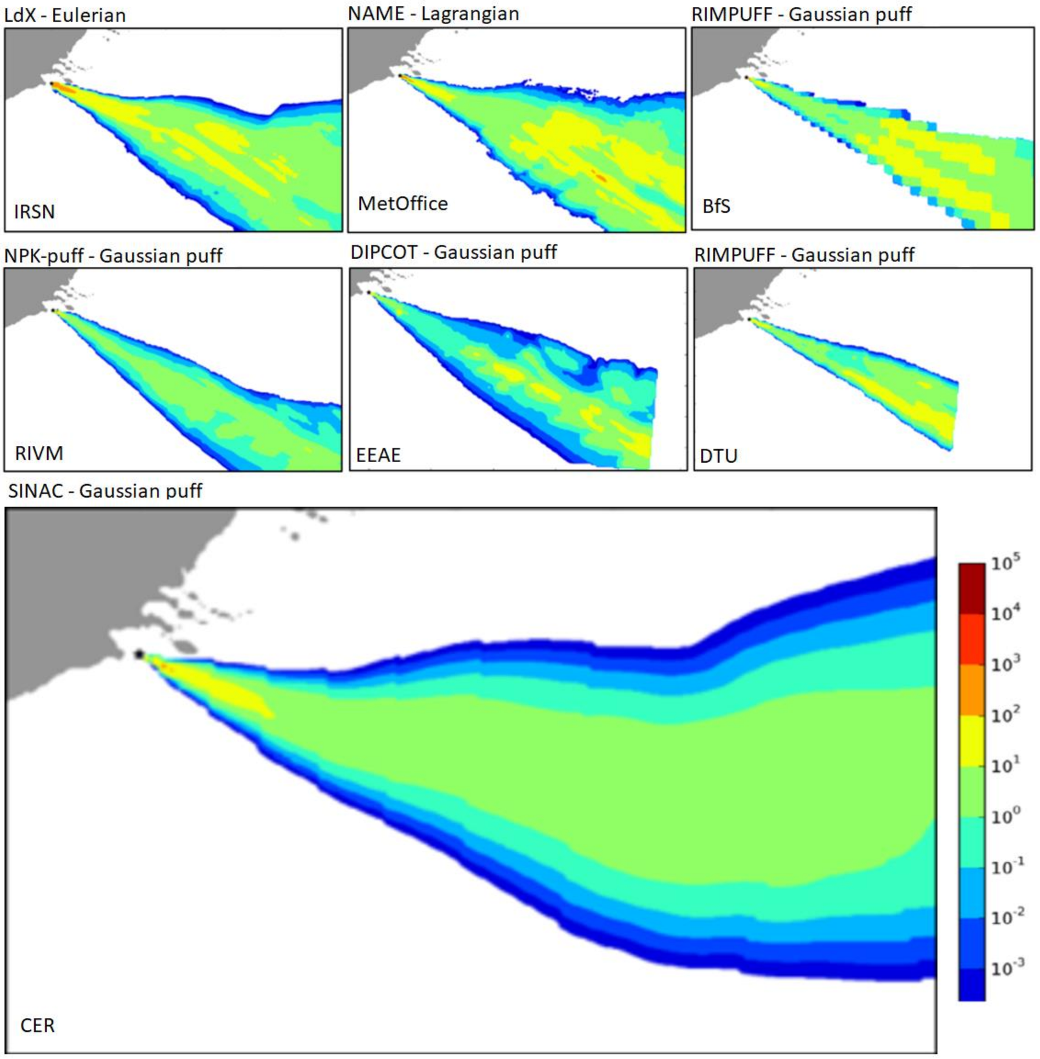

Figure 42. Median of the Cs-137 deposition [Bq/m^2] at 24 h computed for the meteorological ensembles for the seven participants of REM-1 case study (my results shown enlarged on the bottom) [P10][op4]

The results of the maximum distance of threshold exceedance for the considered reference levels are presented in Table 39, averaged over the 10 meteorological members, in Table 40, averaged over both the meteorological and source term perturbations for 24 h. The results show a significant variability among participants, attributed to differences in the models, model parametrization, and modelling domain.

Table 39. The average maximum distance of threshold exceedance for the meteorological perturbations at 24 h (my results indicated with bold font) [op4]

Participant	Average maximum distance of threshold exceedance					
	Cs-137 Deposition		Inhalation thyroid dose		Effective dose	
	10 kBq/m²	37 kBq/m²	10 mSv	50 mSv	10mSv	50 mSv
IRSN	558 km	389 km	209 km	79 km	26 km	1 km
Met	578 km	558 km	130 km	52 km	24 km	0 km
BfS	543 km	447 km	142 km	40 km	16 km	4 km
RIVM	543 km	15 km	40 km	19 km	7 km	0 km
CER	**96 km**	**38 km**	**87 km**	**29 km**	**13 km**	**0 km**
DTU	417 km	403 km	97 km	37 km	11 km	0 km
EEAE	523 km	316 km	46 km	20 km	6 km	0 km

Table 40. The average maximum distance of threshold exceedance for the meteorological and source term perturbations at 24 h (my results indicated with bold font) [op4]

Participant	Average of maximum distance of threshold exceedance					
	Cs-137 Deposition		Inhalation thyroid		Effective dose	
	10 kBq/m²	37 kBq/m²	10 mSv	50 mSv	10mSv	50 mSv
IRSN	409 km	180 km	228 km	90km	35 km	7 km
Met	483 km	361 km	130 km	55 km	28 km	5 km
BfS	505 km	415 km	160 km	36 km	15 km	4 km
RIVM	482 km	222 km	37 km	18 km	7 km	1 km
CER	**184 km**	**46 km**	**85 km**	**28 km**	**12 km**	**0 km**
DTU	417 km	403 km	97 km	37 km	11 km	0 km
EEAE	469 km	237 km	45 km	18 km	6 km	0 km

Another way to visualize the results is to show the areas of threshold exceedance for a given value of a computed quantity. Such results are presented in Figure 48, showing probability maps of threshold exceedance for thyroid dose, considering both the meteorological and source term uncertainties. The results show several projections in the north east direction which is due to the different release times in the source term perturbations.

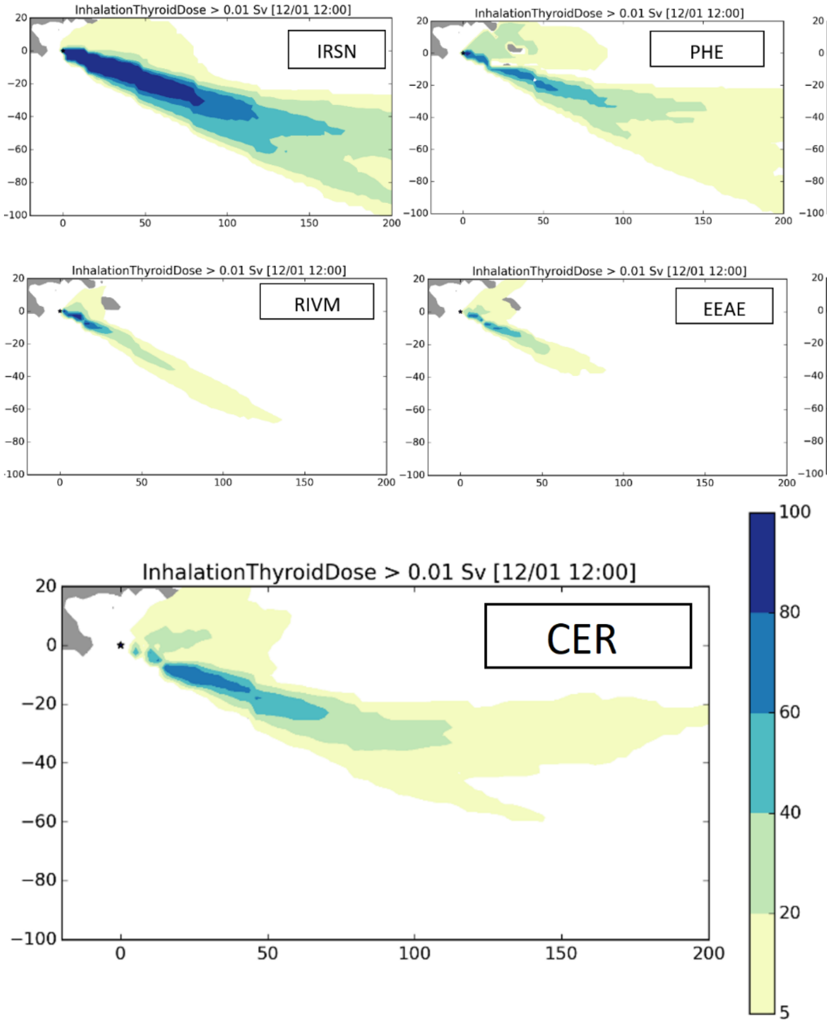

Figure 43. The probability of threshold exceedance maps of 10 mSv thyroid dose for selected percentiles for the meteorological and source term perturbations (my results shown enlarged on the bottom) [op4]

6.2.2.2. Short release with large meteorological variability (REM-2)

To visualize the inter-model variability for the REM-2 case which considers a meteorological scenario with larger variability (changing wind directions and high precipitation), the median of the Cs-137 deposition is shown in Figure 44 for all participants and only taking into account the meteorological ensembles. The figures show a larger deposition as expected due to the high precipitation at the release location. Although the trajectory of the median plume is similar for all participants, there are significant differences in the spread of the plume and also in the deposition values. These variances are within the acceptable range considering that different codes were used and are presumably due to the different wet deposition schemes of the models. For reference, in such comparison studies of various codes, the differences of the obtained results are usually in the one order of magnitude. For example, in an international benchmark of consequence assessment codes [85], the difference of the mean and the 99th percentile of the time-integrated Cs-137 activity concentration at ground level evaluated at 1 km was around 7 and 30 times among the participating software.

.

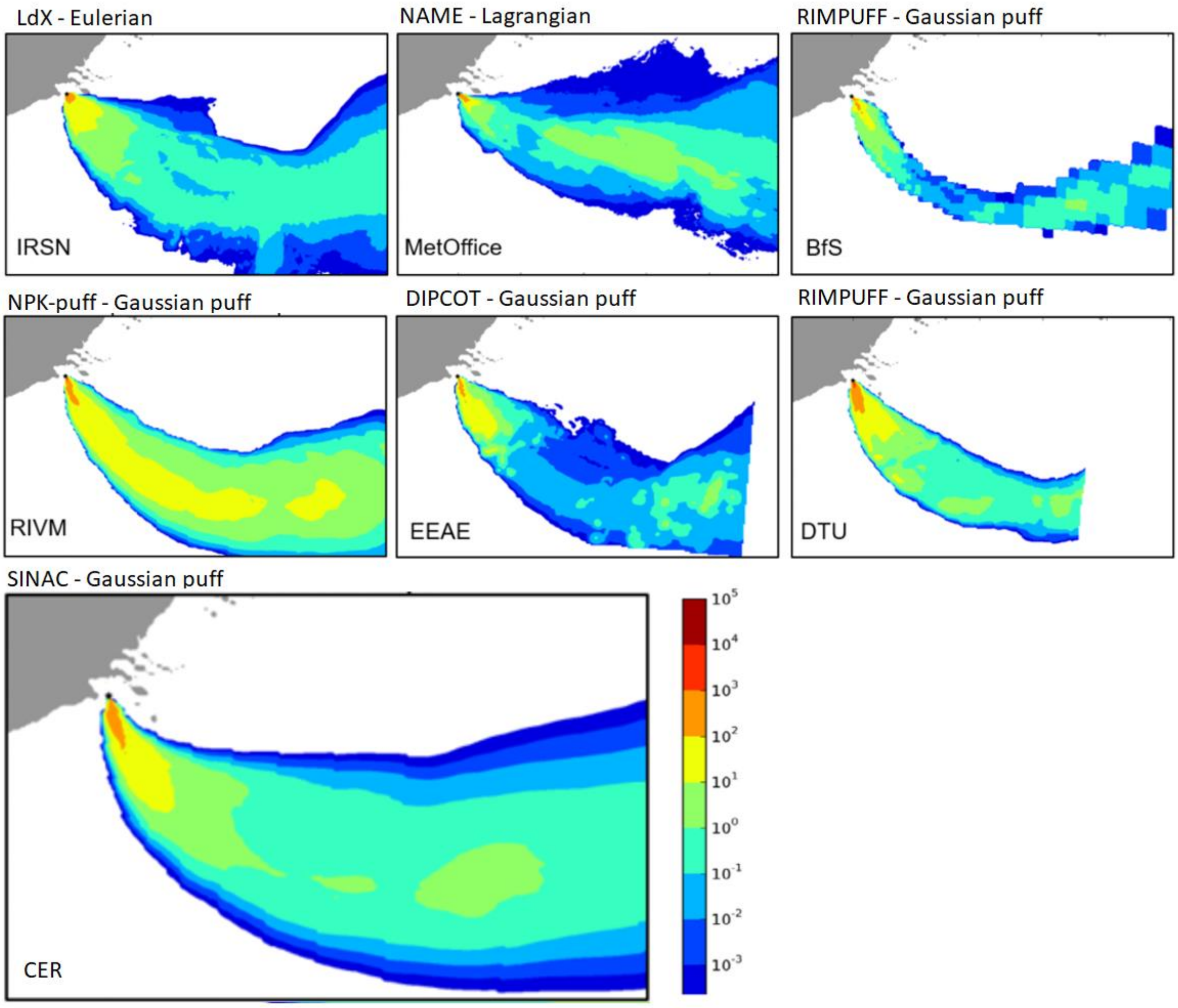

Figure 44. Median of the Cs-137 deposition [Bq/m^2] at 24 h computed for the meteorological ensembles for the seven participants of REM-2 case study (my results shown enlarged on the bottom) [P10][op4]

The maximum threshold exceedance for 37 kBq/m^2 Cs-137 deposition is presented in Figure 45 as boxplots (median shown with red line, 25th and 75th percentile with blue box, the spread with dashed blue line and the outliers with blue crosses). These show reasonably good agreement between the participants except for the results of the MetOffice and RIVM both of which overestimate the distances compared to the others. These outlier values raise the question of how these extreme or worst case results with low probability can be used by decision makers. A possible approach could involve introducing countermeasures in areas where the probability of threshold exceedance is high. In other locations, where the probability is lower, it would be more preferable to prepare and wait for more precise calculation before taking interventions, which can be made as the accident progresses and more information becomes available.

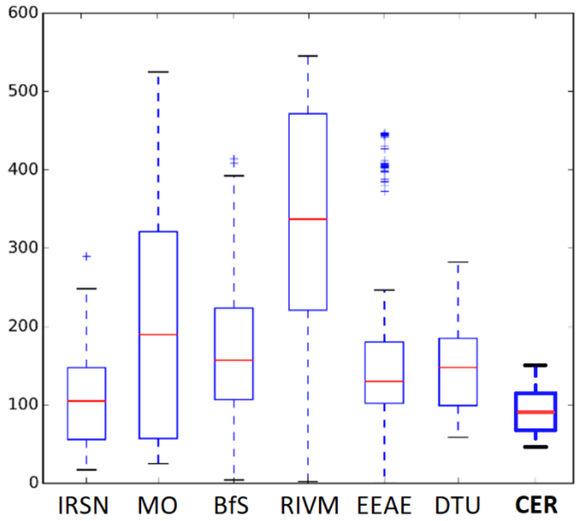

Figure 45. The maximum distance of threshold exceedance values for 37 kBq/m² Cs-137 deposition at 24 h computed for the meteorological and source term ensembles for the seven participants of REM-2 case study (my results indicated with bold font) [P10][op4]

6.2.2.3. Long release with both small and large meteorological variability (REM-L)

The REM-L case is a longer simulation lasting three days which includes both the REM-1 and REM-2 meteorological scenarios. For this calculation, either 10 or 5 ensembles were used by the participants which were compiled to represent the original spread of the source terms. To minimize the computational time of the simulations, I used only the 5 source terms as did BfS, while IRSN, Met Office, DTU and EEAE used 10 source term ensembles. Figure 46 shows the probability of threshold exceedance for 10 kBq/m² I-131 deposition 24 h after the release began. The figure shows the highest deposition values, in my results, which is expected, as the used default values of the scavenging factor for wet deposition was the highest in my calculations among the participants.

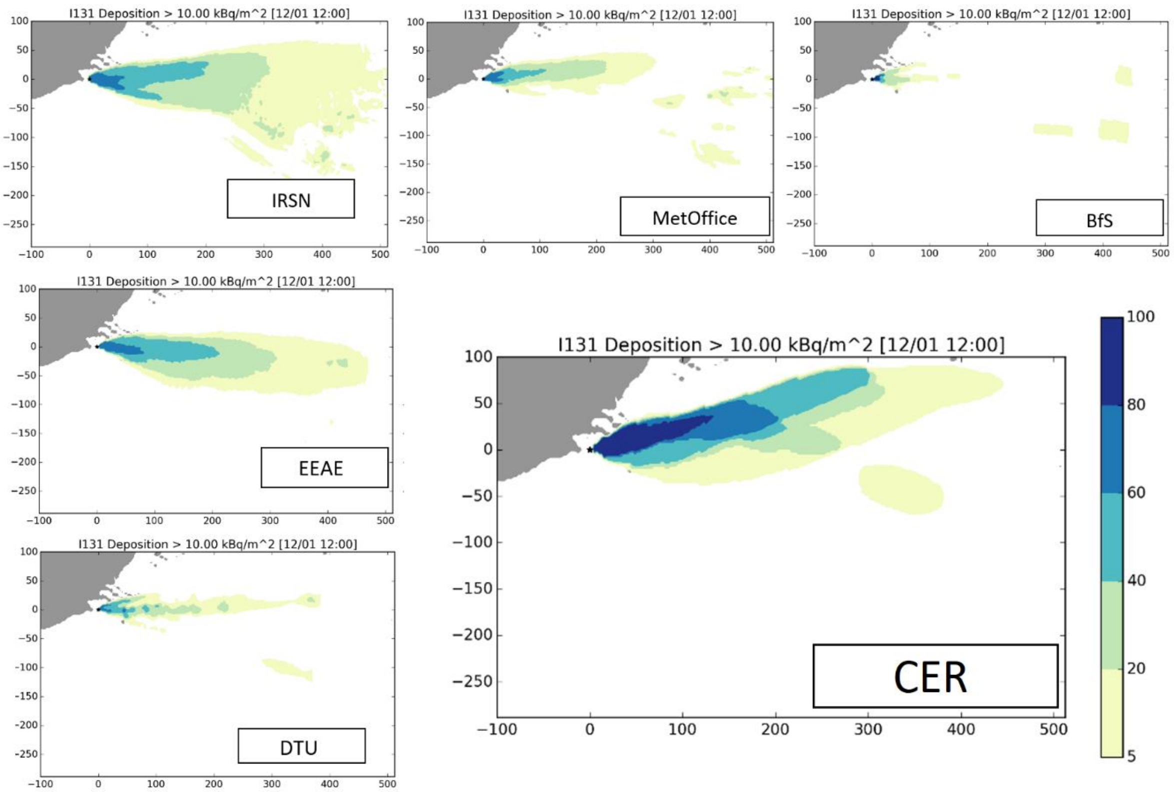

Figure 46. The probability of threshold exceedance maps of 10 kBq/m² I-131 deposition at 24 h computed for selected percentiles for the meteorological and source term perturbations (my results shown enlarged) [op4]

6.3. Optimization of operational use of ensemble input data

The most important characteristics of atmospheric dispersion and dose calculations conducted for emergency preparedness and response are their reliability and rapid computation. Achieving this requires a short runtime for calculation and the statements of uncertainties. As shown previously, while the uncertainties of the simulations can be evaluated with the ensemble methodology, this method is rather computation extensive and requires long computation times. To optimize simulations in order to have reasonably short calculation times, one way is to reduce the model run time for a single ensemble member. To investigate this, I conducted simulations with different input parameters and examined the resulting variation in the uncertainty indicators, specifically the maximum distance of threshold exceedance and the surface area of threshold exceedance [P11][P12][op5]. I carried out the calculations with the SINAC DSS and used the meteorological ensemble data from the REM-2 case with a single source term.

The runtime of the calculation of SINAC is comprised of three parts connected to different simulation tasks.

- first part is the initialization, which contains reading the configuration and input files, as well as the list of outputs and their characteristics;
- second part is the dispersion, which lasts while the released puffs are propagated until a predetermined maximum time or distance;

- final, third part is the calculation of the results, namely the activity concentrations and doses.

In the evaluation, the following parameters were perturbed separately (the baseline values are indicated with bold font):

- number of released puffs: 4, **16**, 64;
- puff propagation time resolution: **4 min**, 8 min, 16 min;
- model domain (maximum calculation distance): 254 km×254 km (400 km), 510 km×510 km (500 km), **767 km×767 km (600 km)**;
- result grid: 100×100 points, 200×200 points, **300×300 points**;
- output time resolution: **1 h**, 2 h, 4 h.

The maximum running time for the atmospheric dispersion calculation was specified as 36 hours.

First, I looked at varying the number of puffs that are released in the simulation, while keeping the total activity released the same (divided equally among the puffs).

The effect the variation in the number of released puff has on the running time is shown in Table 41, namely the mean runtime and their variance based on 10 meteorological ensembles for each calculation step and the total runtime for the entire simulation is presented .

Table 41. The mean and total runtime for the various simulation tasks considering different number of released puffs [P12][op5]

Mean run time (and variance) for each simulation task	Number of released puffs		
	4	16	64
Initialization	44.23 s (2.74 s)	45.00 s (2.70 s)	40.92 s (0.61 s)
Dispersion	26.56 s (4.00 s)	26.06 s (3.82 s)	26.84 s (3.96 s)
Calculation of the endpoints	213.5 s (10.4 s)	385.8 s (45.53 s)	1003.9 s (190 s)
Total run time for 10 ensembles	47.4 min	76.2 min	178.6 min

The largest part of the runtime, about 75-80% was the calculation and writing of the result, which processes were significantly affected by the number of released puffs. The total calculation time for the 10 ensembles was reduced to less than an hour when considering only 4 puffs. However, increasing the number of puffs from 16 to 64 more than doubled the total runtime.

The maximum distance of threshold exceedance for Cs-137 deposition of 10 kBq/m^2, effective dose of 1 mSv and inhalation thyroid dose equivalent of 10 mSv shown in Figure 47 indicate that it is not optimal to release 64 puffs instead of 16 puffs as their results are very similar. But considering that the uncertainty of the Cs-137 deposition expressed with the standard deviation of the values obtained for each puff was logically lower for 16 puffs than for 4 puffs, thus using the 4 puffs is not justified with regard to the precision to be achieved.

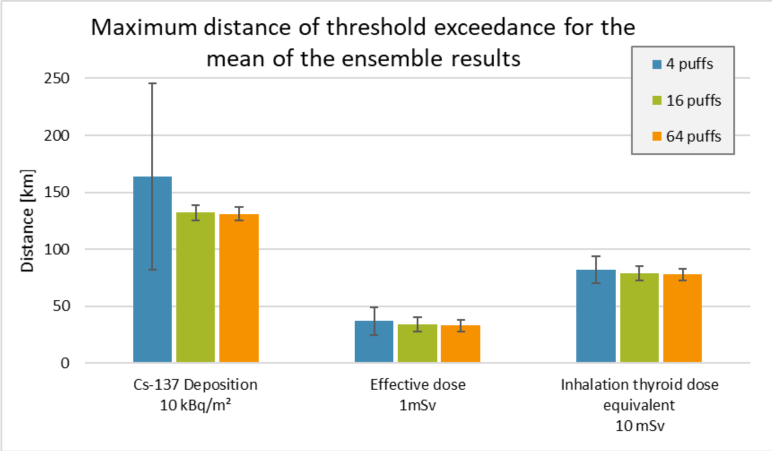

Figure 47. The maximum distance of threshold exceedance with standard deviation bars considering different number of released puffs [P12]

The next optimization approach was to reduce the spatial domain of the computation and focus on a smaller area around the release point. To investigate this, I reduced the size of the rectangular grid by decreasing its side from 300 points to 200 points and then to 100 points as shown in Figure 48.

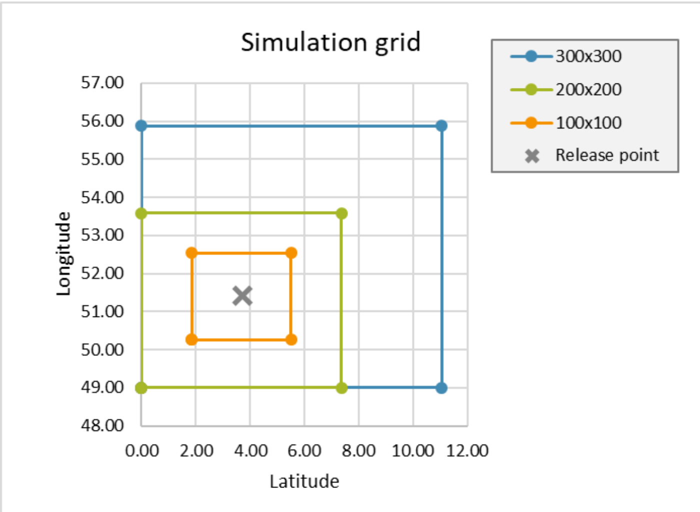

Figure 48. The modelling grid of the simulation and the location of the release point [P12][op5]

The mean and total runtime for the different number of receptor points is shown in Table 42. The run time was reduced to 37% and 13% by decreasing the modeling domain to 4/9 (200×200 points) and 1/9 (100×100 points), respectively. This reduction was the most significant in the results task, because the outputs were computed at fewer points. As the dispersion of the contaminants remained within the smallest grid for all ensemble members, the uncertainty indicators (maximum distance and surface of threshold exceedance) did not change with the reduction of the spatial domain. This type of optimization could be achieved more efficiently with registering the maximum distance of the dispersion and using this value to limit the calculation grid during the computation of the result quantities and writing zero values outside of the relevant area.

Table 42. The mean and total runtime for the various simulation tasks considering different number of receptor points and smaller grid sizes [P12][op5]

Mean run time (and variance) for each simulation task	Number of receptor points (grid size)		
	300×300 (767×767 km^2)	200×200 (510×510 km^2)	100×100 (254×254 km^2)
Initialization	45.00 s (2.70 s)	8.82 s (0.67 s)	1.09 s (0.06 s)
Dispersion	26.06 s (3.82 s)	26.77 s (3.96 s)	26.85 s (3.93 s)
Calculation of the endpoints	385.8 s (45.53 s)	132.72 s (8.57 s)	27.88 s (1.75 s)
Total run time for 10 ensembles	76.2 min	28.1 min	9.3 min

The last optimization method I investigated was changing the time resolution of the output quantities and thus reducing the number of endpoints that need to be computed. In the baseline case, the time resolution of the results, namely the air and ground activity concentration was 1 hour, which I changed to 2 and 4 hours. The mean and total runtime for the different output time resolutions in Table 43 indicate that the time savings were only minimal with this method, given that the total runtime was reduced by 22-26% with the coarser time resolutions.

Varying the time resolution of the results did not change the uncertainty indicators, the mean maximum distance and surface values of threshold exceedance.

Table 43. The mean and total runtime for the various simulation tasks considering different output time resolutions [P12][op5]

Mean run time for each simulation task	Output time resolution		
	1 h	2 h	4 h
Initialization	45.00 s (2.70 s)	41.87 s (1.69 s)	44.81 s (1.94 s)
Dispersion	26.06 s (3.82 s)	25.96 s (3.85 s)	26.02 s (3.81 s)
Calculation of the endpoints	385.8 s (45.53 s)	288.7 s (41.69 s)	268.7 s (44.29 s)
Total run time for 10 ensembles	76.2 min	59.5 min	56.6 min

7. SUMMARY AND OUTLOOK

Regarding the safety of nuclear facilities, it is crucial to investigate the consequences of radioactive releases from such installations which may have significant health impact on the members of public. The dose consequences of an accidental release to the atmosphere – which are usually significantly more severe that liquid releases– can be assessed via modelling the environmental transport of the radioactive material. In modelling, with regard to the investigated phenomenon, the most important processes are considered while other less relevant mechanisms are omitted. In addition to these, there are also uncertainties in modelling, such as the unpredictability and the natural variability of the modelled phenomena (aleatory uncertainty) and the lack of knowledge about the modelled system (epistemic uncertainty), which include

- model uncertainty, arising from simplifications, numerical approximations or incomplete treatment of the modelled phenomena, which can be assessed by comparing different models that compute the same quantity,
- parameter uncertainty, resulting from the uncertainties of the model parameters and input data, that can be evaluated through sensitivity analysis by perturbing single parameters, or uncertainty analysis, when multiple parameters are varied simultaneously.

In my thesis, I investigated the model and input uncertainties of atmospheric dispersion calculations conducted for deterministic safety assessment and for decision support in emergency preparedness and response.

In the context of deterministic assessments and atmospheric release criteria for nuclear facilities, practical application differs from country to country despite ongoing efforts for high level harmonization of the requirements [12]. With the goal of harmonization, an improved methodology was developed for the application of release criteria in practice and implemented in the CARC software. I contributed to this development and compared the new program with commercially available codes for simple scenarios and my results showed acceptable agreement. This indicates that the improved methodology can serve as a reliable tool for deterministic safety assessments and has a potential to contribute significantly to the harmonization of atmospheric release criteria application across different countries. I summarize the main highlights of the comparison in the following:

- The difference of the time-integrated air activity concentration and deposited activity concentration computed with CARC and PC-COSYMA fell between 2% and 50% for the considered meteorological cases (wind speed 1 m/s and 5 m/s, Pasquill stability classes A, D and F, rain intensity 1 mm/h, 5 mm/h and 10 mm/h) and distances (1 km, 3 km, 6.3 km, 10 km).
- The difference of the relative cloudshine and groundshine results obtained with CARC and Microshield ranged from -5% to +13% for the considered energies (from 100 keV to 10 MeV).

- The difference of the relative inhalation dose calculated with CARC and PC-COSYMA was only 1% for the considered radionuclides (Cs-137, I-131, and Sr-90).
- The difference of the relative ingestion doses was between -24% and +26% for the radionuclides that typically have significant contribution to the ingestion dose in case of an accidental release from an NPP (Ce-144, Cs-134, Cs-137, I-131, I-133, Ru-103, Sr-89 and Zr-95).

Through a hypothetical case study, I showed the practical application of the CARC methodology and compared the results with actual DEC safety criteria. The most important benefit of the CARC methodology for which I completed the verification and demonstrated its application is that the methods applied in the safety assessment are very simple and so the methodology could facilitate the harmonization of the practical application of release criteria worldwide.

Regarding the usage of meteorological data, I investigated how the variations of the used meteorological database effect the dose results of deterministic safety assessments which has to be robust and cannot depend significantly on the variation of the meteorological conditions. The main highlights of the evaluation are:

- Using a worst case meteorological scenario for deterministic safety assessment introduces excessive conservativism, leading to unrealistic results the occurrence of which could be omitted due to the very low probability. Instead, the use of a large, site-specific dataset of meteorological measurements, can yield a more realistic yet still conservative outcome. For example, applying the 95th percentile of the considered meteorological cases strikes the right balance between realism and conservatism.
- The difference between the dose result obtained using a predetermined worst case or conservative meteorological data, compared to the actual worst scenario derived from a large meteorological database can be several orders of magnitude.
- In case of a lack of data points in the meteorological database, it is advisable to use a relatively high percentile (e.g. the 95th) as the final result of the calculation. Such percentiles show the lowest variability within the investigated range, thus providing a more reliable basis for deterministic safety assessments.

I conducted my investigations with a 5-years-long meteorological measurement database as an example to demonstrate that selecting meteorological data for deterministic safety assessment requires careful consideration of factor such as missing data and the choice of percentile to use, as these factors can have a significant influence on the final calculation result. The methods I presented are universal and can guide others in effectively applying optimal meteorological databases for deterministic safety assessments.

Future work on the usage of meteorological data for deterministic safety assessment could explore several topics. If there is no available meteorological data for a given location, getting supplementary data from numerical weather prediction models or measurements from nearby locations to assess the uncertainties associated with data extrapolation is an approach that could be investigated. Another interesting possibility to assess the uncertainties of the meteorological data would be to estimate the distribution of meteorological variables similarly to how meteorological hazards associated with extreme meteorological conditions are investigated for risk assessment purposes [116][117]. Concerning what percentile to use as the final result when considering a broad range of meteorological data, I tried to avoid arguing in favor of one specific percentile, as my exact findings only pertains to the specific scenario (location of meteorological measurement data, chosen endpoints of the assessment) that I used in the investigation. Expanding the analysis to meteorological data from different locations and longer time periods (e.g. 10 or 20 years-long data) would provide insight into the sensitivity to specific locations and temporal changes. Regarding the potential impacts from climate change, the conditions that could affect atmospheric dispersion modelling are more frequent occurrence of unstable atmospheres (as presented in [118]) and extreme storms with higher rainfall intensity (as shown in [119]). Unstable atmosphere is generally favorable for in terms of the public dose, because in unstable conditions the plume is more wide and diluted, i.e. the air and ground activity concentration will be lower. On the contrary, the increase in the rain intensity will significantly increase the ground activity concentration, and thus the groundshine dose and the food chain dose will be higher, the air activity concentration will be lower (due to the higher level of wash-out), which will reduce the cloud dose and the inhalation dose. Based on these deductions, it is not clear how the use of future meteorological databases will affect total doses in light of climate change. Nevertheless, my expectation is that, from a robustness point of view, the variance of the actual maximum dose will still be larger than the 95-99 percentiles, precisely because of the more extreme conditions.

The evaluation of uncertainties is also important in the case of decision support systems that are used for providing advice about the introduction of protective measures in real-life emergencies. To investigate the influence of various methods used for atmospheric dispersion calculation, I compared three types of puff propagation models of the SINAC DSS. The various puff propagation methods differ how they consider the time step of the incrementation: the first method uses fixed time steps, the second uses time steps proportional to the size of the puff and the third one adjusts the time step based on the increment of the dispersion parameter. The aim of the analysis was to find the most optimal method that produces precise results with the lowest computation time. My main results are the following:

- If the receptor points of the calculation are relatively close to the release point, the most precise air activity concentration results were produced by the third model (where the time step is based on the increment of the dispersion parameter). However, the computational time of this method was higher than those of the first and second method.
- If the running time of the calculation is the most important, then the second method should be used, as it gives acceptable time-integrated air activity concentration results with the lowest runtime.

Regarding the puff propagation model of the SINAC software, further assessments could be conducted to include a wider range of receptor points with the consideration of various atmospheric stability conditions which influence the dispersion parameter and thus the time step of the calculation in case of the second and third methods.

The uncertainties of atmospheric dispersion models used for emergency response calculations have to be evaluated as well. In order to estimate the uncertainties caused by the meteorological input data of such calculations I conducted a sensitivity analysis with the SINAC DSS. In the analysis, I perturbed key meteorological parameters that are considered in the modeling, such as the wind speed, wind direction, atmospheric stability and precipitation, and determined their influence on the environmental activity concentrations. Based on my assessment, the ranking of the most influential meteorological parameters on the atmospheric dispersion calculation is as follows: wind direction, precipitation, Pasquill stability category and wind speed. This ranking generally aligns with the literature, although there is some discrepancy regarding the wind speed which is often ranked higher in literature due to it's potential of having a large influence in certain scenarios.

Taking part in the CONFIDENCE project, I participated in the assessment of the source term and meteorological uncertainties of atmospheric dispersion modelling considering different radiological release scenarios. In the REM case studies, different meteorological cases and source terms were taken into account as ensembles and various statistical values and probability of exceedance areas were computed as results. Our findings indicated that the variation in the release time caused larger variability than the variability of the meteorological data resulting in lower probabilities of threshold exceedance but larger areas of contamination. The project findings revealed significant differences between the results obtained with various software despite using the same input data. These discrepancies can be attributed to the differences in modelling methods, including dispersion model, deposition schemes and simulation domains. Our work also highlighted the importance of using multiple different outputs (e.g. statistical values and graphical maps) to comprehensively visualize the uncertainties inherent in the calculations.

In addition to the necessity of showing the uncertainties of atmospheric dispersion results of decision support systems aimed at providing reliable advice for protective measures, the computational speed is crucial due to the limited time available during emergencies. The advantage of using ensemble input for the atmospheric dispersion calculation of such systems is that it directly quantifies the uncertainty of the computed quantities. However, the typical runtime of such simulations often exceeds practical limits for operational use in emergencies. To optimize the simulations in an ensemble approach, I investigated different methods of efficiency savings for a specific release scenario and identified which approach would make the computations optimal to be used in an emergency situation without the detriment of the uncertainty indicators of the atmospheric dispersion and dose calculation. The most important results of my assessment are the following:

- The reduction of the number of released puffs substantially improved the run time of the simulation, but excessive reduction of the puff number can cause variation in the uncertainty indicator and decrease precision. Consequently, the lowest number of puffs negligibly alter the results would be the most optimal to use in operation.
- Pre-selection of the most optimal spatial simulation domain for a given release scenario would significantly reduce the run time without changing the model outputs and affecting their uncertainties. This could be achieved with a simpler atmospheric dispersion model (e.g. Gaussian plume model) using an appropriately selected release meteorological scenario that envelopes all the input ensemble members.
- Reducing the number of computed output quantities (e.g. by decreasing their time resolution or selecting the most important endpoints) could also be beneficial in improving the simulation efficiency. While this method only moderately decreases the runtime, but without compromising the precision of the results.

There are other possible ways of optimizing the simulation to reduce the computational time, which could be investigated in the future. Decreasing the number of radionuclides that are considered in the atmospheric dispersion and dose calculation would also make the computations faster, however the appropriate correction of the results is needed in this case to compensate for the contribution of the omitted radionuclides. There is ongoing research for the selection of key radionuclides for atmospheric dispersion and dose calculation, which would be the representatives of groups of other nuclides with similar physical and chemical properties. With appropriate knowledge of each group member's contribution to a given output quantity (e.g. activity concentrations or doses), the computations could be carried out by focusing solely on a few key nuclides. It is important to recognize that the key nuclides may vary depending on different conditions of nuclear power plants, such as operating states, fuel burn-up, accident conditions. The runtime could also be reduced with the optimization of the software enhancing computational efficiency by transforming or changing the computer code. In addition, some parts of the computation could be parallelized, allowing various tasks to be executed concurrently on separate cores or processors of the computer.

THESIS STATEMENTS

The new scientific results of my dissertation are summarized in the following statements:

1. Thesis Statement:

I improved analytical models with regard to the transparency and simplicity of the calculation process and integrated them into the CARC (Calculations for Release Criteria) software for verifying compliance with release criteria for nuclear facilities. I showed that the internal results of calculations obtained with the improved models show differences between 50%-150%, and agree adequately according to such comparisons with the results obtained with other conventional programs used in international practice

- in the environmental activity concentrations there were more significant differences of up to 60-90% in some cases,
- the difference in the external and inhalation dose was less than 13%,
- the difference in the ingestion dose was maximum 26% for the nuclides that typically contribute to the public dose.

I pointed out that most of the differences are caused by the discrepancies between the individual methods of the compared models and model parameters used. I showed that the value of the effective dose determined for deterministic safety analyzes is significantly influenced by some parameters that describe the habits of the population (i.e. breathing rate, time spent outdoors, shielding and food consumption). Of these, changing the breathing rate (between 0.7 m^3/h and 3 m^3/h), the degree of shielding (between 0.01 and 0.4) and the time spent outdoors (between 1 h and 6 h) do not significantly affect the 1-year effective dose (causing a maximum of 24% difference). The consumption of certain contaminated foodstuffs (i.e. leafy vegetables and milk) increased the 1-year effective dose considerably: the difference compared to no consumption ranged between 124%-251% depending on the used meteorological data. I verified the practical applicability of the models and the CARC program through a case study confirming the verification of compliance with a criteria applied in nuclear deterministic safety analyses for a hypothetical release scenario. [P1][P2]

2. Thesis Statement:

I showed that during deterministic safety analyses, the use of an at least 5-years-long database based on real meteorological measurements and a well-chosen dose percentile gives a more robust result than using fixed meteorological parameters associated with the estimated worst case used in general practice. Using a real annual meteorological dataset, I verified that in the case of random omission of points from the meteorological database, the difference of the 95th percentile of the 7-day dose the 95th percentile compared to the result determined with the full dataset is adequate, less than 5%. I confirmed the adequacy of the method and the advantage of using a well-chosen percentile by finding that, compared to the estimated worst case appointed based on expert judgement (not considering site specific real measurement data), the largest deviation between the maximum doses determined for different years can be nearly 5000% depending on the percentile, while for the 95th percentile of using real meteorological data a maximum of 50% was obtained. [P3]

3. Thesis Statement:

I proved that from the various puff propagating models available in the atmospheric dispersion model of the SINAC (Simulator Software for Interactive Modeling of Environmental Consequences of Nuclear Accidents) emergency response decision support system, the closest to the result regarded to be precise but generated with the longest runtime obtained with the method using the smallest fixed time step was given by the quicker autoscaling procedure that considers the increment of the σ_z vertical dispersion parameter (using a step multiplication factor of M_0 =1.001 and 1.004). Obtaining a difference of less than 1% for the specific release scenario, at 1 km, 3 km and 30 km distance and considering fix meteorological parameters (1 m/s wind speed, D Pasquill stability class and 0 mm/h rain intensity). I showed that in the case of emergency preparedness calculations, in order to minimize the running time, it is optimal to use the model in which the step of the puff depends on the value of the σ_r horizontal dispersion parameter. I proved that in this case by choosing the right parameter (e.g. step multiplication factor m_0 =0.5), the running time is significantly shorter (a half or a quarter) compared to other methods, while the time-integrated activity concentration for the plume passage differs by only 3-5% compared to the case that is considered precise. [P4]

4. Thesis Statement:

I pointed out that the uncertainty of meteorological data can have significant effect on the results of atmospheric dispersion calculation model used for emergency preparedness, I identified the parameters that dominantly influence the calculation of environmental activity concentrations and I quantified the extent of their influence. I proved that a change in the wind speed from 1 m/s to 10 m/s close to the emission point (1-5 km) and in the wind direction from 0° to 10° further away (5-30 km) can cause a difference of 3 orders of magnitude in the activity concentration. I developed a new module for the SINAC emergency preparedness decision support system, with which, using ensemble meteorological data, the uncertainty of the atmospheric dispersion calculation derived from meteorological data can be directly determined and displayed without a labor-intensive sensitivity or uncertainty assessment. I verified the applicability of the ensemble method of the SINAC program with calculations carried out in the framework of an international project. [P5][P6][P7][P8][P9][P10]

5. Thesis Statement:

With the series of calculations performed with the SINAC decision support system, I identified the possibilities of optimizing the run time which is critical from the point of view of emergency decision-making. I showed that reducing the original modelling area to 4/9 and 1/9 and reducing the time resolution of the results to two and four times, while keeping the values of the examined results unchanged, reduced the running time for the simulation of 10 ensemble members from 76 min to 28 min, 9 min, 59 min and 57 min, respectively. I proved that reducing the time step of the release, i.e. the number of puffs emitted in a given time, by a quarter (from 64 to 16 then to 4) while beneficially reduced the run time of the 10 ensemble calculation (from 179 min to 76 min then to 47 min), caused a variation of 25% in the expected value of Cs-137 deposition, one of the most important results in terms of radiation protection and increased its standard deviation by more than six times. [P11][P12]

1. Tézispont:

A nukleáris létesítmények kibocsátási kritériumainak való megfelelés igazolására szolgáló analitikus modelleket a számítási folyamat átláthatósága és egyszerűsége szempontjából továbbfejlesztettem és beépítettem a CARC (Calculations for Release Criteria) szoftverbe. Megmutattam, hogy a továbbfejlesztett modellekkel kapott számítási részeredmények egyéb, nemzetközi gyakorlatban elfogadottan használt programokkal kapott eredményektől való eltérése 50%-150% közötti, vagyis az egyezés az ilyen összehasonlításokhoz viszonyítva megfelelő:

- a környezeti aktivitáskoncentrációknál jelentős, egyes esetekben akár 60-90%-os különbségek is adódtak,
- a külső és inhalációs dózis esetén az eltérés kevesebb, mint 13%,
- a tápláléklánc dózisban azon nuklidok esetében, melyek a lakosság sugárterhelésében tipikusan jelentős járulékot adnak, az eltérés maximum 26%.

Rámutattam, hogy az eltérések nagy részét az összehasonlított modellek egyes metódusai és a felhasznált modellparaméterek közötti különbségek okozzák. Megmutattam, hogy a determinisztikus biztonsági elemzések esetén meghatározott effektív dózisok értékét egyes lakossági szokásokat leíró paraméterek (azaz a légzési sebesség, az árnyékolás mértéke, a szabadban való tartózkodás ideje, a fogyasztási szokások) jelentősen befolyásolják. Ezek közül a légzési sebesség (0,7 m^3/h és 3 m^3/h közötti), az árnyékolás mértékének (0,01 és 0,4 közötti) és a szabadban való tartózkodás idejének (1 h és 6 h közötti) változtatása nem befolyásolja jelentősen az 1 éves effektív dózist (maximum 24%-os eltérés okozva). Egyes szennyezett élelmiszerek (a leveles zöldségek és a tej) fogyasztása jelentősen növelte az 1 éves effektív dózist: az eltérés a fogyasztás nélküli esethez képest 124%-251% közöttinek adódott a figyelembevett meteorológiai adatoktól függően. Igazoltam a modellek és a CARC program gyakorlati alkalmazhatóságát egy esettanulmányon keresztül, igazolva a determinisztikus nukleáris biztonsági elemzések során alkalmazott kritériumnak való megfelelést egy hipotetikus kibocsátási esetre. [P1][P2]

2. Tézispont:

Megmutattam, hogy a determinisztikus biztonsági elemzések során egy legalább 5 évet felölelő, valós meteorológiai méréseken alapuló adatbázis és egy jól kiválasztott dózis percentilis használata robusztusabb eredményt ad, mint az általános gyakorlatban elterjedt legkedvezőtlenebb becsléshez („worst case") tartozó fix meteorológiai paraméterek és egy dóziseredmény alkalmazása. Egy éves valós meteorológiai adatsor használatával igazoltam, hogy meteorológiai adatokból véletlenszerű adatelhagyás esetén a 7 napos dózis 95. percentilisének eltérése a hiánymentes meteorológiai adatsorral meghatározott eredményhez képest megfelelő, 5% alatti. A módszer megfelelőségét és a jól megválasztott percentilis alkalmazásának előnyét továbbá azzal a megállapítással is alátámasztottam, hogy a szakértői becslés (nem a telephelyre jellemző, valós mérési adatok) alapján meghatározott legrosszabb becslésű esethez képest a különböző évekre számított maximum dózisok közötti legnagyobb eltérés akár közel 5000% is lehet a percentilis értékétől függően, míg a valós meteorológiai adatokkal meghatározott 95. percentilis maximum 50%-os eltérést mutatott. [P3]

3. Tézis:

Igazoltam, hogy a SINAC (Simulator Software for Interactive Modelling of Environmental Consequences of Nuclear Accidents) balesetelhárítási döntéstámogató rendszer légköri terjedési modelljében rendelkezésre álló pöff léptetési modellek közül a legkisebb fix időlépést alkalmazó módszerrel kapott és pontosnak tekintett, de leghosszabb futtatási idővel szolgáltatott eredményhez legközelebbi eredményt a rövidebb futási idejű, a σ_z vertikális diszperziós paraméter változásától függő autóskálás eljárás adja (M_0 =1,001 és 1,004 léptetési szorzótényezővel). Kevesebb, mint 1% eltérés adódott a vizsgált egyszerű kibocsátási esetben, 1 km, 10 km és 30 km távolságban, fix meteorológiai paraméterek figyelembevételével (1 m/s szélsebesség, D Pasquill kategória és 0 mm/h esőintenzitás). Megmutattam, hogy balesetelhárítási számítás esetén a futási idő minimalizálása céljából azon modell használata az optimális, melyben a pöff léptetése a σ_r horizontális diszperziós paraméter értékétől függ. Bizonyítottam, hogy a megfelelő paraméter választásával (például m_0 =0,5 léptetési szorzótényezővel) a futási idő jelentősen rövidebb (a fele vagy negyede) az egyéb módszerekhez képest, miközben az időintegrált aktivitáskoncentráció a csóva elhaladásának teljes idejére csupán 3-5%-kal tér el a pontosnak tekintett esethez képest. [P4]

4. Tézis:

Rámutattam, hogy a meteorológiai adatok bizonytalansága jelentős hatással lehet a balesetelhárítási légköri terjedésszámítási modellek eredményeire, azonosítottam a környezeti aktivitáskoncentrációk számítását dominánsan befolyásoló paramétereket, és számszerűsítettem a hatásuk mértékét. Igazoltam, hogy a kibocsátási ponthoz közel (1-5 km) a szélsebesség 1 m/s-ról 10 m/s-ra változtatása körülbelül egy nagyságrendnyi, míg távolabb (5-30 km) a szélirány 10 fokkal való eltérése 3 nagyságrendnyi eltérést okozhat az aktivitáskoncentrációban. Új modult dolgoztam ki a SINAC balesetelhárítási döntéstámogató rendszerhez, amellyel ensemble meteorológiai adatok használatával nagy munkaigényű érzékenységi vagy bizonytalansági vizsgálat nélkül, közvetlenül becsülhető és megjeleníthető a légköri terjedésszámítás meteorológiai adatokból származó bizonytalansága. A SINAC program ensemble bemeneti adatokat felhasználó módszerének alkalmazhatóságát nemzetközi projekt keretében végzett számításokkal igazoltam, melyekben bemutattam a bizonytalanságok vizualizációját térképen megjelenítve különböző eredmények határérték átlépési valószínűségének statisztikai jellemzőit. [P5][P6][P7][P8][P9][P10]

5. Tézispont:

Azonosítottam a balesetelhárítási döntéshozatal szempontjából kritikus futtatási idő optimalizálásának lehetőségeit a SINAC döntéstámogató rendszerrel végzett számítássorozattal. Megmutattam, hogy az eredeti modellezési terület 4/9, illetve és 1/9 részre való csökkentése és az eredmények időbeli felbontásának felére és negyedére csökkentése a vizsgált eredmények értékének változatlansága mellett a 10 ensemble tag szimulációjának 76 perces futási idejét rendre 28 percre, 9 percre, 59 percre és 57 percre csökkentette. Bebizonyítottam, hogy a kibocsátás időbeli léptetésének, vagyis az adott idő alatt kibocsátott pöffök számának negyedére való csökkentése (64-ről 16-ra, majd 4-re), ugyan előnyösen csökkentette a 10 ensemble tag számításának futási idejét (179 percről 76 percre, majd 47 percre), de 25%-kal módosította a sugárvédelmi szempontból egyik legmeghatározóbb Cs-137 kiülepedésre vonatkozó várható értéket, a szórását pedig több mint hatszorosára növelte. [P11][P12]

List of Publications

Publications related to the thesis statements

[P1] **Cs. Rudas**, T. Pázmándi, P. Zagyvai, "Evaluation of an Improved Method and Software Tool for Confirming Compliance with Release Criteria for Nuclear Facilities", *Annals of Nuclear Energy*, Vol. 159, 2021, https://doi.org/10.1016/j.anucene.2021.108332

[P2] **Cs. Rudas**, T. Pázmándi, "Case Study with CARC software for Verifying Compliance with Atmospheric Release Criteria of Nuclear Installations", *9th International Conference on Radiation in Various Fields of Research (RAD 2021), Herceg Novi, Montenegro, 14–18 June 2021*, 2021, https://rad2021.rad-conference.org/vs/RAD_2021-Csilla_Rudas.pdf

[P3] **Cs. Rudas**, T. Pázmándi, "Consequences of Selecting Different Subsets of Meteorological Data to Utilize in Deterministic Safety Analysis", *Journal of Environmental Radioactivity*, Vol. 225, 2020, https://doi.org/10.1016/j.jenvrad.2020.106428

[P4] P. Szántó, S. Deme, A. László, T. Pázmándi, **Cs. Rudas**, "Comparing Different Methods of Calculating Atmospheric Dispersion in SINAC", *in Proceedings of the 18th International Conference on Harmonisation within Atmospheric Dispersion Modelling for Regulatory Purposes*, HARMO18, Bologna, Italy, 9-12 Oct 2017

[P5] T. Pázmándi, D. Jakab, **Cs. Rudas**, P. Szántó, "Availability and reliability of meteorological data for atmospheric dispersion models" *in Proceedings of the5th European IRPA Congress, The Hague, The Netherlands, 4-8 June 2018*. pp. 247-252, 2018 https://irpa2018europe.com/wp-content/uploads/2019/08/IRPA2018-Proceedings-v2sec.pdf#page=253

[P6] **Cs. Rudas**, T. Pázmándi, P. Szántó, M. Szűcs, B. Szintai, "The Application of Meteorological Ensembles in the SINAC Decision Support System", *in Proceedings of the 19th International Conference on Harmonisation within Atmospheric Dispersion Modelling for Regulatory Purposes, HARMO19, Bruges, Belgium, 3–6 June 2019*, 2019, https://www.harmo.org/Conferences/Proceedings/_Bruges/publishedSections/H19-095%20Csilla%20Rudas.pdf

[P7] **Cs. Rudas**, P. Szántó, O. Várady-B., M. Szűcs, B. Szintai, T. Pázmándi, "The application of meteorological ensembles in the SINAC decision support system", *44th Annual Meeting on Radiation Protection, Hajdúszoboszló, Hungary 16-18 Apr 2019,* 2019. https://elftsv.hu/svonline/docs/kulonsz/HSZOB2019_Book_of_abstract.pdf#page=28

[P8] I. Korsakissok, S. Andronopoulos, P. Astrup, P. Bedwell, K. Chevalier-Jabet, H. De Vries, G. Geertsema, F. Gering, T. Hamburger, H. Klein, S. Leadbetter, A. Mathieu, T. Pazmandi, R. Périllat, **C. Rudas**, A. Sogachev, P. Szanto, J. Tomas, C. Twenhöfel and J. Wellings, "Comparison of ensembles of atmospheric dispersion simulations: lessons learnt from the confidence project about uncertainty quantification" *in Proceedings of the 19th International*

Conference on Harmonisation within Atmospheric Dispersion Modelling for Regulatory Purposes, HARMO19, Bruges, Belgium, 3–6 June 2019, 2019, https://www.harmo.org/Conferences/Proceedings/_Bruges/publishedSections/H19-081%20Irene%20Korsakissok.pdf

[P9] S. J. Leadbetter, S. Andronopoulos, P Bedwell, K. Chevalier-Jabet, I. Korsakissok, A. Mathieu, R. Périllat, J. Wellings, G. Geertesma, F. Gering, T. Hamburger, A. R. Jones, H. Klein, T. Pázmándi, **Cs. Rudas**, A. Sogachev, P. Szanto, J. Tomas, C. Twenhöfel, H. de Vries, "Ranking Uncertainties in Atmospheric Dispersion Modelling Following the Accidental Release of Radioactive Material", *Radioprotection*, Vol. 55, pp. S51 - S55, 2020. https://doi.org/10.1051/radiopro/2020012

[P10] I. Korsakissok, S. Andronopoulos, P. Astrup, P. Bedwell, E.Berge, T. Charnock, H. De Vries, G.Geertsema, F.Gering, T. Hamburger, I. Ievdin, H. Klein, S. Leadbetter, O. C. Lind, T. Pázmándi, R. Périllat, **Cs. Rudas**, B. Salbu, S. Schantz, R. Scheele, A. Sogachev, N. Syed, J. Tomas, M. Ulimoen, J. Wellings, "Uncertainty propagation in atmospheric dispersion models for radiological emergencies in the pre- and early release phase: summary of case studies", *Radioprotection*, Vol. 55, pp. S57 – S68, 2020. https://doi.org/10.1051/radiopro/2020013

[P11] P. Bedwell, I. Korsakissok, S. Leadbetter, R. Périllat, **Cs. Rudas**, J. Tomas and J. Wellings, "Operationalising an ensemble approach in the description of uncertainty in atmospheric dispersion modelling and an emergency response", *Radioprotection*, Vol. 55, pp. S75 – S79, 2020. https://doi.org/10.1051/radiopro/2020015

[P12] **Cs. Rudas**, P. Szántó, T. Pázmándi, P. Zagyvai, "Efficiency savings in model setup for an ensemble approach used to describe atmospheric dispersion model uncertainty", *CONFIDENCE Dissemination workshop,* Bratislava, Slovak Republic, 5-9 December 2019. https://eu-neris.net/library/archives/concert/confidence/confidence-dissemination-workshop-2-5-december-2019/posters.html

Other publications

[op1] J. Wellings, P. Bedwell, S. Leadbetter, J. Tomas, S. Andronopoulos, I. Korsakissok, R. Périllat, A. Mathieu, G. Geertsema, H. de Vries, H. Klein, T. Hamburger, F. Gering, T. Pázmándi, P. Szanto, **C. Rudas**, A. Sogachev, N. Davis, C. Twenhöfel, "D 9.1.5 - Guidelines for ranking uncertainties in atmospheric dispersion", *European Joint Program for the Integration of Radiation Protection Research CONCERT - CONFIDENCE project, H2020 – 662287,* 2018. https://www.concert-h2020.eu/sites/concert_h2020/files/uploads/Deliverables/D9/Confidence/D9.1-9.20/_Lists_Deliverables_Attachments_56_D9.1_CONFIDENCE_D68_Guidelines-ranking-uncertainties-for-atmospheric-dispersion_updated_approved02032018.pdf

[op2] S. Leadbetter, Reviewers: H. Klein, H. de Vries, C. Rudas, I. Korsakissok, P. Bedwell, M. Hort: D 9.2 – Published dataset of meteorological ensemble data to be used as dispersion and source terms by other WPs (Fukushima and synthetic), *European Joint Program for the*

Integration of Radiation Protection Research CONCERT - CONFIDENCE project, H2020 – 662287, 2017. https://www.concert-h2020.eu/sites/concert_h2020/files/uploads/Deliverables/D9/Confidence/D9.1-9.20/_Lists_Deliverables_Attachments_41_D69_CONCERT_-Published-dataset-of-meteorological_26062017Approved.pdf

[op3] H. De Vries, G. Geertsema, I. Korsakissok, R. Périllat, R. Scheele, J. Tomas; S. Andronopoulos, P. Astrup, P. Bedwell, T. Charnock, T. Hamburger, I. Ievdin, S. Leadbetter, T. Pázmándi, **C. Rudas**, A. Sogachev, P. Szántó, J. Wellings, "D 9.4 – Published sets of probability maps of threshold exceedance for scenarios provided to WP4, WP5 & WP6→ 2", *European Joint Programme for the Integration of Radiation Protection Research, CONCERT - CONFIDENCE project*, 2019. https://www.concert-h2020.eu/sites/concert_h2020/files/uploads/Deliverables/D9/Confidence/D9.1-9.20/_Lists_Deliverables_Attachments_101_D9.4_Published-sets-of-probability-maps-of-threshold-exceedance-for-scenarios_approved28012019.pdf

[op4] H. De Vries, G. Geertsema, I. Korsakissok, S. Leadbetter, R. Périllat, R. Scheele, J. Tomas, S. Andronopoulos, P. Astrup, P. Bedwell, T. Charnock, T. Hamburger, I. Ievdin, S. Leadbetter, T. Pázmándi, R. Périllat, **C. Rudas**, A. Sogachev, P. Szántó, J. Wellings, "D 9.5.1 – Ensemble calculations for the atmospheric dispersion of radionuclides. Hypothetical accident scenarios in Europe: the REM case studies", *European Joint Program for the Integration of Radiation Protection Research CONCERT - CONFIDENCE project, H2020 – 662287*, 2019. https://www.concert-h2020.eu/sites/concert_h2020/files/uploads/Deliverables/D9/Confidence/D9.1-9.20/_Lists_Deliverables_Attachments_170_D9.5_Guidelines-for-the-use-of-ensemble-calculations_approved28112019.pdf

[op5] P. Bedwell, I. Korsakissok, S. Leadbetter, R. Périllat, **C. Rudas**, J. Tomas, J. Wellings, „D9.5.5 – Guidelines for the use of ensembles in the description of uncertainty in atmospheric dispersion modelling: operational applications in the context of an emergency response", *European Joint Programme for the Integration of Radiation Protection Research, CONCERT - CONFIDENCE project*, 2019. https://www.concert-h2020.eu/sites/concert_h2020/files/uploads/Deliverables/D9/Confidence/D9.1-9.20/_Lists_Deliverables_Attachments_170_D9.5_Guidelines-for-the-use-of-ensemble-calculations_approved28112019.pdf

ACKNOWLEDGEMENTS

First and foremost, I would like to express my gratitude to my supervisor Dr. Tamás Pázmándi for his continuous guidance and support throughout my PhD studies. His enthusiasm and encouragements have motivated me to broaden the scope of my work and his excellent ideas and advice helped me through the challenges in my research. I would like to thank my former colleague Péter Szántó for introducing me to the topic of atmospheric dispersion calculations and the SINAC software, his mentorship provided the foundation that enabled me to start my PhD.

I am extremely grateful to my colleague Péter Zagyvai, who through all of his numerous commitments have always found time for consultations and to review my manuscripts and my dissertation. His advice and contribution has been invaluable to my work.

I would like to thank my colleagues in the Radiation Protection Department of the Centre for Energy Research, especially Dorottya Jakab and Anna Pántya for the fruitful discussions, their review of my publications and their professional end emotional support throughout my PhD.

I would like to extend my gratefulness to my co-authors from the CONFIDENCE project, particularly to Irène Korsakissok, Peter Bedwell, Susan Leadbetter, Jasper Tomas and Raphaël Périllat, who helped me during our joint research.

I wish to thank my consultant Dr. Szabolcs Czifrus from the Institute of Nuclear Techniques of the Budapest University of Technology and Economics as well as Dr. Dániel Péter Kiss, Dr. Máté Szieberth and Dr. Gergő Pokol for their support throughout my studies.

I would like to express my deepest gratitude towards my family, my parents, sisters and grandparents for always believing in me, for loving and encouraging me throughout my entire life.

Finally, I owe my greatest gratitude to my husband Viktor, for his unlimited love and tremendous patience, without his support, it would have been impossible for me to reach this point and complete my PhD. I am also eternally grateful to my son Vili, for brightening my life, for reminding me that I am capable of anything, and for sleeping just enough so I can finish writing my dissertation.

I. ANNEX: IMPROVED METHODOLOGY FOR CONFIRMING COMPLIANCE WITH ATMOSPHERIC RELEASE CRITERIA

"The standard practice of confirmation of compliance with release criteria is the determination of the source term, the environmental transport and the resulting dose which is then compared with the respective regulatory limit." [P1]

The dose representative of the radiation exposure at a given location (receptor point) in the area surrounding the discharge point can be expressed as follows:

$$\Delta = S \cdot T \cdot E \tag{29}$$

where:

Δ: is the dose attributed to the radiation exposure,
S: is the source term of the released activity,
T: is the transport factor (transmission),
E: is the exposure factor (dose conversion factors).

"Equation (29) has to be calculated for every release point, every receptor point selected on the basis of the population distribution, habit and meteorological data specific to the surrounding area, taking into account all exposure pathways separately. With appropriately selected boundary conditions, S, T and E can be defined independently from each other. Due to this separation, the effect that the different contributing factors and the impact of their change exerts on the result can be distinguished, S connected with the safety of the nuclear facility, and T and E dependent on external conditions and features of the site (population and habit data). With the proposed improved approach, during safety analysis, if factors T and E are already computed (which in general do not change for a specific location or site, but can be different for different DBC or DEC categories), only very simple calculations are necessary for the determination of environmental consequences of a new source term, since the calculations would only be a multiplication of three vectors representing the appropriate source term, the transport and exposure factors. Thus the entire chain of calculation does not need to be repeated if there is a change in either the source term (S), the parameters of the environmental transport and dilution process processes (T) or exposure characteristics (E).

In the case of site selection for a new nuclear power plant, in the interest of safety the site with appropriate T and E characteristics has to be chosen. After a site has been selected, these characteristics are to be regarded as external conditions, which are beyond our control, especially under circumstances of normal operation. It should be mentioned that despite the fact that in the long term, change in these site specific conditions might occur, calculation of the environmental transport and dilution (T) and the dose exposure (E) are to be updated only during periodical safety analysis review of a facility with static operational parameters, e.g. once every 10 years, or when there is a significant change in the parameters such as the population distribution or the habits of people living in the vicinity of the nuclear facility. For the time between periodical safety analysis reviews, T and E are considered to be constant. This periodical repetition of the calculations is in line with paragraph (b) of Article 8c of the Council Directive 2014/87/Euratom, which states that "the license holder under the regulatory control of the competent regulatory authority, re-assesses systematically and regularly, at least every 10 years, the safety of the nuclear installation [12].

Factors T and E are decoupled from the attributes of the nuclear facility in a given DBC or DEC status to ensure that the meteorological, environmental and social characteristics of the site will not have influence on the judgment of safety of nuclear facility, however these factors shall be calculated for every facility with site specific parameters. Without this separation, for each safety analysis, different meteorological, social and habit data would have to be used. This would be unnecessary considering that the variability of the weather is taken into account by sampling from the meteorological database, and in case of the social and habit data it can be postulated that the yearly changes won't affect the properties of the representative person for which the doses are calculated. From the safety point of view, if the transport and emission factors would be evaluated and possibly changed frequently based on the short-term fluctuation, decisions regarding the operation (including maintenance during operation) of a NPP could be dependent on the actual weather and social conditions (e.g. for an on-shore NPP, the safety level might be reduced in case of favorable wind direction, since in this case, public dose would be negligible and no countermeasures would be necessary in case of a major accident). Thus, the calculation method would not be robust enough to be the basis of regulatory requirements.

Additionally to the computation of release criteria, the calculation formula Eq. (29) could also be used for determining the radiation conditions in the environment and the population doses due to different release scenarios, in which case the three members on the right side of Eq. (29) depend on the properties of the release, the environment and the receptor points. It is also important to note that the same method could be used for existing and planned nuclear power plants, which would increase the comparability of different sites and nuclear facilities and also lead to a more transparent methodology in safety assessment.

This improved methodology has several advantages, as it is transparent, easy to implement, does not introduce new sources of uncertainty and saves computational burden. Throughout the calculation of the radiation exposure, there are several parameters that are not constant. The results of the calculation depend on actual weather conditions, habits of the population and the development level of plants, which are dependent on the seasonal changes. All of these factors increase the uncertainty of the results. In case of safety analysis performed independently from real events, the time dependency of the parameters can be eliminated, but for an emergency situation, actual parameters should be used for decisions to introduce countermeasures. The dose contributions received by the representative person of the population (e.g. a person with averaged attributes of the effected population) via different pathways shall be calculated taking into account certain meteorological conditions (wind direction, wind speed, atmospheric stability, precipitation) for the representative time period. The doses due to low probability events of extreme weather conditions may exceed the results for average meteorological conditions by many orders of magnitude, therefore the calculation should be regarded as fulfilling the compliance if only a negligible fraction of the dose results (a selected percentile value) exceed the limiting criteria. Taking into consideration the variability of the parameters, the improved method is more robust than the deterministic calculations, thus the results will not be as dependent on the highly variable and extreme weather conditions. Hence, the uncertainty of the results can be decreased.

One of the most important application of the above method is the confirmation of fulfilment for the release criteria of an NPP. To confirm that the large and early releases are avoided the calculation steps are the following:

- The determination of release cases (routes and timing) and released nuclides taken into account by the calculation, defining all the parameters that effect the atmospheric dispersion calculation (nuclide properties, released activity per nuclide per case, release height per case, environmental parameters influencing the effective release height). The source term factor is thus ascertained for each release case c and nuclide i (S_i^c). The range of the considered nuclides determined so that the selected ones cause at least 95% of the total dose.
- The determination of the receptor points at the given distances from the release point and the characteristics of the reference person (e.g. age, food consumption, breathing rate, residence attributes). Verification that farther from these receptor points higher dose values only have a low probability of occurrence with a high confidence.
- The determination of the utilized meteorological database (site specific meteorological data usually for at least 5 calendar years prior to the time of the calculation) from which the meteorological data sets used in the calculations are chosen by uniform sampling.
- The determination of the transport factor as the maximum value for each release case c, nuclide i, exposure pathway p and distance d ($T_i^{c,p,d}$). The transport factors are determined as the 95th percentile value of the atmospheric dispersion results for the sampled meteorological states. In practice, the transport factors for all the meteorological data points are sorted ascendingly and the value corresponding with the selected percentile is chose for each release case, nuclide, exposure pathway and distance.
- The determination of the exposure factor for each nuclide i, exposure pathway p, distance d and exposure duration t ($E_i^{p,d,t}$) based on the dose conversion factors for each pathway, and the characteristics of the reference person. The exposure durations correspond with the time interval of the DEC criterion. When analyzing

for the design basis conditions (DBC), the effect of the food chain must be taken into account, while in the case of design extension conditions (DEC), this pathway can be disregarded.

- The receptor point where the dose result is the highest based on T and E is selected, for which the representative exposure for release case c, distance d and exposure duration t (corresponding with a given DEC criterion).
- The release criterion is fulfilled if all representative doses are less than the limiting values.

The formula of Eq. (29) can be expressed in more detail for deterministic assessment of release acceptance criteria:

$$\Delta^{c,d,t} = \gamma \sum_{p} \sum_{i} S_i^c T_i^{c,p,d} E_i^{p,d,t} \tag{30}$$

where:

c: is the index for the release cases,
d: is the index of the distance,
t: is the index of the exposure duration,
p: is the index of the exposure pathways,
i: is the index of the radionuclides,
γ: is a safety factor.

The safety factor compensates the uncertainty of some elements of the calculation (e.g. selection of the receptor points, neglect of the time dependence of the release time and meteorology, the choice of the dose integration time, and the omission of low probability events).” [P1] Its value need to be determined based on the evaluation of the level of conservativism of each computational model, assumptions, omission or uncertainty.

“This is a transparent method, which supports the comparison of the impact of different sites and characteristics, such as site and meteorological conditions, habits, technical solutions effecting the source term, the timing of the release, release height, chemical form.

The determined representative exposure values could be connected to the countermeasures described in national requirements (emergency response plans) and discussed also in the EUR documents [21]. For example, according to a criterion stating dose consequences of release should not exceed the value which would justify the introduction of urgent countermeasures beyond 800 meters. In this case, the representative dose value ($\Delta^{c,d,t}$) should be calculated for all DEC cases (c), at the distance of 800 m from the release point (d) and for an exposure duration of 24 hours (t). The resulting values should be compared with the EUR DEC acceptance criterion of 50 mSv.

It should be emphasized that the calculated variable Δ has dose dimensions [Sv] but does not give an accurate, unbiased estimate of the projected dose of the representative person at the receptor point." [P1] When a given percentile of the transport factor (T^{air} for air activity concentration and T^{ground} for activity concentration on the ground) is chosen, the different meteorological cases are combined due to the difference of the migration, dilution and decay of radionuclides in the environment. Due to the difference in dispersion, deposition and decay properties of the nuclides, the meteorological case corresponding with the chosen percentile may not be the same for all the nuclides (e.g. for the transport factor in air, a meteorological case with no rain gives a higher value, whereas in case of the transport factor for ground, high precipitation conditions will result in higher values).

"Additionally, the representative dose variable (Δ) is not suitable for comparison with the reference levels used in emergency response practice (in a real emergency situation), due to the different methods and parameter values used in the calculations, its usage is solely justified for the confirmation of release criteria fulfilment during safety assessment. It is also important to mention that for similar reasons, the final representative exposure value (Δ) cannot be compared with operational intervention levels (OILs) [84]. For most of the exposure pathways, the dose criterion is the committed effective dose for different time periods, but for thyroid, the dose criterion is the absorbed dose.

This calculation method is similar to the one presented first in the NRC document RG 1.145 [17], with T being a counterpart of the relative air concentration (χ/Q) and E corresponding with the characteristics of the representative person at the receptor point. The difference from the NRC method, and the main advantage of the improved method is that in the improved approach, not only T is specific for a given site and receptor point, but E is site specific as well, with additional considerations taken into account for the determination of radiological consequences (e.g. exposure from food chain, impact of daughter products)." [P1]

More detailed descriptions of the factors S, T and E are given in the following subsections.

Source term

"The source term factor S depends on the type of the nuclear facility and can be different for each postulated incident or accident. A clear distinction shall be exerted between the inventory (the total amount of radioactivity present in the systems, structures and assemblies of the installation) and the actual source term that is considered for the actual release in investigation." [P1]

The methodology does not include the computation of the source term of the release but takes it into account as an input vector containing the released activity of each radionuclide. However, for the chain of calculations to be compatible, the source term of the release needs to be determined according to the following requirements and assumptions.

"The source term shall be determined on the basis of the specific characteristics of the design. In case of analyzing off-normal releases, quantity, timing and chemical species of the fission and activation products released to the environment in the first 24h, 4 days and during the entire accident period should be considered. These parameters can be determined with reactor physics and thermohydraulic calculations. The computer codes used for source term quantification shall be internationally recognized and adequately supported by documentation, including code validation against experimental data [21]. In the calculation of environmental impacts, radioactive decay and generation of progeny elements may also be taken into account, for which the time elapsed between the reactor shut down and the release of radioactive contaminants must also be determined especially for radionuclides with shorter half-life.

If a radionuclide can be present in more than one chemical form (such as radiocarbon or radioiodine), it should be taken into account in the analyses. The chemical form in which the radionuclide is produced, is highly dependent on the operation state of the nuclear power plant when the event occurs. It should be noted that the chemical form of certain radionuclides – inside and outside the facility – can change throughout the propagation both in space and time. In every model, the iodine conversion among the elemental, aerosol and organic form should be considered and their dispersion should be treated separately, or it must be shown that the approximation of omitting the chemical transformation is negligible or conservative in terms of the outcome of the calculation.

Depending on the purpose of the analysis, the dose calculation may be limited to selected number of key radionuclides, in which case the analysis must demonstrate that the results adequately characterize the emerging dose conditions [21]. The produced isotopes can be grouped based on different aspects. The grouping can be done according to the volatility of the resulting radioactive materials, but other practical classifications (for example, inert and reactive gases, cations and anions, organic and inorganic compounds) may also be used. In order to simplify the calculations of the atmospheric dispersion and environmental consequences, the classification is usually based on the characteristics of the propagation (physical state, chemical form) instead of the origin or the production of the elements." [P1]

Transport

"The dose assessment on-site and off-site the facility is carried out by the evaluation of the dilution processes of the radioactive material migrating through different pathways from the discharge point to the receptor point. The discharge point itself should be selected in a thorough evaluation, considering the actual on-site conditions. The T transport factor determines the dilution of the radioactive material emitted into the environment on its way reaching the receptor point. Its value is dependent on the characteristics of the emission such as release height, heat content, size of the discharge point, and meteorological parameters of wind direction, wind speed, atmospheric stability, precipitation and the temperature. Some parameters of the released radionuclides (e.g. deposition velocity, decay constant) also influence the transport factor.

During the calculations all possible routes of atmospheric and liquid emissions must be taken into account.” [P1]

Exposure

“For the determination of the radiation exposure originating from the nuclear facility of the representative person as a member of the public – generally lower than the natural radiation exposure by several orders of magnitude and compared to the dose constraint in DBC 1 and DBC 2 cases for facilities under construction – the following components shall be considered:

a) external exposure of direct gamma and – only in some special cases – neutron radiation from the facility resulting from the operation of the installation (usually negligible outside the facility),
b) external radiation exposure from the plume of the radioactive contaminant released through the ventilation stack or directly from the damaged building and the material deposited from the plume onto the ground and surface objects,
c) internal exposure from the inhalation of radioactive contaminants from atmospheric release,
d) internal exposure from the ingestion of radioactive contaminants through food chain due to the soil contamination and direct deposition onto plants and fruits from atmospheric release,
e) external exposure from liquid release,
f) internal exposure from the ingestion of radioactive contaminants from liquid release (e.g. consumption of contaminated drinking water or fish, activity intake through food chain due to irrigation).

In most cases direct radiation is negligible outside the facility and dose consequences of liquid releases are smaller with several orders of magnitude than releases to the atmosphere, therefore only point b) c) and d) shall be analyzed.

The exposure factor E specifies how much dose is caused for different exposure pathways as a result of the activity concentration at the receptor point. Its value depends on the age of the person residing at the receptor point, local habits like lifestyle patterns, the breathing rate (in case of inhalation), and the food consumption and specific properties of the foodstuff (in case of ingestion).” [P1]

BIBLIOGRAPHY

[1] Z. Gu, 2018. "History review of nuclear reactor safety", *Annals of Nuclear Energy*, Vol. 120, pp 682-690, 2018, doi: 10.1016/j.anucene.2018.06.023.

[2] M. A. Hernández-Ceballos, M. Sangiorgi, B. García-Puerta, M. Montero, C. Trueba, "Dispersion and ground deposition of radioactive material according to airflow patterns for enhancing the preparedness to N/R emergencies" *Journal of Environmental Radioactivity*, Vol. 216, 2020, doi: 10.1016/j.jenvrad.2020.106178

[3] O. Tichý, V. Šmídl, R. Hofman, N. Evangeliou, "Source term estimation of multi-specie atmospheric release of radiation from gamma dose rates" *Q. J. R. Meteorol. Soc.*, Vol. 144, pp. 2781–2797, 2018, doi: 10.1002/qj.3403

[4] K. Shankar Rao, "Uncertainty Analysis in Atmospheric Dispersion Modeling", *Pure and Applied Geophysics*, Vol. 162, pp. 1893–1917, 2005, doi: 10.1007/s00024-005-2697-4

[5] L. Yuanzhong and C. Jianzhu, "Fission product release and its environment impact for normal reactor operations and for relevant accidents" *Nuclear Engineering* and Design, Vol. 2018, pp. 81-90, 2002, doi: 10.1016/S0029-5493(02)00200-5

[6] A. Zali, M. Shamsaei Zafarghandi, S.A. Feghhi, A.M. Taherian, "Public member dose assessment of Bushehr Nuclear Power Plant under normal operation by modeling the fallout from stack using the HYSPLIT atmospheric dispersion model", *Journal of Environmental Radioactivity*, Vol. 171, pp. 1–8, 2017, doi: 10.1016/j.jenvrad.2017.01.025

[7] M. E. Vasyanovich, A.A. Ekidin, A.V. Vasilyev, A.I. Kryshev, T.G. Sazykina, I.V. Kosykh, I.A. Kapustin, "Determination of radionuclide composition of the Russian NPPs atmospheric releases and dose assessment to population", *Journal of Environmental Radioactivity*, Vol. 208–209, 2019, doi: 10.1016/j.jenvrad.2019.106006

[8] A. Pirouzmand, Z. Kowsar, P. Dehghani, "Atmospheric dispersion assessment of radioactive materials during severe accident conditions for Bushehr nuclear power plant using HYSPLIT code" *Progress in Nuclear Energy*, Vol. 108, pp. 169-178, 2018, doi: 10.1016/j.pnucene.2018.05.015

[9] W. H. Leung, W.M. Ma, Philip K.Y. Chan, "Nuclear accident consequence assessment in Hong Kong using JRODOS" *Journal of Environmental Radioactivity*, Vol. 183, pp. 27–36. 2018, doi: 10.1016/j.jenvrad.2017.12.002

[10] International Atomic Energy Agency, "Deterministic Safety Analysis for Nuclear Power Plants", IAEA Safety Standards Series No. SSG-2 (Rev.1), Vienna, 2019.

[11] International Atomic Energy Agency, "Radiation Protection Aspects of Design for Nuclear Power Plants", IAEA Safety Standards Series No. NS-G-1.13, IAEA, Vienna, 2005

[12] “Council Directive 2014/87/Euratom of 8 July 2014 amending Directive 2009/71/Euratom establishing a Community framework for the nuclear safety of nuclear installations, Section 2 Specific obligations Article 8a Nuclear safety objective for nuclear installations” OJ L 219, 25.7.2014, pp. 42–52, 2014.

[13] J. A. Jones, P. A. Mansfield, S. M. Haywood, I. Hasemann, C. Steinhauer, J. Ehrhardt and D. Faude, “PC Cosyma (Version 2): An Accident Consequence Assessment Package for Use on a PC” European Commission, Brussels, 1996.

[14] Grove Software, MicroShield® 6.20. Grove Engineering. 2004.

[15] P. Szántó, S. Deme, E. Láng, I. Németh, and T. Pázmándi, “SINAC – Simulator Software for Interactive Modelling of Environmental Consequences of Nuclear Accidents (Second Generation),” in Proceedings of the 13th IRPA International Congress – IRPA13 Glasgow, 2013, https://www.irpa.net/members/P09.46fp.pdf

[16] S. Deme, I. Németh, T. Pázmándi, P. Szántó, “Description of the models applied in the SINAC program”, (in Hungarian) HUN-REN Centre for Energy Research Report, EK-SVL-2012-262-01-01-03, Budapest, 2013.

[17] J. H. Sørensen, J. Bartnicki, A. M. B. Buhr, H. Feddersen, S. Cordt Hoe, C. Israelson, H. Klein, B. Lauritzen, J. Lindgren, F. Schönfeldt, R. Sigg, “Uncertainties in atmospheric dispersion modelling during nuclear accidents”, *Journal of Environmental Radioactivity*, Vol. 222, 2020, doi:10.1016/j.jenvrad.2020.106356

[18] B. Cao, W. Cui, C. Chen, Y. Chen, “Development and uncertainty analysis of radionuclide atmospheric dispersion modeling codes based on Gaussian plume model,” *Energy*, Vol. 194, 2020, doi: 10.1016/j.energy.2020.116925

[19] B. Salbu, “Environmental impact and risk assessments and key factors contributing to the overall uncertainties”, *Journal of Environmental Radioactivity*, Vol. 151, 2016, doi: 10.1016/j.jenvrad.2015.09.001

[20] U.S. Nuclear Regulatory Commission, “RG 1.145: Atmospheric dispersion models for potential accident consequence assessments at nuclear power plants”, 1982, https://www.nrc.gov/docs/ML0037/ML003740205.pdf

[21] “European Utility Requirements for LWR Nuclear Power Plants (EUR)”, Volume 2, Chapter 1, Safety Requirements, Revision D, October 2012

[22] E. Davakis, S. Andronopoulos, I. Kovalets, N. Gounaris, J.G. Bartzis, S.G. Nychas, “Data assimilation in meteorological pre-processors: Effects on atmospheric dispersion simulations” *Atmospheric Environment*, Vol. 41, Issue 14, pp. 2917-2932, 2007, doi: 10.1016/j.atmosenv.2006.12.031.

[23] Leutbecher, M., Lock, S.J., Ollinaho, P., Lang, S.T.K., Balsamo, G., Bechtold, P., Bonavita, M., Christensen, H.M., Diamantakis, M., Dutra, E., English, S., Fisher, M., Forbes, R.M.,

Goddard, J., Haiden, T., Hogan, R.J., Juricke, S., Lawrence, H., MacLeod, D., Magnusson, L., Malardel, S., Massart, S., Sandu, I., Smolarkiewicz, P.K., Subramanian, A., Vitart, F., Wedi, N., Weisheimer, A., "Stochastic representations of model uncertainties at ECMWF: state of the art and future vision", *Q.J.R. Meteorol. Soc.*, Vol. 143, Issue 707, pp. 2315-2339, 2017, doi: 10.1002/qj.3094

[24] World Meteorological Organization, "Guide to Meteorological Instruments and Methods of Observation", WMO-No. 8. ISBN 978-92-63-10008-5. 2014.

[25] World Meteorological Organization, "Manual on the Global Data-processing and Forecasting System. Volume I – Global Aspects", WMO-No. 485. ISBN 978-92-63-10485-4. 2010.

[26] World Meteorological Organization, "Guidelines on Ensemble Prediction Systems and Forecasting", WMO-No. 1091. ISBN 978-92-63-11091-6. 2012.

[27] Steven R. Hanna, Gary A. Briggs, Rayford P. Hosker, "Handbook on Atmospheric Diffusion", Technical Information Center, U.S. Department of Energy, 1982.

[28] D. Jakab, T. Pázmándi, Cs. Rudas, P. Szántó, "Uncertainty of the meteorological data required for atmospheric dispersion calcualtions and their consequences", (inHungarian) EK-SVL-2017-718-01-01-00 Budapest, 2017.

[29] A. Stohl, M. Hittenberger, G. Wotawa, "Validation of the lagrangian particle dispersion model FLEXPART against large-scale tracer experiment data", *Atmospheric Environment*, Vol. 32, Issue 24, pp. 4245-4264, 1998, doi: 10.1016/S1352-2310(98)00184-8.

[30] A. F. Stein, R. R. Draxler, G. D. Rolph, B. J. B. Stunder, M. D. Cohen, and F. Ngan, "NOAA's HYSPLIT Atmospheric Transport and Dispersion Modeling System," *Bull. Am. Meteorol. Soc.*, Vol. 96, No. 12, pp. 2059–2077, 2015, doi: 10.1175/BAMS-D-14-00110.1.

[31] D.B. Ryall, R.H. Maryon, "Validation of the UK Met. Office's name model against the ETEX dataset", *Atmospheric Environment*, Vol. 32, Issue 24, pp. 4265-4276, 1998, doi: 10.1016/S1352-2310(98)00177-0.

[32] D. Bruce Turner, "Workbook of atmospheric dispersion estimates: an introduction to dispersion modelling" CRC Press; 2nd edition, 1994.

[33] T. Pázmándi, Cs. Rudas, "Development of CARC code for calculations of environmental radiation conditions, Description of the models used in the CARC code" (in Hungarian) HUN-REN Centre for Energy Research Report, EK-SVL-2020-731-01-01-00, Budapest, 2020.

[34] G.A. Briggs, "Plume Rise Predictions" *in Lectures on Air Pollution and Environmental Impact Analyses*, American Meteorological Society, Boston, MA. 1982. doi: 10.1007/978-1-935704-23-2_3

[35] F. Pasquill, "The estimation of the dispersion of windborne material", *The Meteorological Magazine*, Vol. 90, No. 1063, pp 33-49, 1961.

[36] H.-J. Panitz, J. Päsler-Sauer, C. Matzerath, "UFOMOD: Atmospheric dispersion and deposition", KfK-4332, Germany, 1989.

[37] H-J. Panitz, "Accident Consequence Assessment with Different Atmospheric Dispersion Models", KfK-4445, Germany, 1989.

[38] P. Zannetti, "An improved puff algorithm for plume dispersion simulation", *J. Appl. Meteorol.*, Vol. 20, Issue 10, pp. 1203–1211, 1981, doi: 10.1175/1520-0450(1981)020<1203:AIPAFP>2.0.CO;2

[39] Datasheet of Wind Set WA15 https://www.vaisala.com/en/products/instruments-sensors-and-other-measurement-devices/weather-stations-and-sensors/wa15 Accessed: 23.09.2021. 11:58

[40] International Atomic Energy Agency, "Generic Models for Use in Assessing the Impact of Discharges of Radioactive Substances to the Environment", Safety Reports Series No. 19, IAEA, Vienna, 2001.

[41] Milton R. Beychok, "Fundamentals of stack gas dispersion", 4th Edition, MR Beychok 2005.

[42] S. Thykier-Nielsen, S. Deme, T. Mikkelsen, "Description of the atmospheric dispersion module RIMPUFF", Riso National Laboratory, PO Box 49, 1999.

[43] C. Landman, W. Raskob, Dmytro Trybushnyi, I. Ievdin, I.. (2016). Creating and running worldwide accident scenarios with JRodos", *Radioprotection*, Vol. 51, Num. HS1, pp. S27 - S30, 2016, doi: 10.1051/radiopro/2016007

[44] US Nuclear Regulatory Commission, "NUREG 1150-Severe accident risks: an assessment for five US nuclear power plants", Division of Systems Research, Office of Nuclear Regulatory Research, Washington DC. 1990.

[45] S. Karlsson, "Dry Deposition - A Literature Survey", Studsvik Energiteknik AB, 1982.

[46] I. Van der Hoven, "Deposition of particles and gases", *Meteorology and Atomic Energy,* D. Slade (Ed.), TID-24190, NTIS, Springfield, VA, 1968.

[47] H. D. Brenk, K. J. Vogt, "Calculation of wet deposition from radioactive plumes," *Nuclear Safety*, Vol. 22, pp. 362–371, 1981.

[48] International Commission on Radiological Protection, "Use of dose quantities in radiological protection", ICRP Publication 147, Ann. ICRP 50(1). 2021.

[49] International Commission on Radiological Protection, "Conversion Coefficients for Radiological Protection Quantities for External Radiation Exposures", ICRP Publication 116, Ann. ICRP 40(2-5). 2010.

[50] International Commission on Radiological Protection, "The 2007 Recommendations of the International Commission on Radiological Protection", ICRP Publication 103, Ann. ICRP 37 (2-4). 2007.

[51] International Commission on Radiological Protection, "Conversion Coefficients for use in Radiological Protection against External Radiation", ICRP Publication 74, Ann. ICRP 26 (3-4). 1996.

[52] International Commission on Radiological Protection, "Dose coefficients for external exposures to environmental sources", ICRP Publication 144, Ann. ICRP 49(2). 2020.

[53] International Atomic Energy Agency, "Radiation Protection and Safety of Radiation Sources: International Basic Safety Standards", IAEA Safety Standards Series No. GSR Part 3. Vienna, 2014, doi: 10.61092/iaea.u2pu-60vm

[54] International Atomic Energy Agency, "Preparedness and Response for a Nuclear or Radiological Emergency", IAEA Safety Standards Series No. GSR Part 7, Vienna, 2015, doi: 10.61092/iaea.3dbe-055p

[55] International Atomic Energy Agency, "Dispersion of Radioactive Material in Air and Water and Consideration of Population Distribution in Site Evaluation for Nuclear Power Plants", IAEA Safety Standards Series No. NS-G-3.2, Vienna, 2002.

[56] U.S. Nuclear Regulatory Commission, "Regulatory Guide 1.183: Alternative Radiological Source Terms for Evaluating Design Basis Accidents at Nuclear Power Reactors", 2000, https://www.nrc.gov/docs/ML0037/ML003716792.pdf

[57] U.S. Nuclear Regulatory Commission, "NRC Regulations Title 10 Energy", Code of Federal Regulations, 2023, https://www.nrc.gov/reading-rm/doc-collections/cfr/

[58] Act CXVI of 1996 on Atomic Energy

[59] Govt. Decree 118/2011. (VII. 11.) Korm. on the nuclear safety requirements of nuclear facilities and on related regulatory activities

[60] Hungarian Atomic Energy Authority Decree 2/2022. (IV. 29.) on the protection against ionizing radiation and the corresponding licensing, reporting (notification) and inspection system

[61] International Atomic Energy Agency, "Terminology Used in Nuclear Safety, Nuclear Security, Radiation Protection and Emergency Preparedness and Response", IAEA Nuclear Safety and Security Glossary, 2022 (Interim) Edition

[62] Ministerial Decree 16/2000 (VI. 8.) EüM of the Minister of Health on the Implementation of Certain Provisions of the Act CXVI of 1996 on Atomic Energy

[63] Interdepartmental Coordination Committee for Disaster Management, "National Nuclear Emergency Response Plan OBEIT, v3.1" 2020.

[64] J. W. Poston, W. S. Snyder, "A Model for Exposure to a Semi-infinite Cloud of a Photon Emitter", *Health Phys.*, Vol. 26, Issue 4, pp.287-293, 1974, doi: 10.1097/00004032-197404000-00001

[65] D. C. Kocher, "Dose-Rate Conversion Factors for External Exposure to Photons and Electrons", *Health Phys.* Vol. 45, Issue 3, pp. 665-686. 1983, doi: 10.1097/00004032-198309000-00010

[66] Keith F. Eckerman, Jeffrey C. Ryman, "External Exposure To Radionuclides In Air, Water, And Soil", Federal Guidance Report No. 12, EPA-402-R-93-081. U.S. Environmental Protection Agency, 1993.

[67] S.Y.F. Chu, L.P. Ekström, R.B. Firestone, "The Lund/LBNL Nuclear Data Search, Version 2.0," 1999, http://nucleardata.nuclear.lu.se/toi/nucSearch.asp

[68] J.H. Hubbell, S.M. Seltzer, "NIST Standard Reference Database 126", 1996, https://doi.org/https://dx.doi.org/10.18434/T4D01F

[69] K. Saito, N. Petoussi, M. Zankl, R. Veit, P. Jacob, G. Drexler, " Calculation of organ doses from environmental gamma rays using human phantoms and Monte Carlo methods", (GSF--2/90), Germany, 1990.

[70] A.D. Poley, "Modell Description, NUDOS: A Computer Program for Assessing the Consequences of Airborne Releases of Radionuclides", ECN-I-96-057, Petten, Netherlands, 1996.

[71] US Environmental Protection Agency, "Exposure Factors Handbook: 2011 Edition (Final Report)", Washington, DC, EPA/600/R-09/052F, 2011.

[72] Csilla Rudas, "Modeling the Migration of Radionuclides in Food Chain", (in Hungarian) Budapest University of Technology and Economics, Faculty of Natural Sciences, Department of Nuclear Techniques, Master's Thesis, Budapest, 2017.

[73] H. Müller, G. Pröhl, "ECOSYS-87: A Dynamic Model for Assessing Radiological Consequences of Nuclear Accidents", *Health Physics*, Vol. 64, No. 3, pp. 232–252, 1993. doi: 10.1097/00004032-199303000-00002

[74] H. Müller, F. Gering, G. Pröhl, "Model Description of the Terrestrial Food Chain and Dose Module FDMT in RODOS", PV6.0, GSF - Institut für Strahlenschutz, Munich, 2003.

[75] International Atomic Energy Agency, "Generic Models and Parameters for Assessing the Environmental Transfer of Radionuclides from Routine Releases: Exposures of Critical Groups", IAEA Safety Series No. 57", Vienna, 1982.

[76] International Atomic Energy Agency, "Quantification of radionuclide transfer in terrestrial and freshwater environments for radiological assessments", IAEA-TECDOC-1616, Vienna, 2009.

[77] International Atomic Energy Agency, “Handbook of Parameter Values for the Prediction of Radionuclide Transfer in Terrestrial and Freshwater Environments” IAEA Technical Reports Series No. 472, Vienna, 2010.

[78] M. Thorne, R. Walke, P. Maul, “The PRISM Foodchain Modelling Software: Parameter, Values for the Soil/Plant Model”, Food Standars Agency QRS-1198A-3, United Kingdom, 2005.

[79] W. T. Hwang, G. Cho, M. H. Han, “Development of a Dynamic Food Chain Model, DYNACON and Its Application to Korean Agricultural Conditions”, *Journal of Nuclear Science and Technology*, Atomic Energy Society of Japan, Vol. 35, No. 6, pp. 454-461, 1998.

[80] R.D. Sharp, A.L. Sjoreen, R.W. Shor, C.F. Baes III, “A review and analysis of parameters for assessing transport of environmentally released radionuclides through agriculture”, Oak Ridge National Laboratory Report ORNL-5786, 1984, doi: 10.2172/6355677

[81] A.F. Nisbet, R.F. Woodman, „Soil-to-plant transfer factors for radiocesium and radiostrontium in agricultural systems”, *Health Physics*, Vol. 78, No. 3, pp. 279-288, 2000, doi: 10.1097/00004032-200003000-00005

[82] G. Voigt, K. Henrichs, G. Pröhl, H.G. Paretzke, “Measurements of transfer coefficients for 137Cs, 60Co, 54Mn, 22Na, 131I and 95mTc from feed into milk and beef”, *Radiation and Environmental Biophysics*, Vol. 27, No. 2, pp. 143–152, 1988, doi: 10.1007/BF01214604.

[83] G. Voigt, G. Pröhl, H. Müller, T. Bauer, J.P. Lindner, G. Probstmeier, G. Röhrmoser, “Determination of the transfer of cesium and iodine from feed into domestic animals”, *Science of The Total Environment*, Vol. 85, pp. 329–338, 1989, doi: 10.1016/0048-9697(89)90332-X.

[84] International Atomic Energy Agency, “Operational Intervention Levels for Reactor Emergencies, Emergency Preparedness and Response”, IAEA, Vienna, 2017.

[85] European Commission, Organisation for Economic Co-operation and Development Nuclear Energy Agency, “Probabilistic accident consequence assessment codes, Second international comparison”, Brussels, Luxembourg, 1994.

[86] J. A. Mitchell, C. Molenkamp, N. E. Bixler, C. W. Morrow, J. V. Ramsdell, “Comparison of Average Transport and Dispersion Among a Gaussian Model, a Two-Dimensional Model and a Three-Dimensional Model, in: Probabilistic Safety Assessment and Management”, *Springer*, London, 2004, doi: 10.1007/978-0-85729-410-4_516

[87] National Radiological Protection Board, “PC COSYMA Version 2.0 User Guide”, EUR 16240 EN, 1995.

[88] International Commission on Radiological Protection, “Age-dependent Doses to Members of the Public from Intake of Radionuclides - Part 1”, ICRP Publication 56, Ann. ICRP 20 (2). 1990.

[89] International Commission on Radiological Protection, “Age-dependent Doses to Members of the Public from Intake of Radionuclides - Part 2 Ingestion Dose Coefficients”, ICRP Publication 67, Ann. ICRP 23 (3-4) 1993.

[90] International Commission on Radiological Protection, “Age-dependent Doses to Members of the Public from Intake of Radionuclides - Part 3 Ingestion Dose Coefficients”, ICRP Publication 69, Ann. ICRP 25 (1). 1995.

[91] A.W. Phipps, G.M. Kendall, J.W. Stather, T.P. Fell, “Committed equivalent organ doses and committed effective doses from intakes of radionuclides”, National Radiological Protection Board, Chilton, United Kingdom. 1991.

[92] I. Hasemann, J. Ehrhardt, “COSYMA. Dose models and countermeasures for external exposure and inhalation”, KfK 4333, Germany, 1994.

[93] W. Raskob, N. A. Beresford, T. Duranova, I. Korsakissok, A. Mathieu, M. Montero, T. Müller, C. Turcanu and C. Woda, “Coping with uncertainties for improved modelling and decision making in nuclear emergencies. Key results of the CONFIDENCE European research project”, *Radioprotection*, Vol. 55, pp. S7-S15, 2020, doi: 10.1051/radiopro/2020008

[94] MVM Paks Nuclear Power Plant Ltd. Final Safety Analysis Report, Chapter 15.2. Design Basis Accidents, Version 17. 2022.

[95] International Atomic Energy Agency, “Generic Procedures for Assessment and Response during a Radiological Emergency”, IAEA TECDOC 1162, Vienna, 2000.

[96] C. I. Anderson, W. A. Gough, “Accounting for missing data in monthly temperature series: Testing rule-of-thumb omission of months with missing values”, *Int. J. Climatol.* Vol. 38, Issue 13, pp. 4990-5002, 2018, doi: 10.1002/joc.5801

[97] A. Anjomshoaa, M. Salmanzadeh, “Filling missing meteorological data in heating and cooling seasons separately”, Int. J. Climatol. Vol. 39, Issue 2, pp. 701-710, 2019, doi: 10.1002/joc.5836

[98] U.S. Environmental Protection Agency, “Meteorological Monitoring Guidance for Regulatory Modeling Applications”, EPA-454/R-99-005. 2000.

[99] World Meteorological Organization, “Guide to Climatological Practices”, 3rd ed., WMO-No. 100, ISBN 978-92-63-10. Geneva, Switzerland, 2018.

[100] J. M. Colston, T. Ahmed, C. Mahopo, G. Kang, M. Kosek, F. de Sousa Junior, P. S. Shrestha, E. Svensen, A. Turab, B. Zaitchik, “Evaluating meteorological data from weather stations, and from satellites and global models for a multi-site epidemiological study”, *Environmental Research*, Vol. 165, pp. 91-109, 2018, doi: 10.1016/j.envres.2018.02.027

[101] International Atomic Energy Agency, “Arrangements for the Termination of a Nuclear or Radiological Emergency”, IAEA Safety Standards Series No. GSG-11, Vienna, 2018.

[102] Steven R. Hanna, "Chapter 4.0 A review of uncertainty and sensitivity analyses of atmospheric transport and dispersion models," Developments in Environmental Science, Elsevier, Vol. 6, pp.331-351, 2007, doi: 10.1016/S1474-8177(07)06040-8.

[103] Ngoc Bao Tran LE, Irène Korsakissok, Vivien Mallet, Raphaël Périllat, Anne Mathieu, "Uncertainty study on atmospheric dispersion simulations using meteorological ensembles with a Monte Carlo approach, applied to the Fukushima nuclear accident," *Atmospheric Environment: X*, Vol. 10, 2021, doi: 10.1016/j.aeaoa.2021.100112.

[104] S. J. Leadbetter, A. R. Jones, M. C. Hort, "Assessing the value meteorological ensembles add to dispersion modelling using hypothetical releases", *Atmos. Chem. Phys.*, Vol. 22, pp. 577–596, 2022, doi: 10.5194/acp-22-577-2022

[105] Tamás Velenyák, "Modelling atmospheric dispersion of contaminants", (in Hungarian) Budapest University of Technology and Economics, Faculty of Mechanical Engineering, Master's Thesis, Budapest, 2016.

[106] World Meteorological Organization, "Guide to Meteorological Instruments and Methods of Observation", WMO-No. 8. ISBN 978-92-63-10008-5. 2014.

[107] World Meteorological Organization, "Manual on the Global Data-processing and Forecasting System. Volume I – Global Aspects", WMO-No. 485. ISBN 978-92-63-10485-4. 2010.

[108] T. Iversen, A, Deckmyn, C. Santos, K. Sattler, J. B. Bremnes, H. Feddersen, I. L. Frogner, "Evaluation of "GLAMEPS"-a proposed multimodel EPS for short range forecasting", Tellus A: Dynamic Meteorology and Oceanography, Vol. 63, pp. 513–530, 2011, doi: 10.1111/j.1600-0870.2010.00507.x.

[109] L. Descamps, C. Labadie, A. Joly, E. Bazile, P. Arbogast, P. Cébron, "PEARP, the Météo-France short-range ensemble prediction system", *Q.J.R. Meteorol. Soc*, Vol. 141, Issue 690, pp. 1671-1685, 2015, doi: 10.1002/qj.2469

[110] F. Molteni, R. Buizza, T. N. Palmer, T. Petroliagis, "The ECMWF Ensemble Prediction System: Methodology and validation", *Q.J.R. Meteorol. Soc*, Vol. 122, Issue 529, pp. 73–119, 1996, doi: 10.1002/qj.49712252905

[111] G. Geertsema, H. de Vries, R. Sheele, "High resolution meteorological ensemble data for CONFIDENCE research on uncertainties in atmospheric dispersion in the (pre-)release phase of a nuclear accident", *in Proceedings of the 19th International Conference on Harmonisation within Atmospheric Dispersion Modelling for Regulatory Purposes, HARMO19, Bruges, Belgium, 3–6 June 2019*, 2019, https://www.harmo.org/conference.php?id=19 2019.

[112] Y. Seity, P. Brousseau, S. Malardel, G. Hello, P. Bénard, F. Bouttier, C. Lac, V. Masson, "The AROME-France convective-scale operational model", *Monthly Weather Review*, Vol. 139, No. 3, pp. 976-991. 2011.

[113] A. Horányi, M. Mile, Szűcs, "Latest developments around the ALADIN operational short-range ensemble prediction system in Hungary", *Tellus A*, Vol. 63, Issue 3, pp. 642-651, 2011, doi: 10.1111/j.1600-0870.2011.00518.x

[114] K. Chevalier-Jabet, "Design and use of Bayesian networks for the diagnosis/prognosis of severe nuclear accidents", EU program for research and innovation H2020 – FAST Nuclear Emergency Tools (FASTNET) project. Report FASTNET-DATA-D2.3. 2019.

[115] International Atomic Energy Agency, "Criteria for Use in Preparedness and Response for a Nuclear or Radiological Emergency", IAEA Safety Standards Series No. GSG-2, IAEA, Vienna, 2011.

[116] International Atomic Energy Agency, "Meteorological and Hydrological Hazards in Site Evaluation for Nuclear Installations", IAEA Safety Standards, Specific Safety Guide SSG-18, IAEA, Vienna, 2011.

[117] M. Lakatos, B. Izsák, O. Szentes, L. Hoffmann, A. Kircsi, Z. Bihari, "Return values of 60-minute extreme rainfall for Hungary", *Időjárás, Quarterly Journal of the Hungarian Meteorological Service*, Vol. 124, No. 2 pp. 143–309, 2020, doi: 10.28974/idojaras.2020.2.1

[118] J. Chen, A. Dai, "The atmosphere has become increasingly unstable during 1979–2020 over the Northern Hemisphere", *Geophysical Research Letters*, Vol. 50, Issue 20, 2023. doi: 10.1029/2023GL106125

[119] H. Tabari, "Climate change impact on flood and extreme precipitation increases with water availability", *Scientific reports*, Vol. 10, 2020. doi: 10.1038/s41598-020-70816-2